Frost Heave Properties Assessment of the Soils for the Road Pavement design

Final report

Customer:	VAS "Latvijas Valsts ceļi"
Contractor:	SIA "Vides eksperti"
Sub-contractors:	University of Latvia
	SIA "Ceļu eksperts"

Experts:	Māris Krievāns, PhD – University of Latvia
	Jānis Karušs, PhD – University of Latvia
	Ivars Pavasars, PhD – SIA "Vides eksperti"
	Aigars Strežs, MSc– SIA "Ceļu eksperts"

Rīga 2019

KOPSAVILKUMS

Apstiprinu, ______________________________ (vārds, uzvārds, paraksts)		
Pētniecības projekta nosaukums: *Grunšu sala pacēluma īpašību novērtēšana ceļu segas projektēšanas vajadzībām*		
Līguma numurs	LVC2018/1.10/1/AC	
Līguma slēgšanas datums	2018. gada 7. jūnijs	
Pētniecības projekta stadija	Gala ziņojums	
Starpziņojumu kopējais skaits	Viens	
Ziņojuma nodošanas datums	2019. gada 18. marts	
Pētniecības projekta stadijas izstrādes periods	2018. gada 12. novembris - 2019. gada 18. marts	
Lappušu skaits	138 (neieskaitot pielikumus)	
Disks vai cits datu nesējs (ir/nav)	Ir	
Eksemplāru skaits	1	
Pētniecības programma JAUNU TEHNOLOĢIJU IZPĒTES PROGRAMMA 2017. - 2019. GADAM		
Pētniecības projekta izpildītāji	Grāds,Vārds, Uzvārds	Paraksts
Pētniecības projekta vadītājs	PhD, Ivars Pavasars	
Pētnieks	PhD, Jānis Karušs	
Pētnieks	PhD, Māris Krievāns	
Pētnieks	MSc, Aigars Strežs	
Projektu finansē	VAS ″Latvijas valsts ceļi″ / Satiksmes ministrija	
Partneri	SIA "Vides eksperti", Latvijas Universitāte, SIA "Ceļu eksperts"	

Apraksts

Darba izstrādes ietvaros ir veikts zinātniskās literatūras apskats un analīze, kas koncentrējas uz sala pacēluma teorētiskajiem aspektiem, kā arī apskatīti un salīdzināti pašreiz pasaulē lietotie izpētes standarti un metodes sasaluma un atkusuma ietekmes novērtēšanai gruntīm. Sniegts vispārējs Latvijas klimatisko apstākļu apskats, tendences un analizēti LVC meteoroloģisko staciju dati. Rezultāti atspoguļoti arī grafiski uz Latvijas kartes.

Lai novērtētu dažādu Latvijā sastopamo grunšu sala pacēluma īpašības un konstatētu svarīgākos to noteicošos parametrus, savākti Latvijā raksturīgo dažādu grunšu paraugi aptverot pēc iespējas vairāk dažādus grunšu tipus. Veikta atlasīto grunšu pamatīpašību un sala pacēluma testēšana laboratorijā.

Veidojot monitoringa programmu, vispirms analizēta satelītu datu iespējamā izmantošana meteoroloģisko parametru monitoringam uz ceļiem, kas, kā izrādījās, tomēr nav pietiekami precīzi un detalizēti, un līdz ar to nav piemēroti sala pacēluma novērtēšanai uz ceļiem. Tālāk apskatīta ārvalstu pieredze sasaluma dziļuma un sala pacēluma noteikšanā *in situ*, kā arī attiecīgi pielietojamie sensoru tipi un aprīkojums šādu mērījumu veikšanai. Konstatēts, ka sala pacēluma *in situ* mērījumi uz ceļiem pasaulē ir veikti ļoti ierobežotā apjomā, pārsvarā

pielietojot netiešas aprēķinu metodes. Attiecīgi arī tirgū nav pieejamas šādas plaši aprobētas un standartizētas mēriekārtas.
Ir sagatavoti priekšlikumi iespējamajam grunšu temperatūras, mitruma un sala pacēluma in situ mērījumu monitoringa staciju tīklam Latvijā, mēriekārtu parametriem, aprīkojumam un mērīšanas metodikai. Novērtētas arī ar to saistītās iespējamās izmaksas.

Abstract

The report includes an overview of the scientific literature and an analysis focusing on the theoretical aspects of frost heave, as well as on a comparison of currently applied soil testing standards and methods for assessing the impact of soil freezing and thaw. A general overview of Latvian climatic conditions is provided and data from road weather stations are analysed. The results are also represented visually on a map of Latvia.

In order to assess the frost heave properties of different soils typical for Latvia and to determine the crucial parameters, samples of different Latvia-specific soils were collected, covering as many soil types as possible. Laboratory tests were performed on the selected soils in order to determine the key properties and frost heave thereof.

When designing the monitoring programme, the potential use of satellite data for the monitoring of meteorological parameters on the roads was first analysed. The data did not appear to be accurate and detailed enough and consequently were not suitable for the road frost heave assessment needs.

Furthermore, evidence from other countries was reviewed regarding *in situ* measurements of frost depth and frost heave, as well as the relevant sensor types and installations for such measurements. It was found that frost heave *in situ* measurements on the roads are made on a very limited scale worldwide and that frost heave is mostly assessed using indirect calculation methods. Consequently, no widely accepted and standardized measurement instruments are available on the market.

Possible soil temperature, moisture and frost heave *in situ* monitoring station network site locations in Latvia are proposed, along with sensor characteristics, equipment and measurement methodology. The potential associated costs are also assessed.

Pielietojums/pētījuma sfēra	Ceļu projektēšana
Papildus izstrādātie materiāli	-

CONTENTS

DARBA UZDEVUMS
Pētījumam

Grunšu sala pacēluma īpašību novērtēšana ceļu segas projektēšanas vajadzībām

PAMATOJUMS

Projektējot zemes klātni un ceļa segu, ļoti liela nozīme projekta risinājuma izstrādē ir sasaluma/atkusuma un gruntsūdens līmeņu izmaiņu noteikšanai. Sasaluma dziļums ietekmē kā tiek projektēti un būvēti infrastruktūras objekti, ieskaitot ceļa segas, tiltu un ēku pamatus un apakšzemes inženierkomunikācijas. Sala ietekme šādās būvēs tiek novērsta būvējot pamatus zem sasaluma dziļuma robežas. Ceļu būvē, izbūvējot ceļa segas pamatus, lai mazinātu sala radīto iedarbību uz konstruktīvajām kārtām, parasti tiek izmantota nekūkumojoša grunts.

Viena no nozīmīgākajām sala izraisītām problēmām ir zemes klātnes grunts nespējas zudums, ko izraisa sasaluma/atkusuma režīma cikliskā ietekme. Tādēļ dati par sasaluma dziļumu ir nepieciešami, lai noteiktu un prognozētu sasalšanas/atkušanas ietekmi uz ceļa konstruktīvajiem slāņiem. Pašreiz pieejamā grunts sasaluma dziļuma grafiskā karte nesniedz precīzu informāciju par sasaluma dziļumu ceļa konstrukcijā, jo konstruktīvo slāņu blīvums ir lielāks nekā gruntīs, tādēļ iespējama dziļāka sala ietekme.

Cita ar sasalumu saistīta mehāniska parādība ir sala pacēlums, kas veidojas palielinoties grunts tilpumam, sasalstot tajā esošajam ūdenim, un pie nevienmērīgas izplešanās tas var novest pie ceļa segas sabrukuma. Šobrīd autoceļu ģeotehniskajā izpētē sasaluma režīms, grunšu sala pacēlums un mitruma apstākļi tiek pieņemti, izmantojot no dažādiem literatūras avotiem iegūtu informāciju, kas nav aprobēta vai identificēta ar konkrēti Latvijas apstākļos sastopamajām gruntīm un lokālo klimatisko u.c. faktoru iedarbību uz tām.

MĒRĶIS

Veikt literatūras apskatu par grunšu sala pacēluma un sasaluma dziļuma noteikšanas metodēm, piedāvāt potenciālas sasaluma dziļuma ilgtermiņa novērojumu staciju ierīkošanas vietas un salīdzināt laboratorijas apstākļos Latvijā raksturīgāko grunšu īpašības sala ietekmē. Nepieciešams veikt pieejamo tehnoloģisko aprīkojumu salīdzinājumu, ilgtermiņa stacionāriem sasaluma dziļuma novērojumiem, šī pētījuma iespējamajām tālākajām kārtām, gan tehniskajā, gan finansiālajā, gan ģeogrāfiskās pieejamības ziņā.

DARBA SATURS UN METODIKA

1. Ceļa segas sala pacēluma un zemes klātnes sasaluma dziļuma izpētei un monitoringa staciju aprīkojuma izvēlei veicamie darbi:
   1.1. Literatūras apskats, aprakstot ceļa konstrukcijas sasaluma dziļuma ietekmējošos faktorus (piem. gruntsūdens līmenis, vietējie klimatiskie apstākļi, sasaluma periods, temperatūras svārstības, ūdens pieplūdes iespējamība, hidrauliskais spiediens utt.)

1.2. Ārvalstu literatūras un pieredzes apkopojums par sasaluma dziļuma un sasaluma/atkusuma ciklu noteikšanas metodoloģiju, sagaidāmo iegūstamo informāciju un potenciālajām problēmām.

1.3. Kartogrāfiskā materiāla sagatavošana – vispārīgā ģeoloģiskā situācija (sala ietekmes dziļuma) un gaisa temperatūru u.c. ietekmējošo klimata faktoru faktisko novērojumu karšu izveidei. Mērķis – mērījumu staciju izveides vietu izvēlei. Kartogrāfiskais attēlojums (areāls LR teritorija un piegulošie areāli, ja ir pieejama novērojumu informācija):

- ģeoloģiskās virsmas (kvartārģeologiskā, kvartāra nogulumu biezuma, noteiktām ģeogrāfiskām vietām pirmskvartāra) karte ar Latvijas Valsts ceļu (LVC) pārvaldībā esošo ceļu un lielāko pilsētu attēlojumu;
- pēdējās desmitgades (vai cita, pēc Izpildītāja ieskatiem raksturīga laika perioda) minimālo temperatūru karte (ar ilglaicību) apvienojumā ar LVC pārvaldībā esošo ceļu un lielāko pilsētu attēlojumu;
- pieejamie (pirms šī pētījuma) sasaluma dziļuma dati apvienojumā ar LVC pārvaldībā esošo ceļu un lielāko pilsētu attēlojumu;
- jebkura veida citas kartes, kas nepieciešamas vai uzskatāmas par lietderīgām darbu uzdevuma izpildei.

1.4. Mērījumu staciju uzstādīšanas iespējamo vietu identificēšana, izvēloties tās dažādos Latvijas reģionos ar atšķirīgiem grunts tipiem, mitruma un temperatūras režīma apstākļiem.

1.5. Pētījuma uzdevumam atbilstošu dažādu sasaluma/atkusuma sensoru (monitoringa stacijas) identificēšana un informācijas (tehniskās un finansiālās) salīdzināšana par tiem.

1.6. Izpēte par sensoru un citu mērierīču efektīvāko izvietojumu ceļa konstrukcijā un zemes klātnē. Jādefinē nepieciešamais sensoru izvietošanas solis un dziļums.

1.7. Izmaksu aprēķina veikšana sensoru izvietošanai, uzturēšanai un datu monitoringam (datu analīzei) nākamajām pētījuma kārtām. Balstoties uz aprēķinu, jāpiedāvā optimālais izbūvējamo mērījumu staciju skaits.

1.8. Vispārīgas grunts sasaluma monitoringa programmas izstrāde, kas ietver ieteicamos novērojuma nolasīšanas laikus un intervālus, datu apstrādes principus un vērtējamos parametrus, saistīto novērojumu veidus un biežumus.

2. Grunts sastāva un parametru precizēšana sasaluma dziļuma un sasaluma/atkusuma izpētes datu interpretācijai:

2.1. Grunts paraugu noņemšana un testēšana laboratorijā (aptuveni 10 dažāda tipa gruntis). No katra viendabīgā slāņa (ģeotehniskā elementa) paraugs jātestē vismaz 3 dažādos mitruma saturos. Interpretējot testēšanas izpētes datus, lai sasniegtu pētījuma mērķus, nepieciešamības gadījumā testējamo īpašību veids un apjoms var tikt arī mainīts vai papildināts esošā līguma darba pozīciju ietvaros;

2.2. Grunšu klasifikācijas (DIN18196; ISO 14688; GOST 25100) un raksturlielumu noteikšana, veicot vismaz sekojošus laboratoriskos testus:

- Granulometriskais sastāvs saskaņā ar LVS EN 933-1 un LVS CEN ISO/TS 17892-4;
- smalko (māla) daļiņu saturs (< 0,02mm);

- Plasticitātes rādītāji saskaņā ar LVS CEN ISO/TS 17892-12 (mālainām gruntīm);
- Dabiskais mitrums saskaņā ar LVS CEN ISO/TS 17892-1;
- Dabiskais blīvums saskaņā ar LVS CEN ISO/TS 17892-2;
- Grunts daļiņu blīvums LVS CEN ISO/TS 17892-3;
- Siltumvadītspēja;
- Elektrovadītspēja;
- Filtrācijas koeficients saskaņā ar *Ceļu specifikācijas 2017* p.12.3 (smilšainām gruntīm);
- Ķīmiskā analīze;
- Organisko vielu saturs saskaņā ar *Ceļu specifikācijas 2017* p.12.5 (pēc nepieciešamības).

2.3. Atlasīto grunšu sala pacēluma īpašību testēšana laboratorijā. Izvēlētos materiālus sagatavot ar dažādu mitruma saturu, tiem testēt:

- Proktora tilpumsvars un optimālais mitrums;
- Tūlītējās nespējas indekss (TNI) (3 dažādi mitruma saturi);
- Kalifornijas nespējas rādītājs (CBR) (3 dažādi mitruma saturi);
- elastības modulis – VSN 46-83 (3 dažādi mitruma saturi);
- sala pacēlums (3 cikli):
  - gruntij optimālajā mitrumā pie 100 % sablīvējuma;
  - gruntij ar virs optimālā mitruma satura palielinātu mitrumu, pie sablīvējuma ap 90 % - 95 %;
  - gruntij ar zem optimālā mitruma satura samazinātu mitrumu, pie sablīvējuma ap 90 % - 95 %;

DARBA IZPILDES TERMIŅI

N.p.k	Izstrādātā pētniecības projekta pozīcija	Izpildes termiņi	Procenti no kopējā finansējuma
1.	1. starpziņojums	12. novembris 2018.	60%
2.	Gala atskaite	18. marts 2019.	40%

Pirmais starpziņojums par izpildītiem darbiem (Darba uzdevuma Darba satura nodaļas 1.1; 1.2; 1.3; 1.5. un 1.7. punktus) jāiesniedz ne vēlāk kā līdz 2018. gada 12. novembrim.

Atskaite par visa pētniecības darba (ieskaitot Darba uzdevuma Darba satura nodaļas 1.4; 1.6; 1.7. un 1.8. punktus) jāiesniedz ne vēlāk kā līdz 2019. gada 18. martam.

PĒTĪJUMA REZULTĀTI

Ieteikumi sasaluma dziļuma staciju izvietošanai Latvijas teritorijā, to tehniskajam aprīkojumam un izbūves metodikai.

Novērojumu staciju izbūves izmaksu tāme un uzturēšanas izmaksu aplēse datu monitoringa periodam.

Ieteikumi par nepieciešamo datu apjomu (datu nolasīšanas biežums un daudzums) sasaluma dziļuma mērījumu analīzei un interpretācijai.

Atskaite ar testēšanas rezultātiem, to analīze, secinājumi un ieteikumi tālākiem pētījumiem.

DARBA NOFORMĒJUMS UN PIELIKUMI

Darbs izpildāms angļu valodā ar kopsavilkumu latviešu valodā.

Izpildītājam darba programmas, to izmaiņas un papildinājumi, starpziņojumi un gala ziņojums jāsagatavo 1 eksemplārā uz A4 formāta lapām un elektroniski MS Word vai ar to savietojamā formātā. Burtu lielums ir 12 punkti, fonts – Times New Roman, nodaļu virsrakstu burtu lielums – 14 punkti, atstarpe starp rindām – 1,5. Jāievēro atkāpes no lapas malām: 30 mm – no kreisās puses, 20 mm – no labās puses un 20 mm – no augšas un apakšas. Katrai nodaļai jāsākas jaunā lappusē. Lappuse nedrīkst beigties ar virsrakstu. Nodaļu virsrakstus raksta ar lielajiem burtiem, bet apakšnodaļu virsrakstus – ar mazajiem burtiem treknrakstā (Bold). Virsrakstu rakstīšanai ir ieteicams lietot MS Word stilus (Heading).

Iesniegtā dokumentācija jānoformē ar titullapu un satura rādītāju. Satura rādītāju ieteicams veidot automātiskā režīmā, balstoties uz virsrakstu (*Heading*) stiliem, lai pārveidojot teksta izvietojumu vai garumu, automātiski tiktu pārveidots arī satura radītājs. Aiz titullapas jāpievieno Darba kopsavilkums latviešu un angļu valodās.

Ja Darbā kāds no literatūras avotiem tiek izmantots būtiskas Darba sastāvdaļas radīšanai, šāda avota kopija vai oriģināls jānodod pasūtītājam, ievērojot izmantotās literatūras avota autortiesības.

Pasūtītājs	**Izpildītājs**
VAS „Latvijas Valsts ceļi"	SIA „Vides eksperti"
valdes priekšsēdētājs	valdes priekšsēdētājs
Jānis Lange	Ivars Pavasars

INTRODUCTION

This is the final report of the study carried out jointly by SIA “Vides eksperti”, University of Latvia and SIA “Ceļu eksperts” as ordered by the VAS “Latvijas Valsts ceļi” (Latvian State Roads) under the contract of July 7, 2018, No. LVC2018/1.10/1/AC.

When designing earthworks and road overlays, identifying ground freeze/thaw and groundwater level changes are essential in project solution development. The frost depth influences the way infrastructure objects such as road overlays, bridges, building foundations and underground utilities are designed and constructed. The impact of frost on such structures is mitigated by constructing the foundation below the frost depth mark. In road construction, frost-susceptible soil is usually used when building the road overlay foundation, in order to reduce the frost effect on the construction layers.

One of the most pronounced issues caused by frost is a loss of earthwork soil load carrying capacity, caused by the cyclical impact of the freeze/thaw regime. Therefore, frost depth data are required in order to identify and forecast the freeze/thaw impact on road construction layers. The currently available soil frost depth map does not provide accurate information on the frost depth for road construction, as the construction layer density is higher than soil density, thus a deeper frost effect is possible.

Another mechanical phenomenon related to freezing is frost heave, caused when the soil volume increases when the water it contains freezes. If the expansion is uneven this can lead to earthwork collapse. Currently, in geo-technical research, the frost regime, soil frost heave and humidity conditions are assumed using information obtained from various literature sources, which is neither approved for nor identified with the soils present in Latvia and the effect of the local climatic and other factors on the soil

There are numerous standards (BS 812-124, ASTM D5918-13 and GOST 28622-2012) that describe field and laboratory tests that must be carried out to determine frost influence of particular soils.

Nonetheless, there is still a wide range of problems that are associated with frost heave that needs more investigations and testing to be fully understood. Many of obtained equations are empirical and many classifications are based on visual inspections of soil that are carried out on the field. For many coefficients that are included in equations precise values are hard to determine. As a result, despite a wide range of literature that is devoted to the subject of frozen ground, site-specific studies and laboratory investigations should be carried out.

Consequently, the objective of the study in question was to perform an overview of literature sources regarding soil frost heave and frost depth identification methods, offer potential locations for establishing long-term frost depth observation stations and compare properties of the soils most characteristic to Latvia under frost effect in laboratory conditions. A comparison of the available technological equipment in terms of technical, financial and geographical availability is required for stationary long-term frost depth observations and possible future phases of this research.

1. FROZEN GROUND

Frozen ground and permafrost has been studied since first human settlements in regions located close to Earth poles. There are numerous publications that deal with frozen ground engineering and permafrost in general (Harries et. al., 2017; Carter and Bentley, 2016; Anderson and Laddanyi, 2003; Anderson and Laddanyi, 1994; etc.). Some of those publications cover wide aspects of ground and soil mechanical properties from that one is frost heave and influence of temperature variations on soil properties. Some publications are devoted exclusively to frost actions.

1.1. Defining frozen soil and regions where it can appear

Cold regions of the world may be defined in terms of air temperatures, snow depth, ice cover on lakes, or depth of ground freezing. Temperature and frost penetration are of greatest importance to frozen ground engineering. The isotherm for 0°C means temperature during the coldest month of the year has been used to define the southern limit of the cold regions in the northern hemisphere (Bates and Bilello 1966). An arbitrarily selected depth of seasonal frost penetration (300 mm) into the ground once in 10 years is a generally accepted criterion for identification of the southern boundary of cold regions. This boundary is similar to that defined by the 0°C isotherm and with minor exceptions is approximated by the 40^{th} parallel.

Since the actual observations on the distribution and depth of frozen soil are scarce, and since the freezing temperature of soils varies through several degrees depending on the mineral, organic, and water content, use of the 300-mm depth requires the estimation of frost penetration on the basis of a freezing index derived from meteorological data.

This application of the freezing index is complicated by many factors, including mineral and textural composition of the soil and the insulation effect of vegetation and snow cover. It is possible that some areas excluded by this definition can occasionally experience frost problems. For these areas local meteorological and soil data can be used to provide accurate information on frost penetration for a given site.

Frozen ground is defined as soil or rock having a temperature below 0°C. The definition is based solely on temperature, recognizing that the water-ice phase composition of the soil or rock will vary with particle mineral composition, specific surface area of the particles, the presence of solutes, and temperature.

Frozen soil is a four-component system consisting of soil particles, ice, water, and air. The particles (mineral and/or organic matter) come in various sizes and shapes with a thin film of unfrozen water coating most mineral grains.

The top layer of ground in which temperature fluctuates above and below 0°C during the year is defined as the active layer (Figure 1.1). The climatic factors responsible for ground surface temperature variations include surface radiation, convective heat flow, and evaporation and condensation. Terms such as seasonally frozen ground, seasonal frost, and annually thawed layer are sometimes used as synonyms for the active layer. Its thickness depends on many factors, including the severity of winter temperatures (freezing index), soil and rock type, ground moisture content, snow cover, surface vegetation, drainage, and the degree and orientation of slopes.

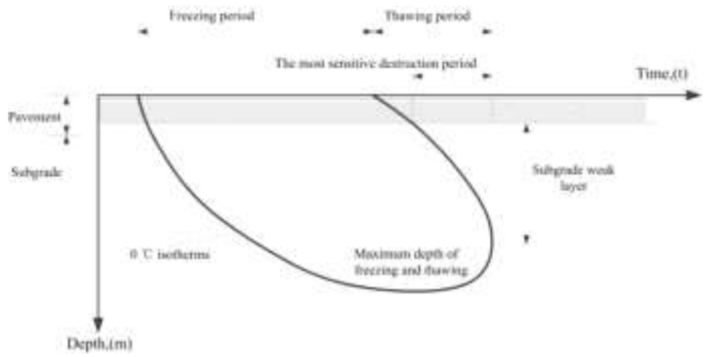

Figure 1.1. Freezing pattern of road pavement (Andersland O.B., Ladanyi, B. 1994).

The geothermal gradient will vary between 0.3 and 1.1°C per 30 m of depth as shown by field temperature measurements at various locations (W.G. Brown, 1963). Because of it at about 9 to 15 m, the temperature remains approximately constant throughout the year.

1.2. Soil temperature profile and frost penetration depth

Ground temperatures are determined by air (or ground surface) temperatures, heat flow from the interior of the earth, and soil thermal properties. Surface temperatures undergo approximately simple periodic fluctuations on both a daily and an annual cycle (Figure 1.2.).

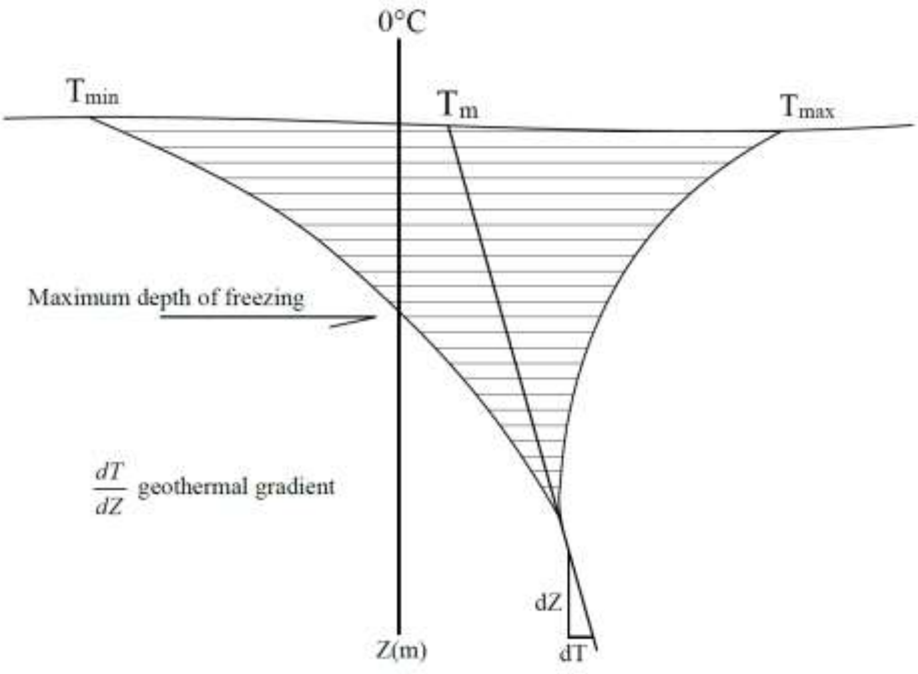

Figure 1.2. Annual changes of surface and ground temperature. Legend: T_m – the mean annual air temperature, T_{min} – annual minimum air temperature, T_{max} – annual maximum air temperature.

This temperature pattern is attenuated with depth and, in a homogeneous soil with no change of state and where heat flow from the interior of the Earth is assumed to be negligible, the temperature at any depth and time can be calculated with equation 1.1.

$$T_{z,t} = T_m + A_s \exp\left(-z\sqrt{\frac{\pi}{\alpha_u p}}\right)\sin\left(\frac{2\pi t}{p} - z\sqrt{\frac{\pi}{\alpha_u p}}\right) \tag{1.1}$$

T_m – the mean annual air temperature (°C);

A_s – surface temperature amplitude (°C);

$T_{z,t}$ – Soil temperature (°C);

p – interval (24h or 365 days);

t – time (day);

z – depth (m);

α_u – soil thermal diffusivity (m^2/day).

Annual minimum soil temperature at any depth can be calculated with equation 1.2.

$$T_z = T_m - A_s \exp\left(-z\sqrt{\frac{\pi}{\alpha_u p}}\right) \quad (1.2)$$

T_m – the mean annual air temperature (°C);

A_s – surface temperature amplitude (°C);

T_z – Soil temperature (°C);

p – interval (24h or 365 days);

t – time (days);

z – depth (m);

α_u – soil thermal diffusivity (m^2/days).

Maximum depth at that soil will freeze (temperature will fall below °C) can be calculated with equation 1.3.

$$z = -\frac{\ln\left(\frac{T_m}{A_s}\right)}{\sqrt{\frac{\pi}{\alpha_u p}}} \quad (1.3)$$

T_m – the mean annual air temperature (°C);

A_s – surface temperature amplitude (°C);

p – interval (24h or 365 days);

z – depth (m);

α_u – soil thermal diffusivity (m^2/days).

To accurately forecast frozen ground behavior not only temperature profile but also frost penetration depth needs to be determined. Solutions for frost depth penetration in non-uniform soils, typical for highway and foundation structures, generally utilize approximate computation techniques. Numerical methods may be adapted to model complex geometrical boundaries and time-dependent thermal properties. One of the Formulas for frost-depth penetration in multilayered soil systems is based on the modified Berggren equation developed by Aldrich and Paynter (1966) (Equation 1.4).

$$X = \lambda\left(172800\frac{kI_{sf}}{L}\right)^{\frac{1}{2}} \quad (1.4)$$

X – depth of frost penetration (m);

λ – correction coefficient (dimensionless);

k – soil thermal conductivity (J/(s*m*°C));

L – soil volumetric latent heat (MJ/m^3);

I_{sf} – the absolute value of surface freezing index (°C*days).

The dimensionless correction coefficient λ is given as a function of two dimensionless parameters (Equation 1.5 and 1.6; Figure 1.3).

$$\alpha = \frac{v_0 t}{I_{sf}} \tag{1.5}$$

$$\mu = \frac{c_v I_{sf}}{Lt} \tag{1.6}$$

α – thermal ratio (dimensionless);

t – duration of freezing period (days);

v_0 – water intake flux (mm/s);

I_{sf} – the absolute value of surface freezing index (°C*days);

μ – fusion parameter (dimensionless);

L – soil volumetric latent heat (MJ/m^3);

c_v – soil volumetric heat capacity (kJ/m^3).

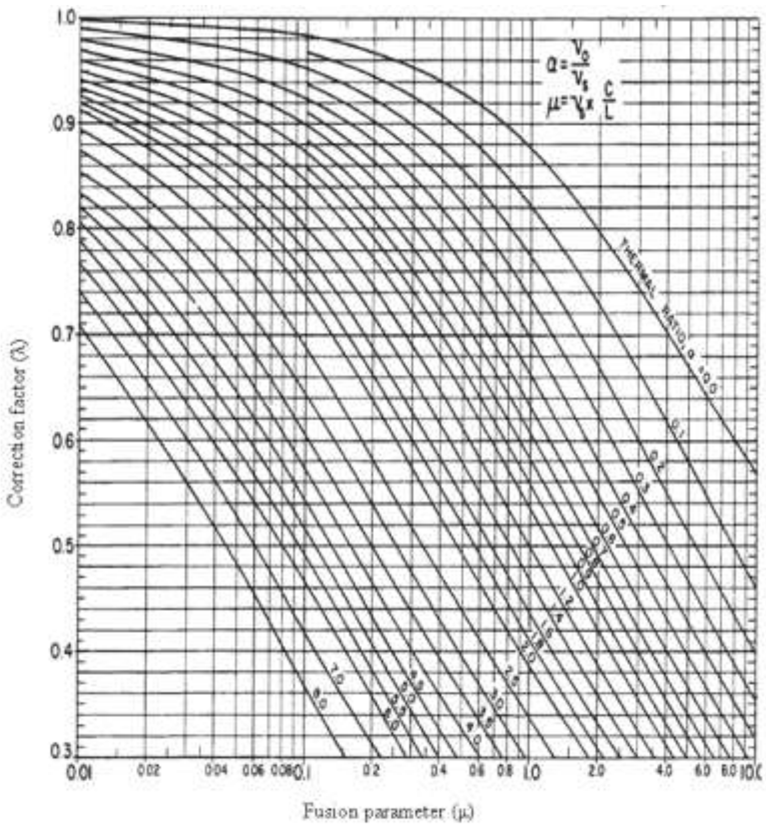

Figure 1.3. correction coefficient in the Berggren equation (Andersland O.B., Ladanyi, B. 1994).

1.3. Frost action process

Frost heave occur in places where significant ice buildup is present. To predict frost heave distribution and preconditions it is necessary to fully understand the freezing process in soil.

The general unsteady heat flow near the ground surface coupled with conditions of crystal ice nucleation and growth is the necessary condition for the formation of alternating bands of soil and ice. In addition, it is essential that the rate of heat extraction exceeds the rate of heat supply (mainly water flow) to the freezing front (Figure 1.4).

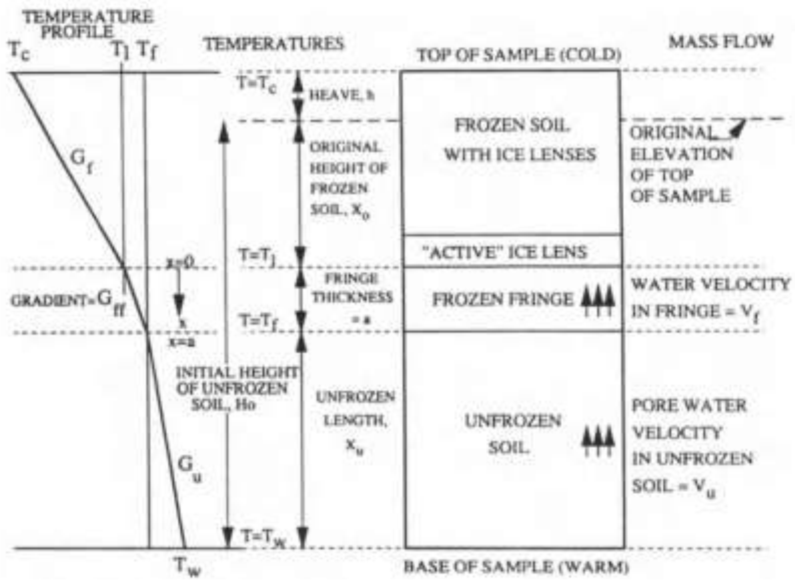

Figure 1.4. Frost heave in an idealized one-dimensional soil column (Andersland O.B., Ladanyi, B. 1994).

The fringe is a region of impeded flow caused by partial filling of soil pores by ice (Nixon, 1991). The soil skeleton, within the fringe, will expand when the pressure in the ice exceeds the overburden pressure plus any pressure required to initiate separation of the soil skeleton. With sufficient ice pressure, the soil skeleton separates and a new ice lens forms.

During slow freezing, near steady-state temperature profiles are maintained in the freezing fringe and unfrozen zones (Nixon, 1992). With a rapid advance of the frost front (unsteady heat flow) and a decrease in temperature, permeability of the frozen fringe will decrease, causing a reduction in the flow of water to the ice lens. This interrelation of heat and water flow results in finer ice lenses near the surface and thicker ice lenses at greater depth, where the temperature gradient is smaller.

The temperature curve (Figure 1.4) with different slopes shows the unsteady heat flow situation near the ground surface. The temperature gradients show the rate of heat extraction above the frost line to be greater than the rate of heat supply below the frost line (Equation 1.7).

$$G_f = \left.\frac{dT}{dz}\right|_f > G_u = \left.\frac{dT}{dz}\right|_u \qquad (1.7)$$

T – temperature (°C);

z – depth (m);

G_f – frozen conditions gradient (°C/m);

G_u – unfrozen state gradient (°C/m).

With ice forming, the volume of the soil-water system must increase. When water moves to the frost line and freezes, the volume increases more than that necessary for a change in density (water to ice). Frost heave occurs at the frost line with T≤0°C. Many developments (Konrad and Morgenstern, 1980; Nixon, 1991, 1992) indicate that the ice lens forms above the 0°C isotherm and that there is a frozen fringe between the ice lens and the unfrozen soil.

In the frozen fringe, liquid water exists in equilibrium with ice at a temperature below the normal freezing point of water with the segregation-freezing temperature located at the base of the growing ice lens. At the frost line, usually assumed to be at 0°C, a heat balance equation can be written (Equation 1.8).

$$k_f \left(\frac{dT}{dz} \right)_f - k_u \left(\frac{dT}{dz} \right)_u = q_z \qquad (1.8)$$

k_f – frozen soil thermal conductivity;

k_u – unfrozen soil thermal conductivity;

q_z – net heat flux.

The net heat flux q_z can freeze the in situ water and/or the water arriving at the frost line (Equation 1.9).

$$q_z = Ln \frac{dz}{dt} + Lv \qquad (1.9)$$

n – soil porosity;

L – the latent heat of the water;

dz/dt – the rate of frost-front advance;

v – the velocity of water arrival at the frost line.

Formation of ice at T<0°C. induces a pressure deficiency (suction gradient) across the frozen fringe and in the unfrozen soil below. The velocity of water flow is dependent on this pressure deficiency and the overall permeability of the unfrozen soil and frozen fringe in accordance with Darcy's law.

Heave results when the water freezes forming ice lenses. The heave rate can be expressed with equation 1.10 where the phase expansion is assumed to be 9%.

$$\frac{dh}{dt} = 1,09v + 0,09n\frac{dz}{dt} \qquad (1.10)$$

dh/dt – the heave advance rate;

dz/dt – the frost-front advance rate;

n – soil porosity;

v – the velocity of water arrival at the frost line.

Heave prediction requires a relation between the velocity of arriving water and the frost-front advance rate. Konrad and Morgenstern (1980) described the heat and mass transfer relationships involved in evaluating the velocity of arriving water and the frost-front advance rate relative to experimental studies on a Devon silt. There is evidence that an advancing frost front can establish a condition such that all heat extraction goes to growing an ice lens. Such a situation can be described using equations 1.11 and 1.12.

$$\frac{dz}{dt} = 0 \qquad (1.11)$$

$$q_z = Lv \qquad (1.12)$$

This condition requires a low rate of heat extraction, a readily available water supply, and a highly frost susceptible soil. This upper-bound approach to frost heave prediction appears to be justified for some design conditions in highly frost susceptible soils.

1.4. Soil thermal properties

1.4.1. Thermal conductivity

Heat conduction in soils involves a transfer of kinetic energy from molecules of a warm part of the mass to those in a cooler part. The amount of heat transferred by conduction in soil increases as dry density increases and as its degree of saturation increases. Thermal conductivities of some of the soil constituents are given in table 1.1. Volumetric proportions of the various soil constituents will influence the effective soil thermal conductivity.

Table 1.1. Thermal properties of various materials (Andersland O.B., Ladanyi, B. 1994).

Material	Density (kg/m^3)	Heat capacity (kJ/(kg°C))	Thermal conductivity (W/(m*K))
Air (10°C)	1,25	1,00	0,026
Snow, loose	85	2,09	0,08
Snow, compacted	500	2,09	0,7
Ice (-40°C)	900	2,09	2,66
Ice (0°C)	900	2,09	2,21
Water (0°C)	999,87	4,2177	0,56
Water (10°C)	999,73	4,1922	0,58
Peat, dry	250	2,09	0,07
Clay, dry	1700	0,92	0,9
Sand, dry	2000	0,80	1,1
Concrete, asphalt	2150	-	1,28
Rock, typical	2500	0,84	2,2
Quartz	2660	0,733	8,4
Granite	-	-	1,7-4,0
Shale	-	-	1,5

Various methods for calculating the thermal conductivity of soils have been reviewed by Farouki (1981). Johansen's (1975) method generally gives the best results for unfrozen and frozen soils, coarse or fine, at degrees of saturation above 0.1 (equation 1.13).

$$k_u = \left(k_{sat} - k_{dry}\right) K_e + k_{dry} \qquad (1.13)$$

k_{sat} – saturated thermal conductivity;

k_{dry} – dry thermal conductivity;

K_e – Kersten number.

For all types of frozen soil Kersten number is equal to saturation (S_r (Volume %)). For dry natural soils, Johansen (1975) developed semiempirical (equation 1.14). He also observed that crushed rocks give higher values (equation 1.15).

$$k_{dry} = \frac{0,137\rho_d + 64,7}{2700 - 0,947\rho_d} \pm 20\% \qquad (1.14)$$

$$k_{dry} = 0,039n^{-2,2} \pm 25\% \qquad (1.15)$$

k_{dry} – dry thermal conductivity(W/(m*K));
ρ_d – dry density (kg/(m^3));
n – soil porosity.

For saturated soils, Johansen (1975) observed that variations in microstructure had little effect on thermal conductivity. He proposed these of a geometric mean equation based on thermal conductivities of the soil constituents and their respective volume fractions. For saturated frozen soils containing some unfrozen water equation, 1.16 can be used.

$$k_{sat} = k_s^{1-n} k_i^{n-w_u} k_w^{w_u} \qquad (1.16)$$

k_{sat} – saturated thermal conductivity (W/(m*K));
k_i – thermal conductivity of ice (2,2 W/(m*K));
k_w – thermal conductivity of water (0,57 W/(m*K));
k_s – thermal conductivity of solid phase (W/(m*K));
w_u – volumetric fraction of unfrozen water;
n – porosity.

Johansen (1975) suggested the use of a geometric mean equation to determine k (Equation 1.17), where k_q and k_o are the thermal conductivities of quartz and other minerals, respectively, and q is the quartz fraction of the total solids content. Johansen (1975) used k_q = 7.7 W 1m· K and k_o = 2.0 W 1m· K. For coarse-grained soils with a quartz content of less than 20%, Johansen (1975) used k_o = 3.0 W 1m. K to account for the probable mineral composition of such soils.

$$k_s = k_q^q k_o^{1-q} \qquad (1.17)$$

k_s - thermal conductivity of solid phase (W/(m*K));
k_q - thermal conductivity of quartz (W/(m*K));

k_o – thermal conductivity of other minerals (W/(m*K));
q – fraction of solid phase.

Johansen's (1975) method for computation of the soil thermal conductivity is a technique for interpolation between dry and saturated values. It does not take into account possible moisture migration at intermediate degrees of saturation.

Natural soils will vary in composition over relatively short distances; hence average thermal conductivities are appropriate for many thermal problems. General usage describes soils in terms of cohesionless materials (sands and gravels), fine-grained soils (silts and clays), and highly organic soils (peat).

1.4.2. Heat capacity

The heat capacity* [(J/g)/DC] of a soil sample is the amount of heat required to raise its temperature 1 degree. The specific heat of a material is defined as the ratio of its heat capacity to that of water, measured in the same units. Soil consists of various constituents, including solids, water, ice (if frozen), and air. The heat capacity of the soil can be computed by adding the heat capacities of the different constituents in a unit mass of soil (equation 1.18 and 1.19).

$$c_v = \rho_d \left(c_s + c_w w_u + c_i w_i \right) \tag{1.18}$$

c_v – volumetric heat capacity of frozen soil (MJ/(m3*°C));
ρ_d – dry phase density (kg/m^3);
c_s – heat capacity of solids (J/(g*°C));
c_w – heat capacity of water (J/(g*°C));
c_i – heat capacity of ice (J/(g*°C));
w_u – unfrozen water content;
w_i – frozen water content.

$$c_m = \frac{c_v}{\rho} \tag{1.19}$$

c_m – mass heat capacity ();
c_v – volumetric heat capacity of frozen soil (MJ/(m3*°C));
ρ – total soil density (kg/m^3).

1.4.3. Soil latent heat

The amount of heat energy absorbed when a unit mass of ice is converted into a liquid at the melting point is defined as its latent heat of fusion. For soils, the total energy involved in the phase change process will depend on the total water contained in a given soil volume and the fraction of this water that changes phase (equation 1.20).

$$L = \rho_d L' \frac{w - w_u}{100} \tag{1.20}$$

L – soil volumetric latent heat of fusion (kJ/m^3);
ρ_d – dry soil density (kg/m^3);
L' – the mass latent heat for water (kJ/kg);
w – total water content (% dry mass basis);
w_u – unfrozen water content (% dry mass basis).

For those soils (sands and gravels) with little or no unfrozen water, the *Wu* term will be very small. For many practical problems, the assumption that *Wu* is zero will give acceptable *L* values for estimation purposes.

1.4.4. Thermal diffusivity.

The rate at which heat is transferred in a soil mass is dependent on the thermal conductivity. The rise in temperature that this heat will produce will vary with the heat capacity and the bulk density of the soil mass. The ratio of these quantities is defined as the soil thermal diffusivity (equation 1.21).

$$\alpha_u = \frac{k}{c\rho} \tag{1.21}$$

α_u – thermal diffusivity (m^2/s);
k – thermal conductivity (W/(m*°C));
c – heat capacity (kJ/(kg*°C));
ρ – density (kg/m^3).

1.4.5. Air and surface freezing index

Ground surface temperatures are generally not available for most locations; hence air temperatures are used. The index determined for air temperatures measured at 1.5 m above ground is commonly designated as the air freezing index.

The index is a measure of the combined duration and magnitude of below-freezing temperatures occurring during any given season. The usual design index is defined as the average air freezing index of the three coldest winters in the latest 30 years of record. If 30 years of record are not available, the index for the coldest winter in the latest 10-year period may be used. Over one season, the air freezing index (I_{af}) is the number of negatives ($T < 0°C$) degree-days between the highest and lowest points on a curve of cumulative degree-days versus time.

Mean annual ground surface temperatures (1 cm depth) differ from mean annual air temperatures with no constant difference between them (Brown, 1963). Some factors accounting for this difference include net radiation, vegetation, snow cover, ground thermal properties, surface relief, and subsurface drainage. The surface freezing index is calculated using air freezing index and dimensionless factor (equation 1.22). Calculations by using this dimensionless factor are regarded as a simplification of the real situation.

$$I_{sf} = n_f I_{af} \tag{1.22}$$

I_{sf} – surface freezing index (°C*days);

n_f – empirically determined factor (Table 1.2);

I_{af} – air freezing index (°C*days).

Table 1.2. Examples of n factor (Andersland O.B., Ladanyi, B. 1994).

Surface	n_f
Snow	1
Pavement free of snow and ice	0,9
Sand and gravel	0,9
Turf	0,5
Mineral soil surface (Vegetation and 6 cm soil stripped)	0,33
Gravel	0,6-1,0
Asphalt pavement	0,29-1
Concrete pavement	0,25-0,95

1.5. Description and classification of frozen soils

Different terms are used in conjunction with the description of frozen ground areas (table 1.3. and figure 1.5.) The system for describing and classifying frozen soil involves three parts. In part 1 the soil phase is identified independently of the frozen state using the Unified Soil Classification System. Part 2 involves adding characteristics resulting from the frozen state to the soil description. In part 3, ice strata found in the soil are described. This approach provides a frozen soil description and classification that is independent of the geologic history and mode of origin and is flexible enough to provide any desired degree of detail.

Table 1.3. Used terms for description of frozen ground areas (D4083-89).

Term	**Definition**
Annual frost zone (active layer)	The top layer of the ground subject to annual freezing and thawing.
Frost table	The frozen surface, usually irregular, that represents the level, to which thawing of seasonally frozen ground has penetrated.
Frozen zone	A range of depth within which the soil is frozen. The frozen zone may be bounded both top and bottom by unfrozen soil, or at the top by the ground surface.
Ground ice	A body of more or less clear ice within frozen ground.
Ice wedge	A wedge-shaped mass in permafrost, usually associated with fissures in polygons.
Icing	A surface ice mass formed by freezing of successive sheets of water.
Permafrost	The thermal condition in soil or rock, wherein the materials have existed at a temperature below 0°C continuously for a number of years. Pore fluids or ice may or may not be present.
Permafrost table	The surface that represents the upper limit of permafrost.

Polygons (polygonal ground)	More or less regularized surface patterns created by thermal contraction of the ground. Two types are common: (*a*) those with depressed centres and (*b*) those with raised centres.
Residual thaw zone	A layer of unfrozen ground between the permafrost and the annual frost zone. This layer does not exist where annual frost extends to permafrost.

Examination of the frozen samples starts with the identification of one of the main groups to that the sample belongs: soils in which segregated ice is not visible to the unaided eye (designation N) and soils in which segregated ice is visible (designation V). Further classification proceeds as described in table 1.4. Visual examples of soil samples are shown in figure 1.6.

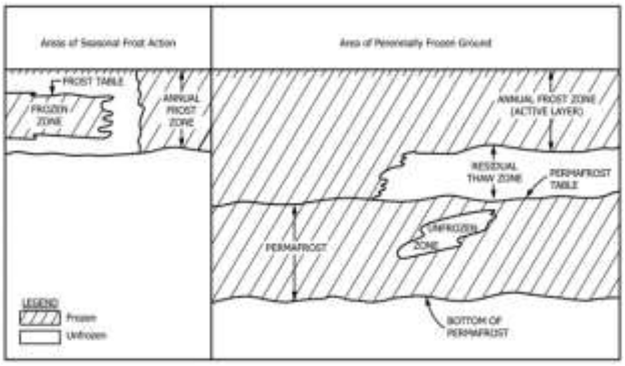

Figure 1.5. Illustration of frozen soil terminology (D4083-89).

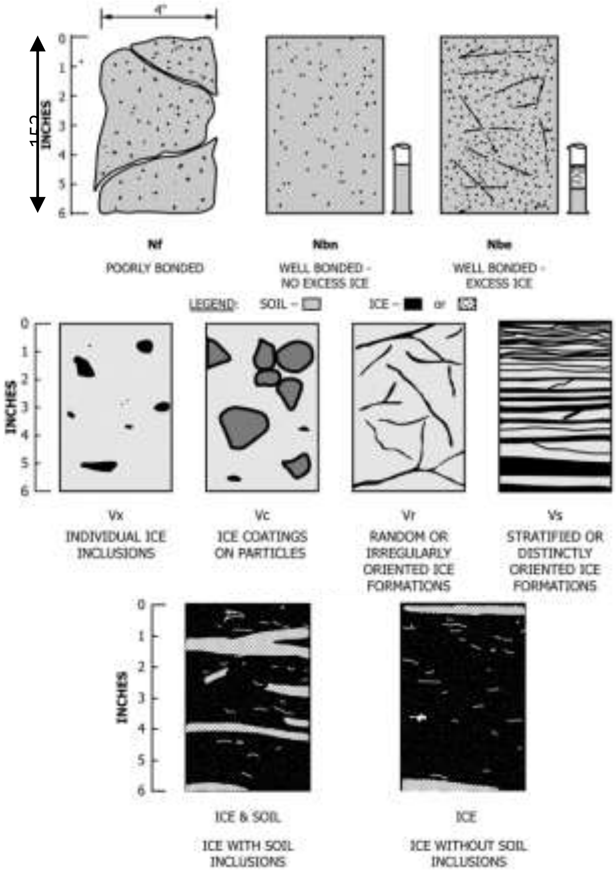

Figure 1.6. Ice inclusions in frozen soil classified using table 1.4.

Table 1.4. Description and classification of frozen soils[a] (Linnell and Kaplar 1966).

<table>
<tr><td>Part I: Description of soil phase (independent of frozen state)</td><td colspan="7">Classify soil phase by the Unified Soil Classification System</td></tr>
<tr><td rowspan="9">(1)
Part II: Description of Frozen soil</td><td colspan="2">Major group</td><td colspan="3">Subgroup</td><td rowspan="2">Field identification (6)</td><td rowspan="2">Pertinent properties of frozen materials which may be measured by physical tests to supplement Field identification (7)</td></tr>
<tr><td>Description (2)</td><td>Designation (3)</td><td>Description (4)</td><td colspan="2">Designation (5)</td></tr>
<tr><td rowspan="3">Segregated ice is not visible by eye[c]</td><td rowspan="3">N</td><td>Poorly bonded or friable</td><td colspan="2">Nf</td><td rowspan="3">Identify by visual examination. To determine presence of excess ice, use procedure under footnote d and hand magnifying lens as necessary For soils no fully saturated, estimate degree of ice saturation: medium, low. Note presence of crystals, or ice coatings around larger particles</td><td rowspan="7">In-place temperature
Density and void ratio
a. In frozen state
b. After thawing in place

Water content (total H_2O, Including ice)
a. Average
b. Distribution

Strength
a. Compressive
b. Tensile
c. Shear
d. Adfreeze
Elastic properties
Plastic properties
Thermal properties

Ice crystal structure (using optical instruments)
a. Orientation of axes
b. Crystal size
c. Crystal shape</td></tr>
<tr><td rowspan="2">No excess ice</td><td rowspan="2">Nb</td><td>n</td></tr>
<tr><td>e</td></tr>
<tr><td rowspan="4">Segregated ice is visible by eye (ice 1 in. or less in thickness)[c]</td><td rowspan="4">V</td><td>Individual ice crystals or inclusions</td><td colspan="2">Vx</td><td rowspan="4">For ice phase, record the following as applicable: Location, Size, Orientation, Shape, Thickness, Pattern of arrangement, Length, Spacing (Hardness, Structure and Colour per part III below)</td></tr>
<tr><td>Ice coatings on particles</td><td colspan="2">Vc</td></tr>
<tr><td>Random or irregularly oriented ice formations</td><td colspan="2">Vr</td></tr>
<tr><td>Stratified or distinctly</td><td colspan="2">Vs</td></tr>
</table>

			oriented ice formations		Estimate volume of visible segregated ice present as percent of total sample volume	d. Pattern of arrangement
Part III: Description of substantial ice strata	Ice (greater thatn 1 in. in thickness)	ICE	Ice with soil inclusions	ICE + soil type	Designated material as ICE[e] and use descriptive terms as fallows, usually one item from each group, as applicable: Hardness (Hard; soft; mass not individual crystals), Structure (clear; cloudy, porous, candled, granular, stratified), Color, Admixtures	Same as Part II, as applicable, with special emphasis on ice crystal structure
			Ice without soil inclusions	ICE		

[a] The following terms are used to describe the characteristics of the frozen earth: (next page):

Ice coatings on particles are discernible layers of ice found on or below the larger soil particles in a frozen soil mass. They are sometimes associated with hoarfrost crystals, which have grown into voids produced by the freezing action.

Ice crystal is a very small individual ice particle visible in the face of a soil mass. Crystals may be present alone or in a combination with other ice formations.

Clear ice is transparent and contains only a moderate number of air bubbles (see footnote f).

Cloudy ice is translucent but essentially sound and non-pervious (see footnote f).

Porous ice contains numerous voids, usually interconnected and usually resulting from melting at air bubbles or along crystal interfaces from the presence of salt or other materials in the water, or from the freezing of saturated snow. Although porous, the mass retains its structural unity.

Candled ice is ice that has rotted or otherwise formed into long columnar crystals, very loosely bonded together.

Granular ice is composed of course, more or less equidimensional ice crystals weakly bonded together.

Ice lenses are lenticular ice formations in soil occurring essentially parallel to each other, generally normal to the direction of heat loss and commonly in repeated layers.

Ice segregation is the growth of ice as distinct lenses, layers, veins, and masses in soils, commonly but not always oriented normal to direction of heat loss.

Well-bonded signifies that the soil particles arc strongly held together by the ice and that the frozen soil possesses relatively high resistance to chipping or breaking.

Poorly bonded signifies that the soil particles are weakly held together by the ice and that the frozen soil consequently has poor resistance to chipping or breaking.

Friable denotes a condition in which material is easily broken up under light to moderate pressure.

Notes:

[b]When rock is encountered, standard rock classification terminology should be used.

[c]Frozen soils in the N group may, on close examination, indicate the presence of ice within the voids of the material by crystalline reflections or by a sheen on fractured or trimmed surfaces. However, the impression to the unaided eye is that none of the frozen water occupies space in excess of the original voids in the soil. The opposite is true of frozen soils in the V group.

[d]When visual methods may be inadequate, a simple field test to aid evaluation of volume of excess ice can be made by placing some frozen soil in a small jar, allowing it to melt, and observing the quality of supernatant water as a percent of total volume.

[e]Where special forms of ice, such as hoarfrost, can be distinguished, more explicit description should be given.

[f]Observer should be careful to avoid being misled by surface scratches or frost coating on ice.

Frozen soil contains ice in several forms, ranging from coatings on individual soil particles and small lenses to large ice inclusions and massive ice deposits. For relatively low ice contents the ice may not be visible or will be revealed only by crystalline reflections on a fractured or trimmed surface. Frequently, for ice content evaluation, iceness ratio is used (Equation 1.23).

$$i_r = \frac{M_i}{M_w} = \frac{w - w_u}{w} \tag{1.23}$$

M_i – mass of ice;

M_w – total mass of water;

w – total water content;

w_u – unfrozen water content.

1.6. Factors that influence soil freezing

Factors necessary for frost action to occur include (1) the presence of frost-susceptible soil, (2) seasonal ground temperatures below O°C, and (3) a source of capillary water or groundwater sufficient to form and supply ice lenses forming in the freezing soil. To reduce or prevent the effects of frost action, one or more of these factors must be reduced or removed.

1.6.1. Temperature

Temperature significantly influences the freezing process of ground, as a result in every ground freezing study soil temperature must be measured.

Formation of ice in soil pores involves cooling of a soil-water system as illustrated in Figure 1.7. The pore water does not start to freeze until the temperature drops to T_{sc} The supercooled water is in a metastable equilibrium state until an abrupt transformation of free water to ice is triggered by nucleation centres. These nuclei can be aggregations of water molecules or soil particles. Formation of ice releases latent heat, causing a rise in temperature to T_f, the initial freezing temperature. For cohesionless soils with small specific surface areas, T_f will be close to 0°C. For fine-grained soils (silts and clays) the temperature depression (ΔT) can be as much as -5°C. Free water in the soil pores will now freeze at the temperature T_f. As free water changes to ice, release of latent heat will slow the rate of cooling until a temperature T_e is reached. All the free water and most of the bound water (unfrozen water film on the soil particles) is frozen at T_e (about - 70°C). A significant amount of unfrozen water can exist at higher temperatures for fine-grained soils with high-specific-surface areas.

The water-ice phase composition of the soil or rock will vary with particle mineral composition, the specific surface area of the particles, the presence of solutes, and temperature. Availability of a prediction equation for unfrozen water contents, an understanding of water-ice phase relationships, and information on the effect of solutes on freezing contribute to our knowledge of frozen soil behaviour relative to engineering construction problems.

Data reported by Anderson and Tice (1972) show that part of water remains unfrozen in the form of thin, liquid like layers on the particle surfaces. Current practice neglects the vapor phase and divides the total water content into two categories: unfrozen water and ice.

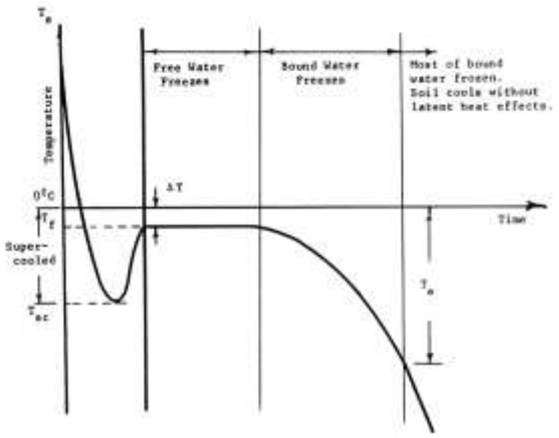

Figure 1.7. Soil temperature curve during freezing.

Tice, Anderson, and Banin (1976) have summarized experimental unfrozen water contents for several soils with varying total water contents and different physical properties. The experimental data have been represented by a simple equation 1.24. Parameters α and β are summarized in table 1.5.

$$w_u = \alpha\theta^{\beta} \tag{1.24}$$

W_u – soil water content (% of dry soil mass);

α, β – soil parameters;

θ – temperature (°C below 0 expressed as a positive term).

Table 1.5. Unfrozen water content parameters (Tice et. al., 1976).

Soil	Specific surface (m^2/g)	α	β
West Lebanon gravel	15	2,1	-0,408
Manchester silt	18	2,5	-0,515
Kaolinite	23	5,8	-0,864
Chena silt	40	3,2	-0,531
Leda clay	58	10,8	-0,649
Morin clay	60	9,5	-0,479
O'Brien clay	61	10,4	-0,484
Goodrich clay	68	8,64	-0,456
Tuto clay	78	12,8	-0,603
Sweden VFB 478 clay	113	27,1	-0,472
Suffield silty clay	148	11,1	-0,254
Frederick clay	159	14	-0,297
Ellsworth clay	184	11,2	-0,293
Regina clay	291	21,1	-0,238
Niagara silt	37	6,6	-0,41
Norway LE-1 clay	52	9,9	-0,523
Kaolinite #7	72	19,8	-0,689
Athena silt loam	83	6	-0,301
Sweden CTH 201 clay	106	19,7	-0,492
Hectorite	419	38,4	-0,369
Fairbank silt	40	4,8	-0,326

Tice, Anderson, and Banin (1976) developed a simple procedure for calculation of α and β based on liquid-limit data. Application of this procedure to a given soil requires measurement of the water contents ($W_{N=25}$ and $W_{N=100}$ corresponding to N = 25 and N = 100 (where N = number of blows required to close the standard groove in the liquid-limit test) and the following empirical relationships (1.25 and 1.26).

$$w_{u,\theta=-1} = 0,346 w_{N=25} - 3,01 \tag{1.25}$$

$$w_{u,\theta=-2} = 0,338 w_{N=100} - 3,72 \tag{1.26}$$

The agreement between measured and predicted W_u values for several soils is excellent. Unfrozen water contents computed on the basis of equation 1.24 are considered adequate for many engineering applications provided that the soils being considered do not contain excessive amounts of soluble salts.

1.6.2. Effect of Solutes on Freezing

Water within soil pores may contain dissolved salts which increase the freezing-point depression and will increase the unfrozen water content. The presence of dissolved salts results in a reduced soil frost susceptibility under seasonal temperature conditions due to a decrease in the freezing index and an increase in the thawing index.

The lowest temperature at which a solution will remain completely liquid is called the eutectic temperature. The eutectic temperature for the H_20-NaCl system is -21°C at about 23.3% NaCl. The eutectic temperature for an H_20-$CaCl_2$ system is - 51°C.

Banin and Anderson (1974) described how the presence of salts in soil pore water lowers the freezing-temperature depression. As the water freezes, solutes are forced into a smaller and smaller volume of solution. The freezing temperature, T_n for a salinity, S_n can be estimated (Patterson and Smith, 1983) using equation 1.27.

$$T_n = T_i + \frac{S_n}{A\left(\frac{w_u}{w}\right)} \tag{1.27}$$

S_n – salinity (g/l of NaCl);

A – -17 (g/l°C);

w_u – unfrozen water in non-saline soil (% of dry soil mass);

w – the total soil water content (% of dry soil mass);

T_i – temperature at which w_u is determined (°C).

A simpler method for estimating the temperature shift, ΔT, due to salinity S_n uses an empirical equation developed by Velli and Grishin (1983) equation 1.28.

$$\Delta T = T_k \left[\frac{S_n}{1000 + S_n} \right] \tag{1.28}$$

ΔT – temperature shift (°C);

T_k – reference temperature (°C);

S_n – salinity (g/l).

Reference temperature equals to 57°C for sea salt, 62°C for NaCl, and 32,5°C for $CaCl_2$.

1.6.3. Water inflow

Ice lenses form in all soil types by the addition of water during stationary or slow movement of the freezing front. The supply of water and ease of movement will often determine the ice lens size or thickness.

Significant heave can develop in places where there is constant water supply to growing ice lenses (Figure 1.8). In field situations, open systems are encountered wherever the vertical distance between the water table and the freezing depth is smaller than the height of capillary rise of the soil.

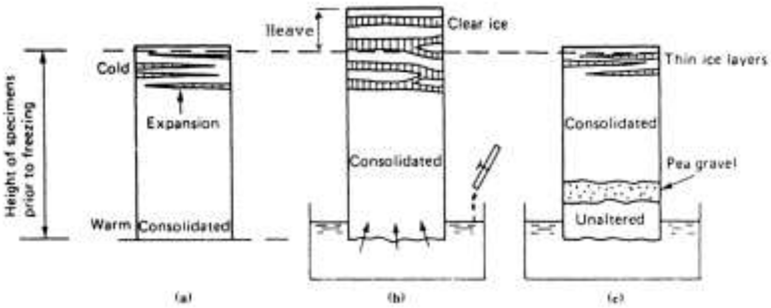

Figure 1.8. Ice formation in soils. Legend: a) closed system; b) open system; c) pea gravel layer changes upper part of the specimen into a closed system.

1.6.4. Organic matter content

Organic matter content is determined by using ASTM D2974 standard ”Standard test methods for moisture, ash, and organic matter of peat and other organic soils”.

1.7. Frost susceptibility of soils

A frost-susceptible soil is defined in terms of its frost-heaving and thaw-weakening behaviour. Both can cause considerable damage to engineering structures. Frost heave is not necessary for thaw weakening. Some clay soils develop segregated ice (and hence thaw weakening) while exhibiting little or no heave. Shrinkage or consolidation of layers adjacent to an ice lens cancels the heave normally associated with ice segregation, particularly where the water supply is limited and soil permeability is low. Frost-susceptibility index tests permit evaluation of the potential for frost heaving and thaw weakening of subgrade soils and unbound base and subbase materials for roads, railroads, and airfields.

Most of the transportation departments throughout the world have developed their own frost-susceptibility index criteria based on laboratory tests but these criteria fail to discriminate between marginally frost-susceptible material and that which is frost susceptible. As part of intensive research on the effects of frost action on pavements, Johnson et al. (1986) selected the U.S. Army Corps of Engineers frost design and soil classification system (Table 1.6, Figure 1.9). In Europe, soils are classified in accordance with their suitability for civil engineering purposes according to DIN 18196 (appendix 1). In Latvia, soils shall be identified, described and classified in accordance with LVS 437, ISO 14688-1 and 14688-2. These standards do not include soil frost susceptibility class.

To successfully apply this classification three levels of screening are required: (I) the percentage of particles smaller than 0.02 mm, (II) soil type based on the Unified Soil Classification System, (III) and a laboratory freezing test.

The simplest rating (based on level I tests) is the classification of negligible frost susceptibility given to gravels with less than 1.5% finer than 0.02 mm and sands with less than 3% finer than 0.02 mm. All soils failing this criterion require complete soil classification tests (level II). Gravels with 1.5 to 3% finer than 0.02 mm and sands with 3 to 10% finer than 0.02 mm also require a laboratory frost heave test (level III).

Table 1.6. U.S. Army Corps of Engineers frost design soil classification system.

Frost susceptibility	Frost group	Kind of soil	Amount finer than 0,02 mm (wt%)	Typical soil type under USCS
Negligible to low	NFS	Gravels Sands	0-1,5 0-3	GW, GP SW, SP
Possibly	PFS	Gravels Sands	1,5-3 3-10	GW, GP SW, SP
Low to medium	S1	Gravel	3-6	GW, GP, GW-GM, GP-GM
Very low to high	S2	Sands	3-6	SW, SP, SW-SM, SP-SM
Very low to high	F1	Gravels	6-10	GM, GW-GM, GP-GM
Medium to high	F2	Gravel	10-20	GM, GM-GC, GW-GM, GP-GM
Very low to very high		Sands	6-15	SM, SW-SM, SP-SM
Medium to high	F3	Gravel	>20	GM, GC
Low to high		Sands except very fine silty sands	>15	SM, SC
Very low to very high		Clays, I_p>12	-	CL, CH
Low to very high	F4	All silts	-	ML, MH
Very low to high		Very fine silty sands	>15	SM
Low to very high		Clays, I_p>12	-	CL, CL-ML

Very low to very high		Varved clays and other fine-grained banded sediments	-	CL and ML; CL, ML and SM; CL, CH and ML; CL, CH, ML< and SM

NFS – Non-frost susceptible.

PFS – Requires laboratory frost-heave test to determine frost susceptibility.

The range of possible degrees of frost susceptibility is very wide for most soils. For this reason, the Corps of Engineers procedure recommends that a freezing test willbe performed when precise information on soil frost susceptibility is required.

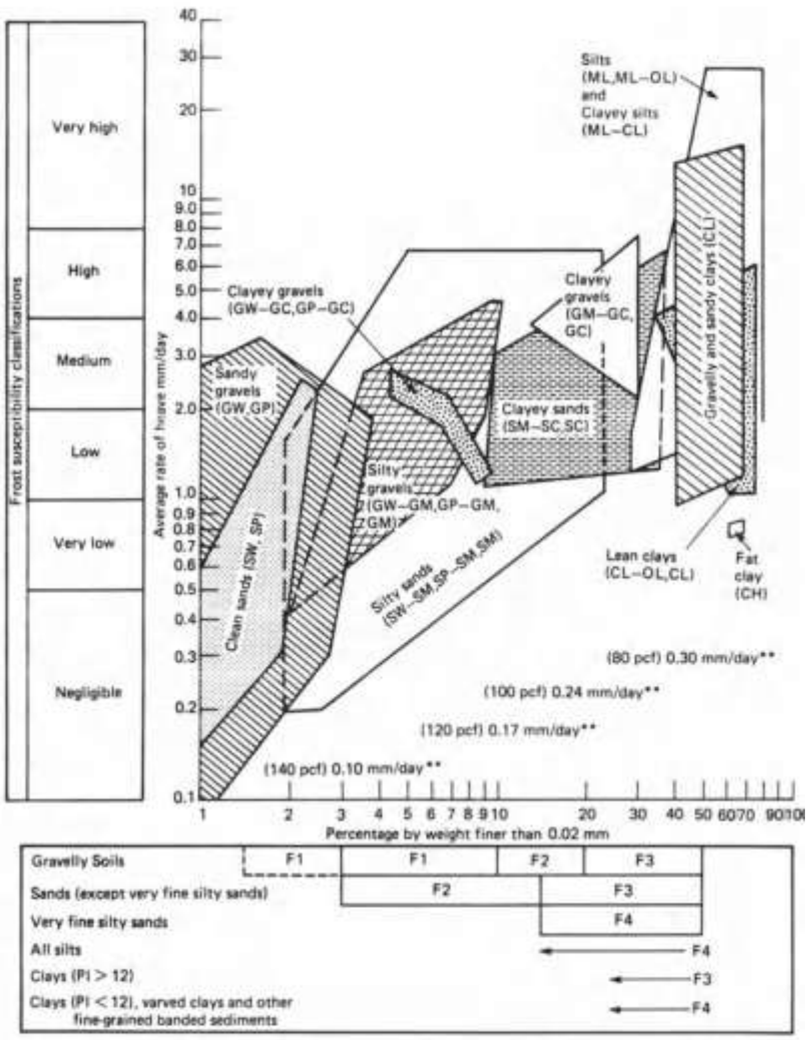

Figure 1.9. Frost susceptibility of soils (Johnson et al. 1986).

An alternative approach for evaluating frost susceptibility and heave involves determination of the segregation potential for the soil in question.

Konrad and Morgenstern (1980) have proposed a detailed model for one-dimensional frost heave. They suggested that after an ice lens has formed, the frozen soil above the ice lens does not participate in mass transport, but that water is transported to the ice lens from the unfrozen soil through a thin zone of partially frozen soil referred to as the frozen fringe. The driving force arrives from suction generated at the ice-fringe interface, and the fringe impedes flow to the lens because of its low permeability. They give a simple linear analysis of the frozen fringe, assuming that the Clausius Clapeyron equation is valid at the base of the ice lens, that water flow is continuous across the frozen fringe, that the fringe can be characterized by an overall permeability k_{f0}, and that the temperature in the frozen fringe varies linearly between the segregation freezing temperature T_{s0}, at the lens and the freezing temperature of bulk water T_i at the bottom of the fringe (Figure 1.10).

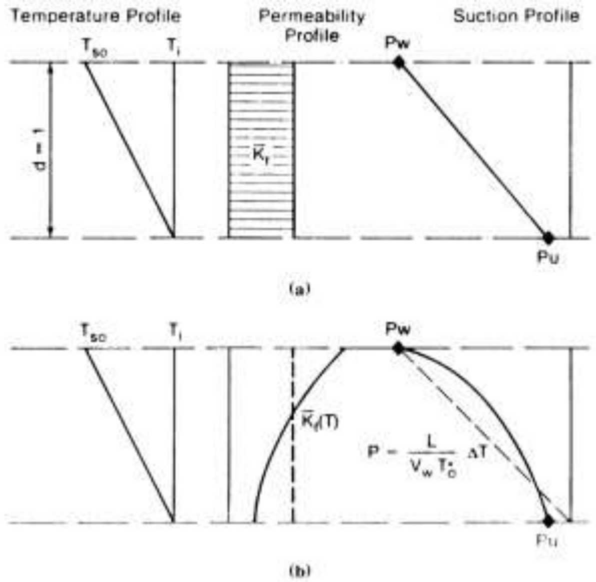

Figure 1.10. Characteristics of frozen fringe (Konrad and Morgenstern, 1980). a) simplified; b) actual

According to Konrad and Morgenstern (1981), when a soil sample freezes, the water intake flux v_0 at the formation of the final ice lens is proportional to the temperature gradient in the frozen fringe (Equation 1.29).

$$v_0 = SP \cdot grad\left(T\right) \tag{1.29}$$

v_0 – water intake flux (mm/s);

SP – segregation potential (mm^2/(s°C));

grad(T) – temperature (°C/mm).

The proportionality factor SP has been termed the segregation potential. Its value was found to be a function of the total suction potential at the freezing front p_w the suction potential at the frozen-unfrozen interface p_u, the segregation freezing temperature T_s and the overall hydraulic conductivity in the frozen fringe (Konrad, 1987) (Equation 1.30).

The segregation potential, once evaluated at near steady-state conditions and under a negligible overburden pressure, may be considered as an index property of a soil that uniquely characterizes its frost-heave susceptibility. Although the SP is usually determined at a constant suction at the frost front, the relationship between SP and p_u can be determined by applying Darcy's equation to the unfrozen zone once the permeability and the velocity of moisture migration are known (Konrad and Morgenstern, 1981; Morgenstern, 1981; Konrad, 1988).

$$p_u = v\frac{l_u}{k} \tag{1.30}$$

p_u – suction potential at the frozen-unfrozen interface (kPa);

v – velocity of moisture migration;

l_u – the length of flow in the unfrozen soil;

k – permeability.

The segregation potential of a given freezing soil decreases with increasing applied pressure. Konrad and Morgenstern (1984) expressed the influence of a surcharge by an empirical power law (Equation 1.31).

$$SP = SP_0 \exp(-ap_e) \tag{1.31}$$

SP – segregation potential ($mm^2/(s°C)$);

SP_0 – segregation potential for 0 applied pressure ($mm^2/(s°C)$);

p_e – applied pressure;

a – soil constant.

According to Konrad and Morgenstern (1982), heave *(h)* under field conditions can be predicted using the equation 1.32.

$$\frac{dh}{dt} = 1,09SP \cdot G_f + 0,09n\frac{dX}{dt} \tag{1.32}$$

dh/dt – heave rate;

X – frost depth;

n – porosity reduced to account for the percentage of in situ pore water that will not freeze (Volume %);

G_f – thermal gradient in the frozen soil.

For field conditions, Nixon (1987) modified equation 1.32 for prediction of the heave rate to equation 1.33.

$$\frac{dh}{dt} = \frac{1,09V_{ff} \cdot G_f}{G_{ff}\left(1 + \frac{L \cdot V_{ff}}{G_{ff} k_f}\right)} \tag{1.33}$$

dh/dt – heave rate;

L – volumetric latent heat of water;

V_{ff} – pore water velocity in the frozen fringe;

G_f – thermal gradient in the frozen soil;

G_{ff} – thermal gradient in the fringe;

k_f – frozen soil thermal conductivity.

Nixon (1991) has shown that the hydraulic conductivity parameters required for heave prediction can be extracted from a set of frost-heave test data. The fringe pore-water velocity V_{ff} per unit temperature gradient in a one-dimensional test can be written as follows (equation 1.34).

$$\frac{V_{ff}}{G_{ff}} = \left[\frac{L}{k_f} + \frac{\left[\left(1,09p_0 - p_u\right)\left(\frac{1+A}{A}\right)\right]^A}{k_0 B^{(1+A)}}\right]^{-1} \tag{1.34}$$

V_{ff} – pore water velocity in the frozen fringe;

G_{ff} – thermal gradient in the fringe;

L – volumetric latent heat of water;

k_f – frozen soil thermal conductivity;

B – thermodynamic constant (12400 cm H_2O pressure/°C);

p_u – suction potential at the frozen-unfrozen interface (g/cm^2);

p_0 – (g/cm^2);

k_0 – hydraulic conductivity at -1°C (cm/s);

2. SOIL INVESTIGATION METHODS

2.1. Field investigations of frozen soil.

Information that is necessary for calculations and frozen soil behavior forecasting, is obtained in the field by conducting various field measurements and soil sampling. Valuable information can also be obtained at the site using in situ test methods and geophysical techniques.

Temperature greatly influences the properties and behaviour of frozen materials, particularly those containing ice and unfrozen water. Measurement of ground temperatures is most important and should be included in any field investigation. For most engineering purposes, an accuracy of ± 0.2°C is desirable and can be obtained either with thermocouples or with thermistors, provided that great care is taken in planning the installation, fabricating the probes, connectors, switches, and circuitry, in the installation of the probes, and in selecting and using the readout instruments.

For most installations, the cable can be placed directly in the hole so that the sensors are in intimate contact with the surrounding soil. The hole should be carefully backfilled, particularly near the ground surface, to prevent percolation of surface water down the hole. The ground surface should be marked on the cable at the time of installation so that any movement due to frost action or thaw settlement and the subsequent position of sensors can be determined. Cables placed in deep holes or those that arc to measure temperature precisely and/or over long periods of time may have to be cased to protect them from damage or moisture and to make it possible to retrieve the thermistors for recalibration.

Depending on the amount of disturbance caused by the drilling operation, it may take several days or weeks before thermal equilibrium is reestablished in most drill holes. Mackay (1974) and Klein et al. (1986) found that temperatures measured in plugged, air-filled drill holes 6 to 30 m deep stabilized within 1 day.

The type and number of samples to be taken from a vertical profile will depend primarily on the variability of the materials encountered and the ultimate use of the samples (i.e., what information is required and what tests are to be performed). These factors will also determine the methods that should be employed to obtain the samples. Techniques used for sampling frozen ground are similar to those used for unfrozen materials, but much greater attention must be paid to avoiding thermal disturbance. At present, there are no set standards or guidelines for sampling frozen materials. The selection of appropriate methods and equipment will depend greatly on the experience and judgment of the field engineer and project needs. Samples can be obtained from natural exposures, test pits, or boreholes (Cass, 1959; Johnston, 1963a). Test pits, which can be excavated to depths of 2 to 10 m by several methods, permit the complete profile to be examined, logged, and sampled in situ.

The success of several geophysical prospecting methods tried in permafrost depends on freezing the interstitial water in soils and rocks, which causes changes in their physical properties. Since the physical properties that change most when interstitial water freezes are the elastic moduli and the electrical conductivity, seismic and electrical methods are the most useful geophysical methods for permafrost studies.

It should be noted that seismic and electrical methods are sensitive primarily to the presence of ice in soil or rock pores and do not give information on the thermal regime that defines permafrost. For that reason, their results may be misleading in dry or saltwater areas (Barnes, 1963). The velocity of elastic waves and the electrical resistivity increase as the water component is transformed into ice. The greatest change in these parameters takes place between 0 and - 10°C, and they do not change linearly with the amount of ice.

The dc electrical resistivity of frozen ground are affected by temperature to a greater extent than seismic velocities in the temperature range from 0 to - 100°C. Data compiled by Barnes (1963) show that, the resistivity of frozen soils and rocks may be 10 to more than 100 times larger than the resistivity of the same materials when unfrozen. However, differentiating between frozen and unfrozen ground solely on the basis of resistivity is not always possible because the resistivity of frozen clay can be less than the resistivity of unfrozen silt, sand, or rock. In addition, the resistivity is especially sensitive to the amount of ionic conduction in the interstitial fluids, so that an increasing salinity of pore water results in a corresponding reduction in resistivity. Therefore, resistivity surveys alone are not sufficient for mapping permafrost; they must be supplemented with other geophysical or geological information.

GPR is particularly sensitive and capable of detecting zones and interfaces with strong dielectric contrasts, such as dry-wet and unfrozen-frozen interfaces. Thus, wherever shallow structural features in a material are manifested by a change in electrical properties, GPR is an applicable technique.

2.2. Laboratory examination of frost heave

The purpose of this test is to determine the frost heave of soil when compacted into cylindrical specimens at a predetermined moisture content and density. The test may also be carried out on cylindrical specimens of undisturbed soil. The procedure is lengthy and is described in following standards: BS 812-124, ASTM D5918-13 and GOST 28622-2012.

2.2.1. Frost heave determination according to BS 812-124:2009 “Testing aggregates. Part 124: Method for determination of frost heave”

BS 812-124:2009 describes a test procedure for the determination of the frost resistance of unbound aggregate mixtures that have been compacted to form a cylindrical specimen with a predetermined water content and density. It is applicable to unbound aggregate mixtures used in the construction of roads and other paved areas at a depth that might experience frost penetration.

The test procedure described in British standard uses three frost heave test specimens for each test on an unbound aggregate mixture. The SRU can accommodate nine specimens. This means that three different unbound mixtures can be tested at one time. If three comparator specimens are used, two unbound mixtures can be tested at one time.

Method principle

Cylindrical specimens of unbound aggregate mixtures, compacted at a predetermined water content and density, are placed in a self-refrigerated unit (SRU). The SRU subjects the upper surface of each test specimen to freezing air at −17 °C whilst their lower ends have access to water maintained at +4 °C. Comparator specimens can be used to confirm that the SRU is operating correctly.

The temperature gradient in the SRU causes water to be drawn into the freezing zone and might lead to the formation of ice lenses that increase the height of the specimens. The change in height is measured at intervals over a period of 96 h. The maximum increase is recorded and is used to calculate the frost heave of the mixture.

The apparatus for determining the frost resistance of the material shall be as specified in BS 812-124:2009. Unless otherwise stated, all apparatus shall conform to BS EN 932-5.

Preliminary testing procedure

Determine the particle-size distribution of a test portion taken from the laboratory sample in accordance with BS EN 933-1. The apparatus for the determination of the particle size distribution shall be as specified in BS EN 933-1.

Determine the optimum water content and maximum dry density of test specimens taken from the laboratory sample in accordance with BS EN 13286-4. The apparatus for determining the relationship between the dry density and water content of the unbound aggregate mixture shall be as specified in BS EN 13286-4. Initial preparation of a frost heave test specimen described in BS 812-124:2009 clause 7.2.2.

Preparation of test specimens

The laboratory sample mass required for determining the frost heave is at least 15 kg for use as a subsample for the frost heave test. Detailed soil sample mixing and method for preparing a single test described in BS 812-124:2009 clause 8.

Procedure for the determination of frost heave

Loading test specimens into the self-refrigerated unit.

Number the specimen positions as shown in figure 2.1. If comparator specimens are not used, load the three test specimens for the first unbound mixture in positions 1 to 3, for the second unbound mixture in positions 4 to 6 and for the third unbound mixture in positions 7 to 9. If comparator test specimens are used, place the three comparator specimens into positions 3, 5 and 7 (see figure 2.1.). Fill the other six positions with specimens, a minimum of three for each material to be tested.

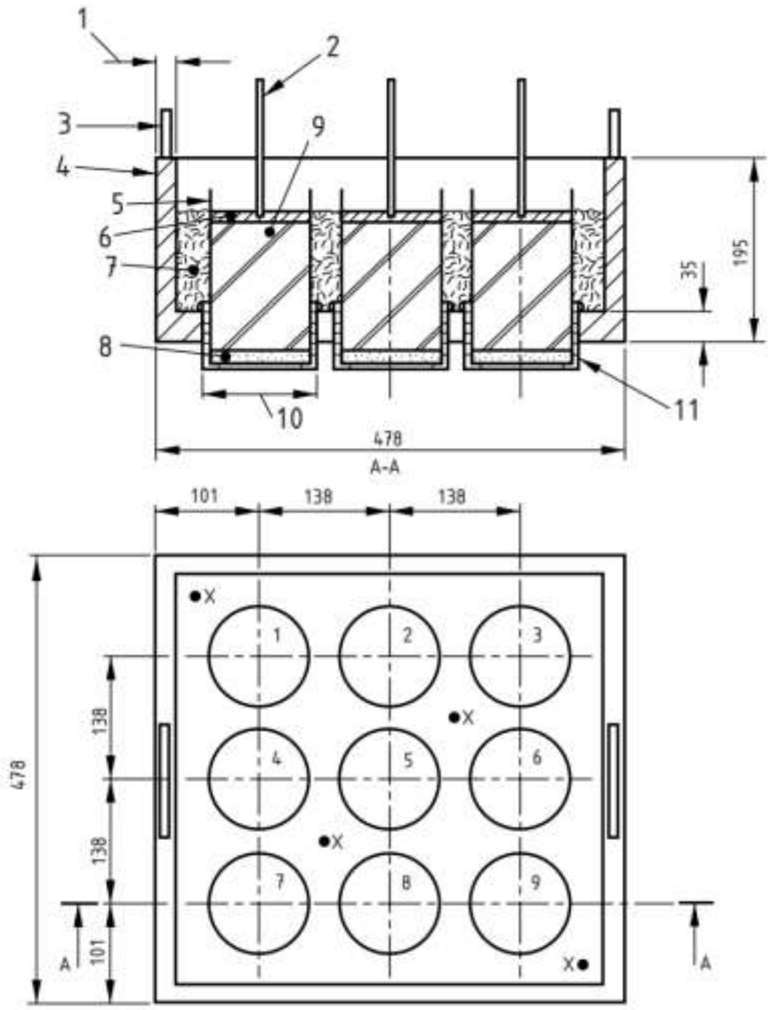

Figure 2.1. Specimen cradle showing specimen position numbers. Legend: 1 – typical: 19 mm; 2 – brass rod Ø 6.0 × 750 mm long; 3 – handle; 4 – specimen cradle; 5 – waxed paper; 6 – rigid disc; 7 – coarse sand fill; 8 – porous disc; 9 – specimen; 10 – typical hole size: Ø 112 mm; 11 – specimen carrier; X – positions of four thermocouples in the air.

Locate a thermocouple between the bottom of the porous disc under the test specimen and the copper specimen carrier in positions 1, 3, 5, 7 and 9. Ensure that the tip of the thermocouple is not in contact with the copper carrier, is 5 mm to 10 mm into the water bath when the carrier is loaded with specimens and is as central as possible in each specimen position.

Fix another thermocouple under the rigid disc on top of the test specimen in position 5, so that the junction is exposed at the of the disc and in contact with the upper surface of the test specimen. If fewer than nine specimens are to be tested, fill the vacant positions with dummy specimens.

When nine test specimens are in position, locate four more thermocouples so that there is one above each of the spots marked "X" on the floor of the cradle in figure 2.1., at a level 250 mm above the plane containing the lower faces of the specimens. This can be achieved by attaching each thermocouple to a 6 mm diameter wooden dowel approximately 300 mm long so that the junction is exposed (205 ± 2) mm from the lower end of the dowel. Position the four dowels on the floor of the cradle. Support the dowels either by drilling holes of the correct diameter or by using flexible tubing placed on the dowel ends which are then pushed onto present studs on the floor of the cradle.

Place coarse sand (clean and dry single-sized coarse silica sand from either the 5mm to 2.36 mm or the 2.36 mm to 1.18 mm fractions) carefully in the space around the specimens (and around the vertical dowels if these are used) until the sand is level with the tops of the specimens. Take care to remove any sand particles accidentally spilt on the rigid discs, particularly in the recesses. Care should be taken to ensure that the particles of sand do not get under the dowels, thus raising the thermocouples. When the sand is in place, the waxed paper around each test specimen should stand approximately 50 mm above the level of the sand.
Check the positions of the thermocouples and any control sensors and then close the lid of the test chamber. Locate the support (datum) frame on the SRU (figure 2.2.). Pass the brass rods (750 mm long and 6.0 mm in diameter) through the holes in the frame and in the chamber lid, and locate each one in the central recess of the corresponding rigid disc on top of the test specimen. Start the constant-level device (a means of maintaining the water in the water-bath at a constant level between 8 mm and 11 mm from the underside of the specimen cradle) by opening the outlet tap, O (figure 2.3.), to allow water to flow into the water-bath and restore the correct level. The water level is controlled automatically for the remainder of the test.

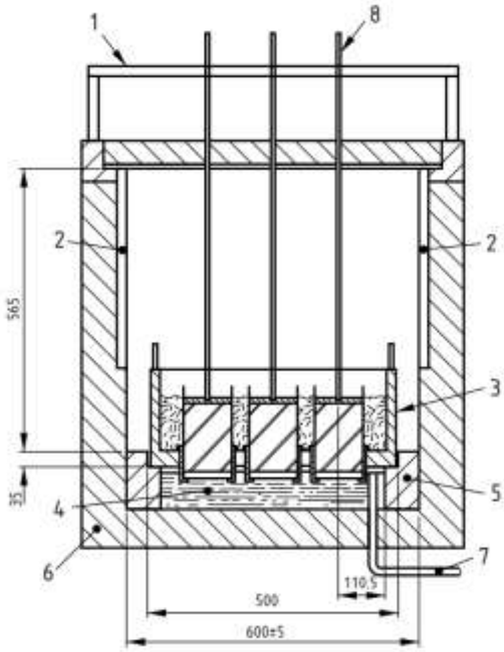

Figure 2.2. Main features and dimensions of the test chamber. Legend: 1 – support frame 150 ± 25 mm; 2 – cooling coils; 3 – specimen cradle; 4 – water bath; 5 – solid insulating material;

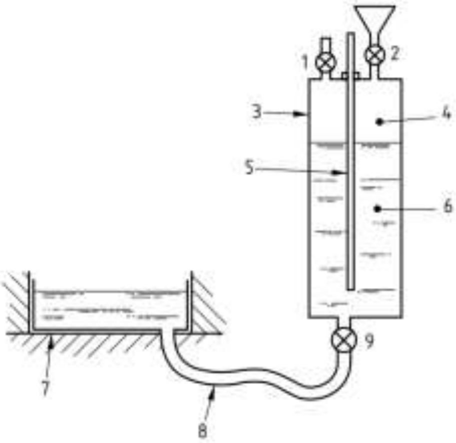

6 – insulating material; 7 – overflow pipe; 8 – brass rod.

Figure 2.3. The principle of a constant level device to control water supply to frost resistance specimens. Legend: 1 – vent tap “V”; 2 – filler tap “F”; 3 – air-tight vessel capacity 6–8 L; 4 – vacuum; 5 – capillary tube, inside diameter approx. 3.0 mm; 6 – water; 7 – water bath; 8 – flexible connection; 9 – outlet tap “O”.

Complete the loading of the SRU within one working day. Leave the loaded SRU undisturbed for (115 ± 5) h from the time that the last specimen was inserted in the cradle before proceeding. Use the temperature recorder to monitor the temperatures in the test chamber during this period. Do not activate the refrigeration function at this stage.

Freezing the specimens and measuring frost resistance

After (115 ± 5) h from the time that the last specimen was inserted in the cradle before proceeding, check the location of the brass rods. Use surgery wool or similar absorbent material to plug the gaps between each rod and the hole in the test-chamber lid through which it passes. For each brass rod, record the distance between the top of the rod and the top of the support (datum) frame to the nearest 0.5 mm. Record the temperature of each thermocouple. Switch on the SRU to start the freezing process. Record the time. Ensure the operating temperatures are reached in a time between 4 h and 14 h from switching on the SRU. Maintain these operating temperatures for the duration of the test. Measure the frost heave after a period of (24 ± 2) h from the time of switching on the refrigeration using the following procedure:

a) Rotate the brass rods to ensure that they have not stuck. Check the surgery wool and replace if necessary.

b) For each brass rod, record the distance between the top of the rod and the top of the support (datum) frame to the nearest 0.5 mm.

c) Calculate the value of any heave that has occurred by subtraction. Record this value as the "frost heave".

Continue to record the frost heave as described previously at intervals of (24 ± 2) h until at least 96 h has elapsed from the time of switching on the SRU. At least daily, record the temperature at each thermocouple sequentially at intervals not exceeding 5 s. Calculate the instantaneous water temperature and the instantaneous air temperature. Detailed monitoring of the temperature conditions is in the BS 812-124-129.

Unloading the self-refrigerated unit

After at least 96 h, or earlier if it has been decided to abandon the test, unload the SRU using the following procedures. At first switch off the refrigeration system. The water-bath circulation/heating system should still be running at this stage, to prevent the water temperature falling too far while it is exposed to the very cold air in the test chamber.

Remove the surgery wool from the holes in the test-chamber lid and discard. Remove the brass rods and allow them to return to room temperature. Remove the support (datum) frame and open the test-chamber lid. Carefully remove the thermocouples in the air above the specimens.

Remove the coarse sand. The sand should not be used again until it has returned to room temperature. Remove the test specimens from the cradle, taking care not to damage any thermocouples as they are detached. Discard the test specimens and the waxed paper around them. Clean and dry the rigid discs, porous discs and copper specimen carriers. Check that the porous discs have not become blocked, particularly when fine-grained materials have been tested. If any are found to be no longer permeable, replace them before future tests.

Remove the wooden cradle. Allow it to return to room temperature, clean and dry. Leave the SRU with the lid open until the air in the test chamber has warmed to above 0 °C. Switch off the water-bath controls and completely drain both the bath and the constant-level device. Discard the waste water.

Finally defrost the SRU and the test chamber (including the water-bath) and thoroughly clean and dry. Do not use the SRU for another test until it has returned to room temperature.

Calculation and expression of results

Review the calculated values of frost heave for each of the nine test specimens taken over the test period. If the values show that the frost heave of two or more of the nine test specimens has fallen by more than 1 mm, consider the test run to be invalid. Do not report the result and repeat the test using new test specimens.

For each test specimen, determine the maximum value of frost heave observed during the test period. For each set of three test specimens, calculate the mean of the maximum values, to the nearest 0.1 mm. If comparator test specimens have not been used, use the mean value calculated as described in previous sentence as the frost heave value for the mixture, subject to the following conditions:

a) If the maximum value of frost heave of all nine specimens is less than 2.0 mm, the results are suspiciously low. Repeat the test unless the results are consistent with previous experience for that mixture.

b) If the mean value of frost heave for a set of three test specimens is less than 18.0 mm, calculate the range (i.e. highest – lowest) of the maximum values for the three test specimens. If the range for the set of three exceeds 6.0 mm, consider the test run to be invalid. Repeat the test using new test specimens.

c) If the mean value of frost heave is 18.0 mm or greater, the test result is valid. No further testing is required.

If the test was carried out using comparator specimens, for each test specimen, determine the maximum value of frost heave observed during the test period. For each set of three test specimens, calculate the mean of the maximum values, to the nearest 0.1 mm. The mean value calculated as the frost heave value for the mixture, subject to the following conditions.

a) The mean value of frost heave for the three comparator specimens is in the range (13.6 ± 4.0) mm.

b) The range (i.e. highest – lowest) of the maximum values for the three sets of test specimens does not exceed 6 mm.

If either of these conditions is not satisfied, consider the test run to be invalid. Repeat the test using new test specimens.

2.2.2. Frost heave determination according to D5918-13 “Standard Test Methods for Frost Heave and Thaw Weakening Susceptibility of Soils”

In this standard described laboratory test methods cover the frost heave and thaw weakening susceptibilities of soil that is tested in the laboratory by comparing the heave rate and thawed bearing ratio with values in an established classification system. This test was developed to classify the frost susceptibility of soils used in pavements. It should be used for soils where frost susceptibility considerations, based on particle size such as the limit of 3 % finer than 20 mm in Specification D2940, are uncertain. This is most important for frost-susceptibility criteria such as those used by the Corps of Engineers, that require a freezing test for aggregates of inconclusive frost classification. The frost heave susceptibility is determined from the heave rate during freezing.

Two freeze-thaw cycles are imposed on compacted soil specimens, 146 mm in diameter and 150 mm in height. The soil specimen is frozen and thawed by applying specified constant temperatures in steps at the top and bottom of the specimen, with or without water freely available at the base; a surcharge of 3.5 kPa is applied to the top. The temperatures imposed on the specimen are adjusted to take into account the freezing point depression attributable to salts in the soil. At the end of the second thawing cycle, the bearing ratio is determined. The entire testing procedure can be completed within a five-day period. This testing procedure may be conducted manually or it may be controlled by a computer.

These test methods can be used to determine the relative frost-susceptibility of soils used in pavement systems. Both the frost heave susceptibility and the thaw weakening susceptibility can be determined. These test methods should be used only for seasonal frost conditions and not for permanent or long-term freezing of soil. These test methods also have not been validated for anything other than pavement systems. These test methods cannot be used to predict the amount of frost heave or thaw weakening in the field. Its purpose is to determine the relative frost-susceptibility classification for use in empirical pavement design methods for seasonal frost regions.

Heave and consolidation measuring apparatus

Heave and consolidation measuring apparatus consist of a vertical post with a minimum diameter of 16 mm and a minimum height of 508 mm fixed to the base plate of the test specimen, shall provide support for an adjustable arm to hold the displacement dial gage or displacement transducer, or both (see figure 2.4.). The dial gages and displacement transducers shall be capable of measuring vertical movements of 25.4 mm with an accuracy of 0.025 mm. The transducers must be calibrated frequently. This can easily be done for each test if a dial gage is coupled to the displacement transducer as shown in figure 2.4.

Temperature control baths. Two sources of temperature-controlled circulating liquid, such as an ethylene glycol-water 50 % solution, are required. One source is to be used to control the temperature of the top temperature control plate and the second source is to control the temperature of the bottom temperature control plate. Both sources shall have a controllable temperature range from −15°C to 15°C and be capable of maintaining the temperature at each temperature control plate to within +0.2°C of the present temperatures.

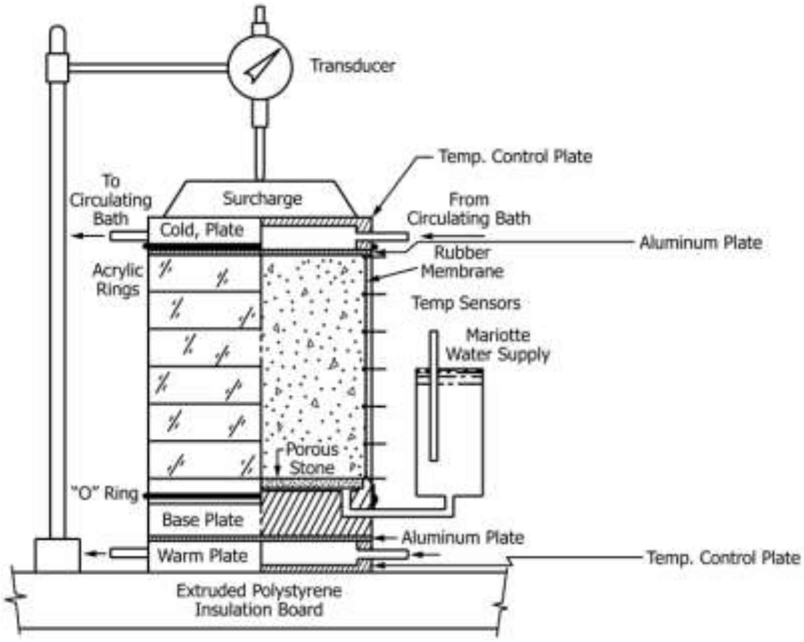

Figure 2.4. Specimen assembly for freezing test.

The temperature control chamber in which the freeze-thaw tests are to be conducted shall have inside dimensions that will house the test specimen freezing assembly. Figure 2.5. shows a 0.35 m^3 capacity chest-type freezer adapted to accommodate four test specimens. A refrigerator or cold room could also be used. The cold chamber shall have the capability of maintaining the ambient air temperature around the test specimen assemblies at 2°C within ±1.0°C.

The temperature measuring system shall have a range from −15°C to 15°C and shall be capable of measuring temperatures within ±0.1°C (0.2°F). The temperature sensors shall be small enough (less than 3.2 mm) to permit their insertion into the soil test specimen with a minimum of disturbance to the soil (see figure 2.6.). The temperature readings are to be taken periodically and may be taken manually. It is preferable that the temperatures be read with an automated data logging system.

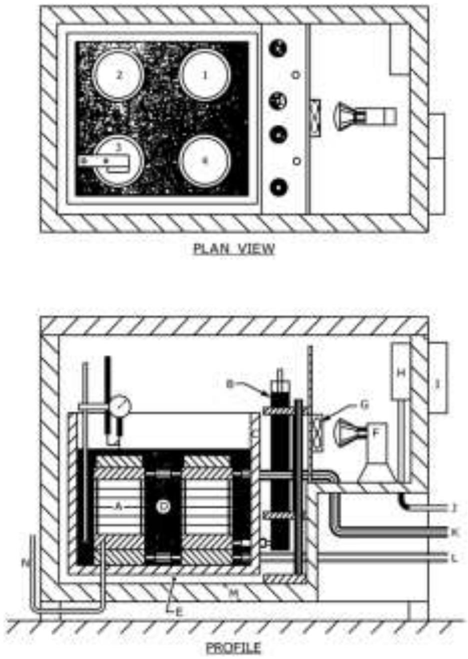

Figure 2.5. Freeze cabinet assembly for freezing test. Legend: A – specimen assembly; B – water supply; C – rigid insulation; D – granular insulation; E – ambient air space; F – heat source; G – fan; H – electronics panel; I – air temperature controller; J - lines to datalogger; K – top plate circulation tubing; L – bottom plate circulation tubes; M – freezer chest; N – drainage lines.

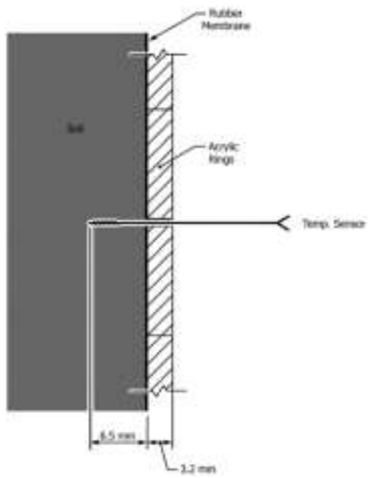

Figure 2.6. Location of temperature sensors in the test specimen.

Specimen preparation.

For testing use intact soil samples when possible. Intact specimens usually can only be prepared for fine-grained soils, in particular competent silt and clay soils found in the subgrade of roads. Where the soil is to be remolded and compacted in the field, use laboratory-compacted soils. Detailed intact samples and remolded samples preparation is described in D 5918-13.

After samples are prepared determine the mass of the assembled specimen, including the acrylic rings with the filament tape, the rubber membrane, and the acrylic spacer disks. Record the results and calculate the wet and dry density, void ratio, porosity, and degree of saturation. Determination of freezing point depression, mounting the specimen for testing, saturating the specimen, placing the specimen in the temperature control chamber, installation of temperature sensors and completing the test assembly in details are described in D 5918-13.

Procedure

Boundary temperatures. The top and bottom cooling plates are set at fixed temperatures (see table 2.1) for specified time periods to induce a conditioning period and two freeze-thaw cycles. If the freezing point depression temperature is lower than −0.25°C, then the specified temperatures in table 2.1 should be lowered by the amount of the freezing point depression.

Table 2.1. Boundary temperature conditions.

Day	Elapsed time, h	Top plate temperature,°C	Bottom plate temperature, °C	Comments
1	0	3	3	24-h conditioning
2	24	-3	3	First 8-h freeze to bottom
	32	-12	0	
3	48	12	3	First thaw
	64	3	3	
4	72	-3	3	Second 8-h freeze to bottom
	80	-12	0	
5	96	12	3	Second thaw
	112 to 120	3	3	

Conditioning the specimen. The first 24 h is a conditioning period. Both the top and bottom plates are held at 3°C.

First freezing period. The first freeze starts at the beginning of the second 24h period. First record the initial dial gage or transducer readings; record each if both are being used. Lower the temperature of the top plate, and hold it at −3°C and the bottom plate at 3°C for 8 h. After 8 h, lower the temperatures of the top plate to −12°C and the bottom plate to 0°C. Hold these temperatures for 16 h. Table 2.1 shows the details of the cooling plate temperature settings.

Nucleation. If the top temperature sensor reading is 1°C lower than the freezing temperature of the soil pore water, initiate ice nucleation by delivering two sharp blows with a metal rod to the top of the cold plate. The readings from the top temperature sensor will rise if nucleation occurred. Other evidence of nucleation may be a positive frost heave rate. Repeat this process for each additional 0.5°C drop below the freezing point of the soil pore water until ice nucleation is achieved. Spontaneous nucleation will occur without applying the sharp blows; however, the nucleation temperature may be very low and instantaneous freezing of the top several centimeters of the specimens may occur. This should be avoided; only unidirectional progressive freezing is desired.

First thawing period. The first thaw starts at the beginning of the third 24-h period. Raise the top plate temperature and hold it at 12°C and raise the bottom plate temperature and hold it at 3°C for 16 h. During the next 8 h, hold both the top and bottom plate temperatures at 3°C. See table 2.1 and figure 2.7 for the temperature settings and timing.

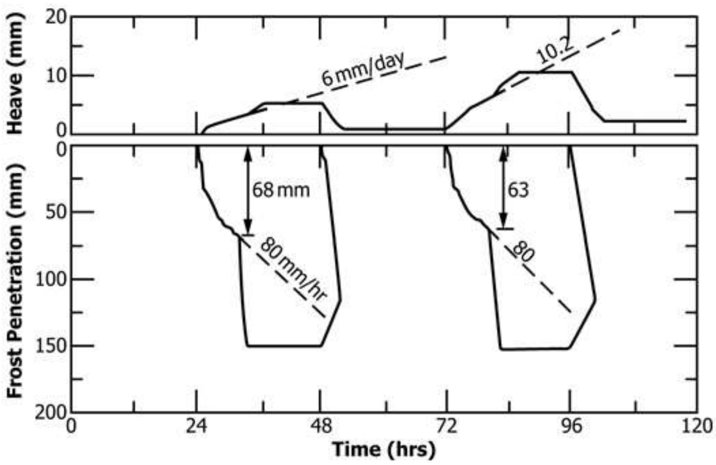

Figure 2.7. Example of the freeze-thaw test results and selection of the frost heave rate.

Second freezing period. The second freeze starts at the beginning of the fourth 24-h period. This procedure is the same as that used in the first freeze.

Second thawing period. The second thaw starts at the beginning of the fifth 24-h period. This procedure is the same as that used for the first thaw.

Measurements during the freeze-thaw test. Read all temperature sensors and displacement transducers at least every half hour throughout the first 8-h of freezing and at 1-h intervals thereafter.

Completing the freeze-thaw test. At the end of the second thaw period (120 h after the start of the test), record the dial gage reading. Turn off the circulating liquid to the temperature control plates. Remove the dial gage and the displacement transducer assembles. Remove the surcharge weights and the top temperature control plate assembly. Remove enough of the loose insulation to allow access to the temperature sensors and the water lines. Remove the temperature sensors from the side of the specimen by pulling them gently away from the acrylic rings. Now, remove the specimen assembly, complete with base plate, from the temperature control chamber.

Conducting the bearing ratio test after thawing

Move the specimen from the base and carefully place it on an aluminium pie plate of known tare mass. Determine the mass of the specimen and the pie plate. Slide a 150-mm diameter hose clamp over each acrylic ring and tighten. Remove the plastic film from the top of the specimen. Conduct a bearing ratio test on the specimen, in accordance with Test method D1883 (Test method for California bearing ratio of laboratory-compacted soils), but limit the penetration to 7.6 mm of depth. Take a small water content specimen from the area where the bearing ratio piston penetrated the specimen. Determine the wet and dry masses and water content. Remove the hose clamps, acrylic rings, and rubber membrane from the specimen, and cut the specimen into six horizontal slices of approximately equal thickness. Determine the water content of each slice.

The bearing ratio should also be determined for a specimen that has not been frozen. This specimen should be prepared at the same moisture and density conditions as the freeze-thaw test specimen.

Determining the frost-susceptibility

Use the two heave rates and the bearing ratio values to determine the frost-susceptibility using the criteria given in table 2.2. Compare the 8-h frost heave rates observed during the first and second freeze-thaw cycles with each other. If there is a significant increase (or decrease) during the second freeze, then the heave rate selected will depend on the site conditions. If the site is in a very temperate region where many freeze-thaw cycles occur and the water table is near the zone of freezing and thawing, then the 8-h heave rate during the second freeze should be selected. If the site is in a more severe winter climate where the frost penetration is more continuous during the winter and does not reach the water table, then the 8-h heave rate during the first freeze should be selected.

Table 2.2. Tentative Frost-Susceptibility Criteria*

Frost-Susceptibility Classification	**Symbol**	**8-h Heave Rate, mm/day**	**Bearing Ratio After Thaw, %**
Negligible	NFS	<1	>20
Very low	VL	1 to 2	20 to 15
Low	L	2 to 4	15 to 10
Medium	M	4 to 8	10 to 5
High	H	8 to 16	5 to 2
Very high	VH	>16	<2

* The criteria will be updated with experience. The bearing ratio criteria should be used only as a guide; if the CBR test is used for design, it should be noted that the thaw CBR value occurs only for a few weeks per year.

The heave rate criteria allow the determination of the frost heave susceptibility of a material that can be related to pavement roughness during the freezing period. The thaw bearing ratio value allows the determination of the thaw weakening susceptibility of the material. Compare the thaw bearing ratio value with the bearing value for no freezing or the design bearing value to determine the frost-susceptibility. Tentative criteria in table 2.2. can be used to determine the thaw weakening susceptibility if no bearing ratio specifications are available. The thaw weakening susceptibility criteria are based upon comparisons of bearing ratios (after two freeze-thaw cycles in the laboratory) with pavement deflection measurements (made during spring thaw with simulated wheel loadings). The thaw weakening period is normally two to four weeks in seasonal frost regions. Thus, the thaw bearing ratio value covers only this period of time.

2.2.3. Frost-heave determination according to GOST 28622-90 “Laboratory method for determination of frost-heave degree”

Soil frost-heaving tests were done in compliance with GOST 28622-90 “Laboratory method for determination of frost-heave degree”.

In compliances with GOST 28622-90 soil susceptibility to frost heave is assessed by the relative deformation of the frost elevation obtained in a specific apparatus by freezing through the test soil at a given temperature mode, and by measuring surface displacement.

Table 2.3. Soil heaving degree depending on relative deformation:

Frost heave characteristic	**Soil sample frost-heave relative deformation**
Not sensitive to heave	< 0,01
Weakly sensitive to heave	≥ 0,01 – < 0,04
Moderately sensitive to heave	≥ 0,04 – < 0,07
Very sensitive to heave	≥ 0,07 – < 0,10
Excessive sensitive to heave	≥ 0,10

Depending on necessity, both undisturbed natural soil samples and samples with the required moisture and density can be tested.

Testing shall be carried out on at least three parallel test soil samples. The test result is calculated as the arithmetic mean of all parallel results. If the values of the test results of the parallel samples differ by more than 30%, the number of samples to be tested should be increased.

The size of the coarse particles in the test soil must not exceed 20 mm.

The prepared dusty-clayey soil samples should be pre-frosted and thawed beforehand. At least two freezing-thawing cycles must be performed.

The upper and lower edges of the samples must be flat and parallel to each other.

Equipment for testing soil heave:

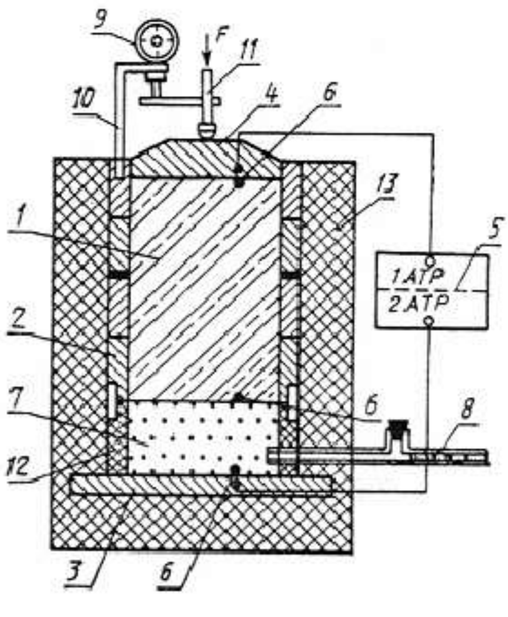

Figure 2.8. Equipment for testing frost heave of the soils

1 – soil sample

2 - cartridge

3 – lower thermostatic plate

4 – upper thermostatic plate

5 – Automatic thermoregulation unit

6 – temperature sensors

7 – capillary-porous material

8 – Water supply device

9 – Indicator of displacement

10 – hanger

11 – load-up bar of the soil

12 – pad

13 – insulated housing

Testing

The soil sample (prepared with the required humidity and density) is placed in the frost heaving testing machine and preloaded till 0,5 MPa (depending on the predicted pressure of the upper layers on the soil in the specific horizon from which the soil sample was taken), it is placed in the freezer for at least for 24 hours at temperature +1 (± 0.5) ° C.

The sample is then started to freeze at 4 (± 0,2) °C until the sample is frozen to the bottom, gradually lowering the base panel temperature from +1 °C to 0 °C, which is achieved by automatically maintaining the temperature of the lower thermostatic panel + 1 (± 0,2) °C. The sample shall then be thawed and re-frozen. The test shall be stopped when a temperature of 0 °C is reached at the bottom of the sample.

For the sample shall measure the actual depth of frozen soil (not including plastical-frozen ground) in millimetres. Relative deformation is calculated by dividing the measured soil displacement with the measured depth of frozen soil.

2.2.4. Comparison of different ground frost test methods

ГОСТ 28622-2012 ″Грунты. Методы лабораторного определения степени пучинистости″ (Soils. Laboratory method for determination of frost-heave degree)

ASTM D 5918-06 ″Standard Test Methods for Frost Heave and Thaw Weakening Susceptibility of Soils″

BS 812-124: 2009 ″Testing aggregates. Method for determination of frost-heave″

Properties to be tested:

GOST 28622-2012	ASTM D 5918-06	BS 812-124: 2009
Relative deformation of the frost heave, units $\varepsilon f\mathrm{h} = \mathrm{h}f \;/\; di$	Speed of the frost heave, mm/day $\vartheta f\mathrm{h} = \mathrm{h}f \;/\; T$	Absolute deformation of the frost heave, mm $\mathrm{h}f$

Soil classification according to frost heave:

Frost heave characteristic	GOST 28622	ASTM D 5918	
	Relative deformation, units	**Speed of deformation 8h, mm/day**	**Bearing capacity, %**
Not sensitive to heave	< 0,01	<1	> 20
Very weakly sensitive to heave	-	1 – 2	20 – 15
Weakly sensitive to heave	0,010 – 0,035	2 – 4	15 – 10
Moderately sensitive to heave	0,035 – 0,070	4 – 8	10 – 5
Very sensitive to heave	0,07 – 0,10	8 – 18	5 – 2
Excessive sensitive to heave	> 0,10	> 16	<2
The bearing capacity index is determined as the ratio between CBR of frozen soil and CBR of non-frozen soil			

Testing equipment:

Parameters of the equipment	GOST 28622-2012	ASTM D 5918-06	BS 812-124: 2009
Number of samples	1	4	9
Geometry of the sample	∅ 100 × 150 mm	∅ 146 × 150 mm	∅ 100 × 150 mm
Vertical load	≤ 50 kPa	3,5 кPa	not applied
Temperature sensors	At the top, bottom, base	At the top, bottom, 7 sensors in sample in different depth	4 in air, 5 in base, 1 at the top of the sample

Parameters of the equipment	GOST 28622-2012	ASTM D 5918-06	BS 812-124: 2009
Temperature at the top and bottom of the sample	- 4 °C + 1 °C	- 12 °C + 12 °C	- 4 °C + 3 ÷ 4,5 °C
Temperature of the environment	+ 1 °C	+ 2 °C	+ 15 ÷ 25 °C
Temperature of freezing	yes	is determined	no
Freezing/thawing	no	yes	no
Number of cycles	no (2 cycles for preparing sample)	2	no
Preparing/testing time	1 day no	1 day 5 days	5 days 4 days
Time of freezing through the sample	not measuring	measuring	provides
Permanent water level	no	yes	yes
Freezing deepness	yes	no	no

3. CLIMATIC CONDITIONS IN LATVIA

Climate features characteristic to Latvia are determined by the amount of solar radiation, air mass transfer with atmospheric circulation from the northern part of the Atlantic Ocean, the proximity of the Baltic Sea and the Gulf of Riga, as well as the land relief (Kļaviņš et al., 2008).

In order to provide a representative characterisation of the climatic conditions of a particular territory, a summary of meteorological conditions for a thirty-year period is usually applied. According to the World Meteorological Organization technical guidelines, standard norms of the climatic parameters or the characteristic climatic conditions can be defined as average values of climatic parameters calculated for a period of 30 consecutive years. Currently, an internationally accepted climatic standard norm period runs from 1 January 1981 to 31 December 2010. Every decade, the climatic standard norm is recalculated, so at the end of this decade, the standard norm will correspond to the period from 1 January 1991 to 31 December 2020 (Avotniece et al, 2017).

Along with the climatic norms, the climatic reference point is also used in climatology. According to the current World Meteorological Organization technical guidelines for assessing long-term climate changes and climate variability characterisation, a 30-year reference period is applied from 1 January 1961 to 31 December 1990. This period is used to make it possible to assess the extent of climate change and variability, as well as to compare the changes observed among different countries worldwide against the defined standard or reference climate conditions (WMO, 2011).

3.1. Air Temperature Regime

As mentioned above, the distribution and regime of air temperatures in the territory of Latvia are defined by the sun radiation received and atmospheric circulation peculiarities, as well as influenced by the Baltic Sea, Gulf of Riga and land relief. The relatively plane relief causes the warm and humid air masses that form above the Atlantic Ocean influenced by sea air planetary flows to move from west to east, penetrating far into the continent of Europe. The temperature fluctuations in the coastal regions are smaller. Because the seawater accumulates a large amount of heat during the summer, winters and autumns are warmer than further into the terrestrial areas. In spring, by contrast, it is cooler at the coast, as water warms up more slowly than soil (Nikodemus et al., 2018).

The lowest average air temperature during the climatic norm of the last 30 years over the period (1981-2010) was in February (-3.6 °C). The February air temperature distribution corresponds to the decrease in the oceanic air mass proportion from west to east (Figure 3.1.) (Nikodemus et al., 2018).

Over a long period from 1950 to 2010, the statistically most significant air temperature increase is observed for average annual temperatures. In terms of months, the statistically most significant increase is shown for average air temperatures in March and April. Statistically significant temperature changes over the period 1950-2010 have not been found in October, November or December (Nikodemus et al., 2018).

Figure 3.1. Average Air Temperature (°C) in Latvia in February (1981-2010) (Nikodemus et al., 2018).

3.2. Average Annual Minimum Daily Air Temperatures

Similar to the territorial distribution of the average annual air temperature, the lowest daily average air temperature values are observed in the eastern part of the country, with the highest values on the western coast of Kurzeme, where the frost periods are shorter, less stable and of lower intensity. Yet, unlike the average annual air temperature with the most specific reference to the south-western regions of the country, the minimum daily average air temperature values are higher in the north-western part of Kurzeme. On average, the minimum daily air temperature values vary between -8.8 and -29.1 °C (Avotniece, Aņiskeviča and Maļinovskis, 2017) (Figure 3.2.)

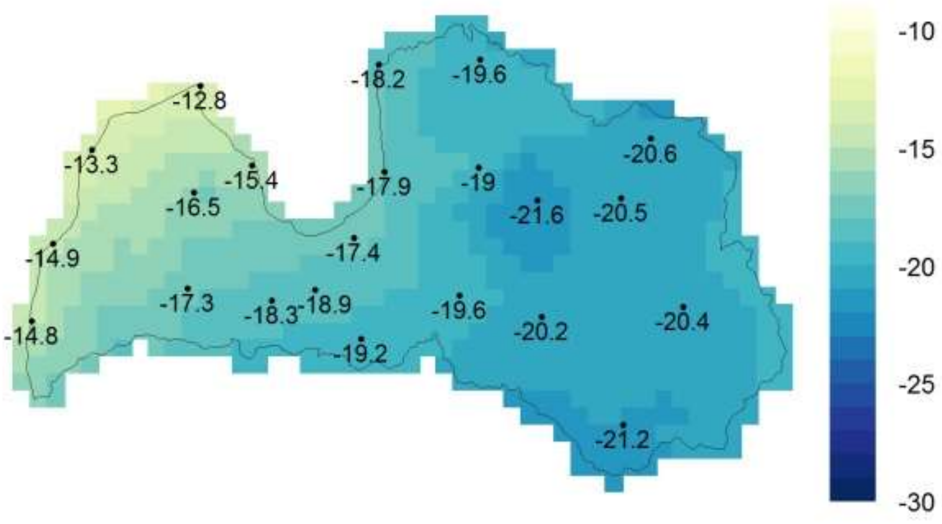

Figure 3.2. Multiannual Average Annual Minimum Daily Air Temperature (°C) in Latvia over the Period from 1961 till 2001.

The average annual minimum daily air temperature values characterise a single highest daily average air temperature value in terms of a year; consequently, the distribution of these values by years can differ considerably, both in terms of territory and intensity.

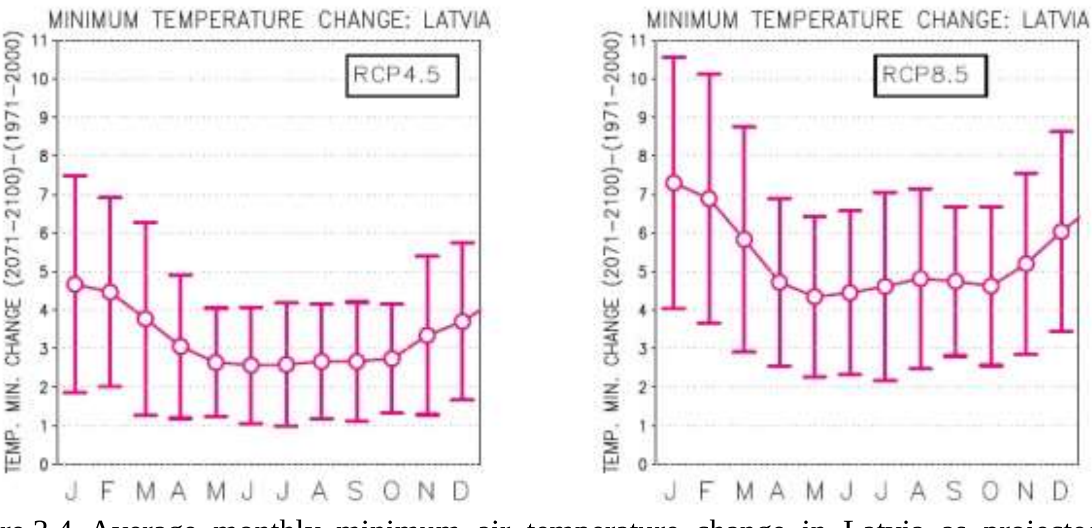

Figure.3.4 Average monthly minimum air temperature change in Latvia as projected by ensemble of global climate models (change in °C 2071.-2100.g. compared to 1971.-2000.g. values) according to RCP 4,5 (left) and RCP 8,5 (right) climate change scenarios

Climate model projections show that depending on a particular month (Figure 3.4) until the end of the century the minimum air temperature according to RCP 4,5 scenario in Latvia will rise by 2,5-5°C, and according to RCP 8,5 scenario – by 4-7,5°C. Similar to mean air temperature change, also minimum air temperatures will most significantly rise during the period from November to April - by 3-5,5°C and 5-7,5°C respectively, thus substantially influencing the amount of cold and snowy winters in the future. And according to both climate change scenarios the most pronounced air temperature rise in winter season will be in the Eastern part of Latvia (figure 3.5 and 3.6), thus in a radical and complex way altering the climatic conditions of this coldest and most snow-rich region of the country (Avotniece, Aņiskeviča and Maļinovskis, 2017)

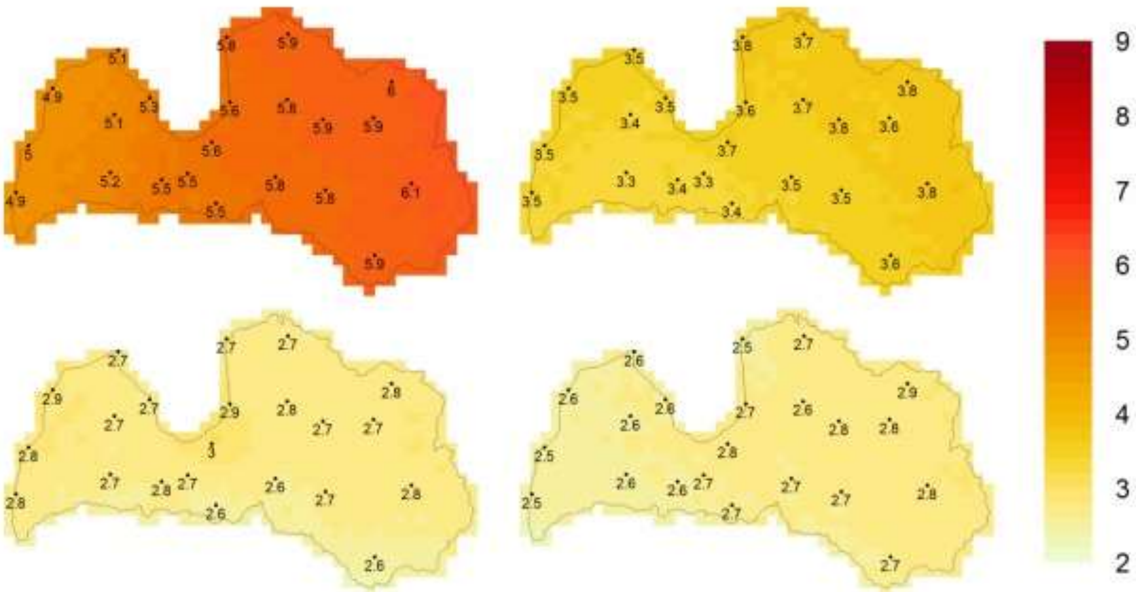

Figure 3.5. Average seasonal minimum air temperature change in Latvia as projected by ensemble of global climate models (upper raw from left to right - winter, spring, lower raw – summer, autumn) (change in °C, 2071.-2100.g. compared to 1961.-1990.g. values) according to RCP 4,5 climate change scenario.

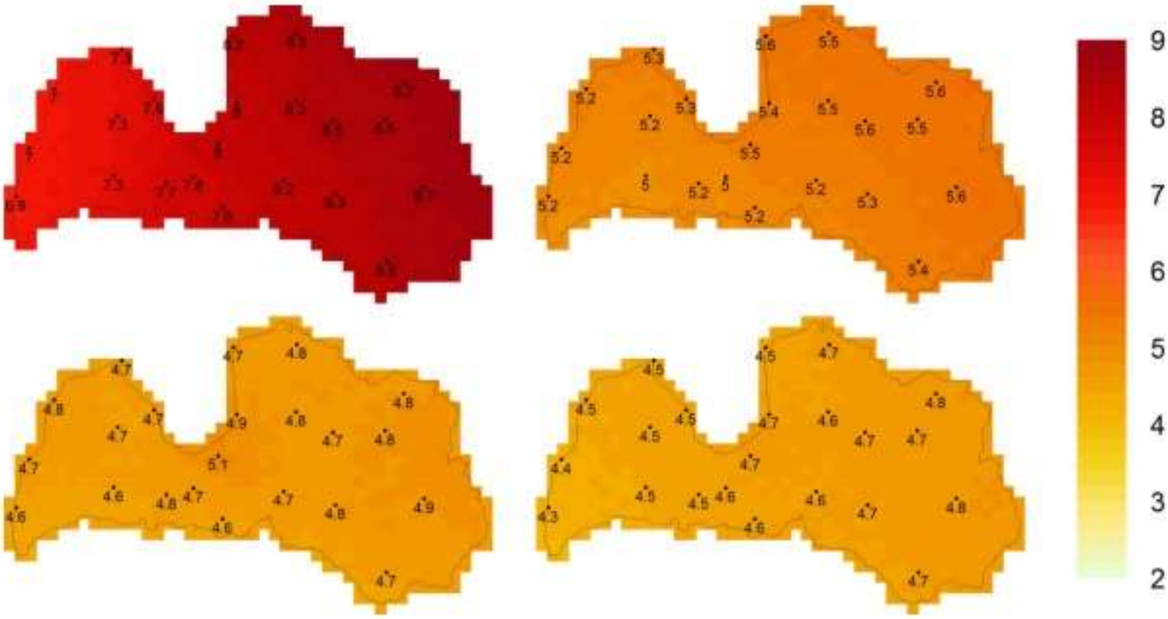

Figure 3.6. Average seasonal minimum air temperature change in Latvia as projected by ensemble of global climate models (upper raw from left to right - winter, spring, lower raw – summer, autumn) (change in °C, 2071.-2100.g. compared to 1961.-1990.g. values) according to RCP 8,5 climate change scenario.

3.3. Snow Cover

Weather conditions in winter and snow cover formation are significant indicators in the climate system. Seasonal snow cover can contain high quantities of water, which, when melting, influences the hydrological regime of both surface and underground waters. Snow depth and persistence are significant factors for road maintenance (Nikodemus et al., 2018).

The geographical location of a site influences not only snow cover duration but also its depth (both seasonal average and ten-day period maximum). The depth is considered one of the most essential snow cover indicators. The average snow cover depth changes during the winter season in Latvia are shown in Figure 3.7.

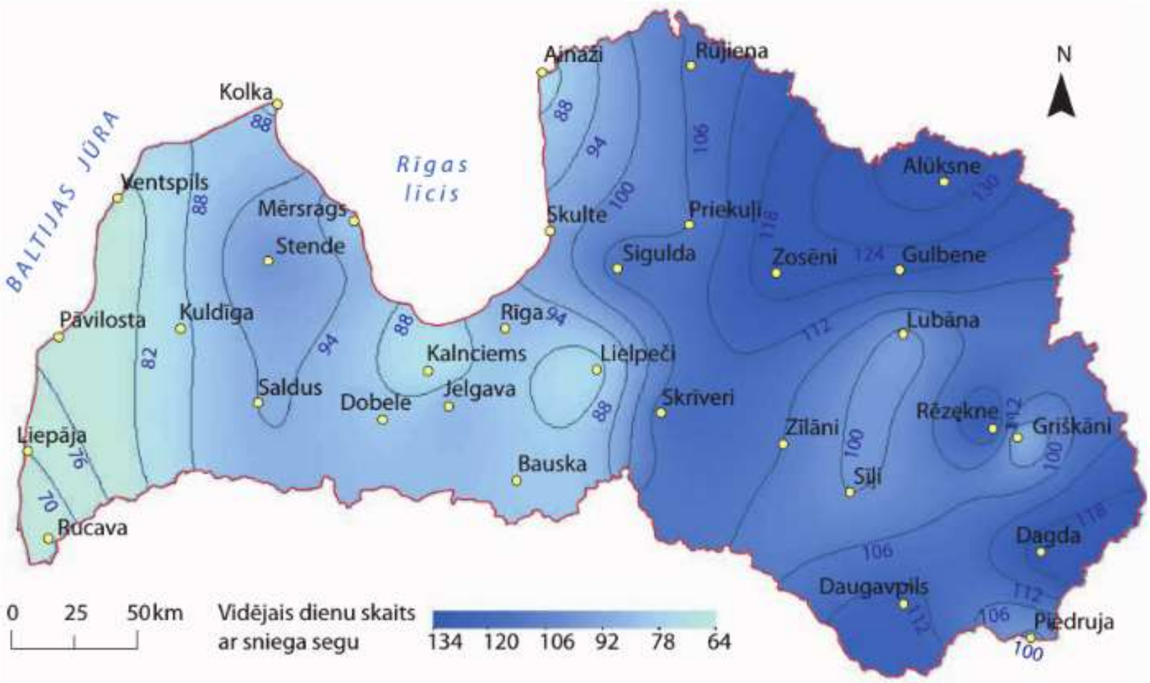

Figure 3.7. Average Number of Days with Snow in Latvia (1950 -2010) (Kļaviņš and Zaļoksnis, 2016).

In general, snow cover in Latvia is characterised by a relatively high variety. This applies both to the number of days when a constant snow cover is formed and exists, and to the snow depth. The snow cover forms during the cold period of the year when the air temperature is mostly below zero, but the annual snow cover duration changes. The regional variability is defined by the air temperature distribution. Moving further from the Baltic Sea and Gulf of Riga coasts, the snow cover persistence period and depth increase, especially in regions where the surface height above sea level and position to the prevailing winds encourage the upward movement of the air masses. It has been proved that the Baltic Sea influence can be clearly felt over a 30-100 km wide coastline (Nikodemus et al. 2018).

The first snow cover appears between 1 and 23 November: at the Baltic Sea coast, it usually only forms during the last ten days of November, but during the second ten-day period, it appears at the Gulf of Riga coast and on the Zemgale plain, as well as on the Kurzeme plateau. Its earliest appearance, during the first ten-day period, is on the Vidzeme plateau and regions to the north of it, the lowlands of Eastern Latvia and Latgale. According to multiannual indicators, snow cover in Alūksne usually appears on the 1 November, but in Dagda and Zosēni on the 5th of November. A persistent snow cover in Latvia is formed on average 30-45 days after the formation of the first snow cover, i.e. between the 6 December and 6 January (in Alūksne and Ventspils), but over the largest part of the territory during the second and third ten-day periods in December (Nikodemus et al. 2018).

A persistent snow cover does not even form or forms very late in a rather wide part of the territory of Latvia, but winters with non-persistent snow cover are very rare in the eastern regions of the country. At all stations the snow depth reaches its maximum during the last ten days of February. On average, the deepest snow cover is formed in the last ten days of February (ranging from 7 cm in the western part, up to 42 cm in the central part). The deepest snow cover recorded by weather stations is 130 cm, in the Vidzeme highlands (Figure 3.8) (Nikodemus et al. 2018).

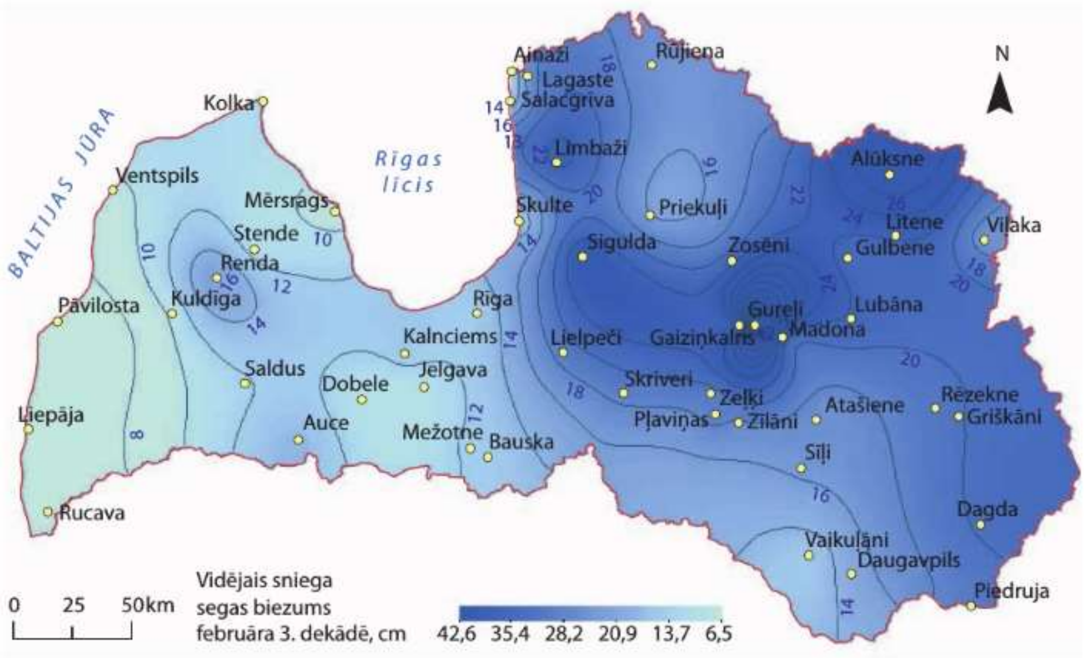

Figure 3.8: Average in Latvia during the of February (1950 -2010) (Kļaviņš and Zaļoksnis, 2016)

3.4. Road weather station data analysis

The following terms have been used in this analysis:

Cold season – period between the first and the last day of the year, when the minimum air temperature was negative (see. Figure 3.11., 3.14., 3.15.);

Frost season – period between the cumulative minimum air temperature maximum and minimum dates (Figure 3.12.)

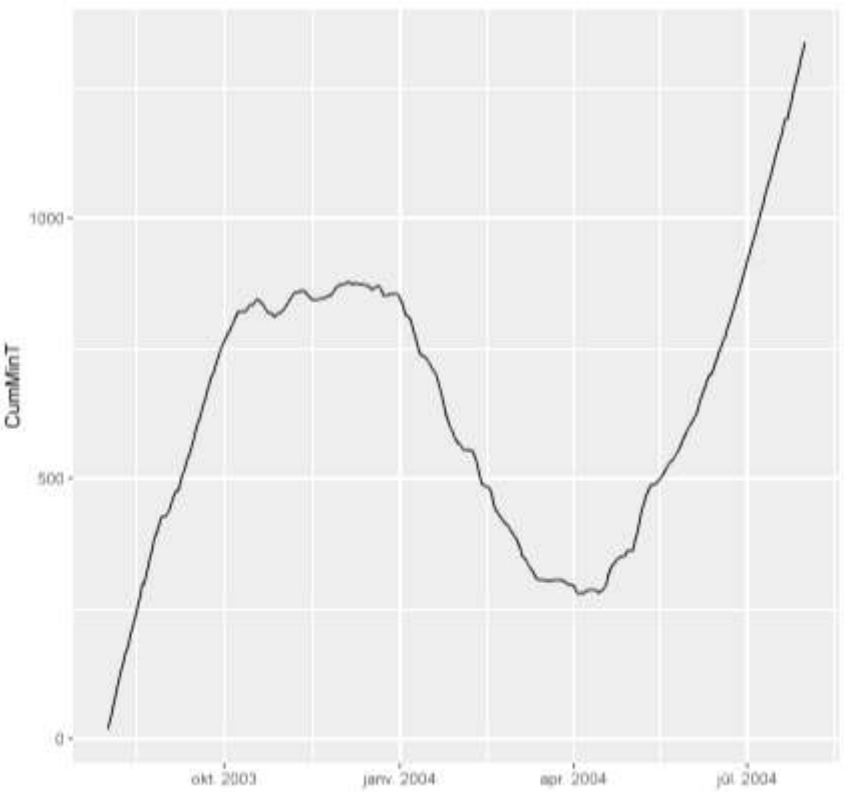

Figure 3.9. Road weather station (RWS) No. LV15, 2003.-2004. season's cumulative minimum air temperature.

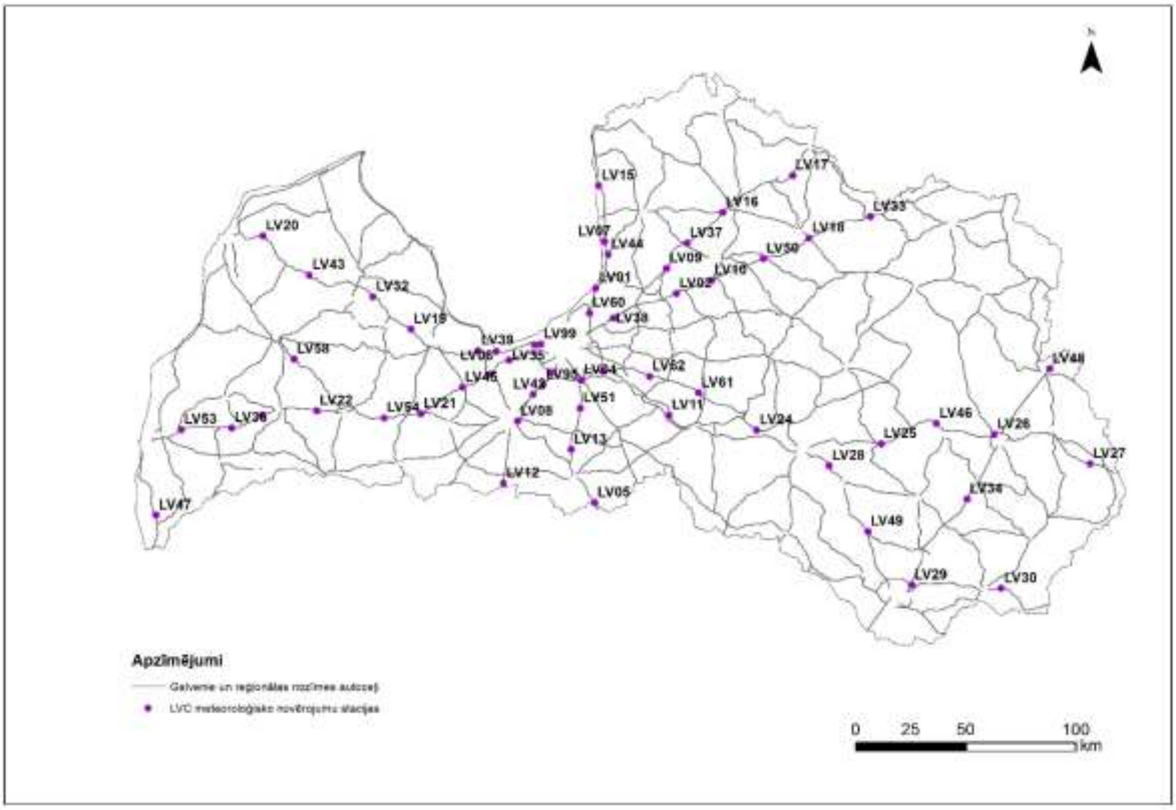

Figure 3.10. Location of Latvian RWS

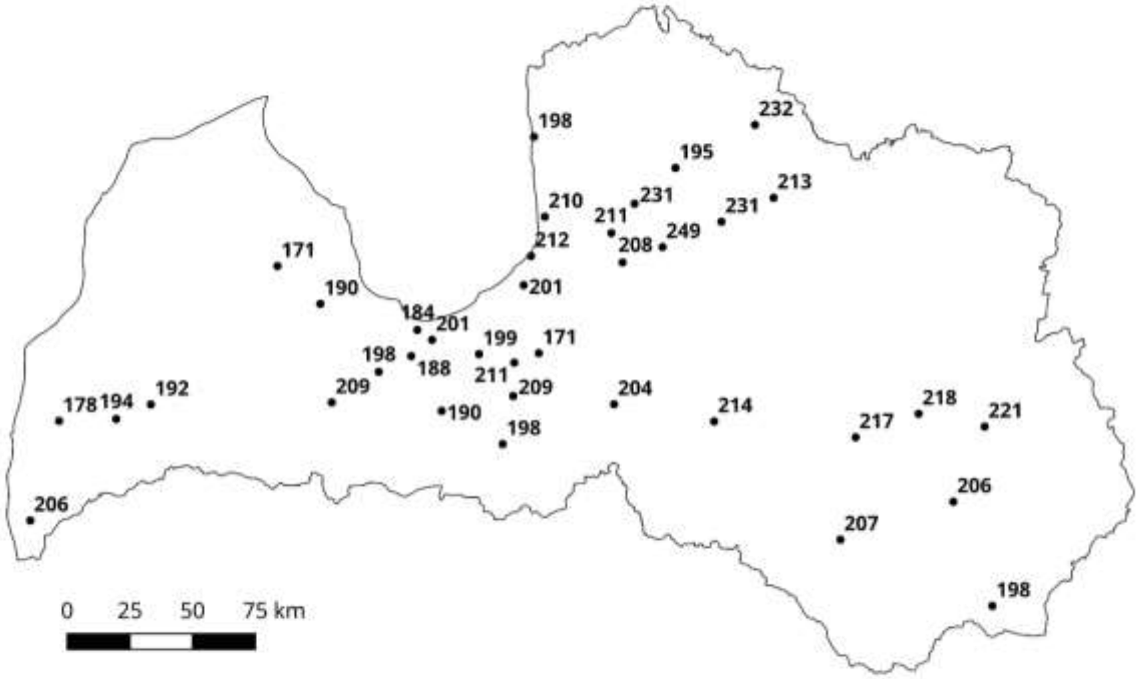

Figure 3.11. Average number of days in Cold season in the period 2001 – 2018, according to the Latvian RWS data.

As we can see in Figure 3.6 the average number of days in Cold season is much greater in Eastern (Latgale) and Northern (Vidzeme) part of Latvia . Also the same situation is Frost season (Figure 3.11 and 3.12).

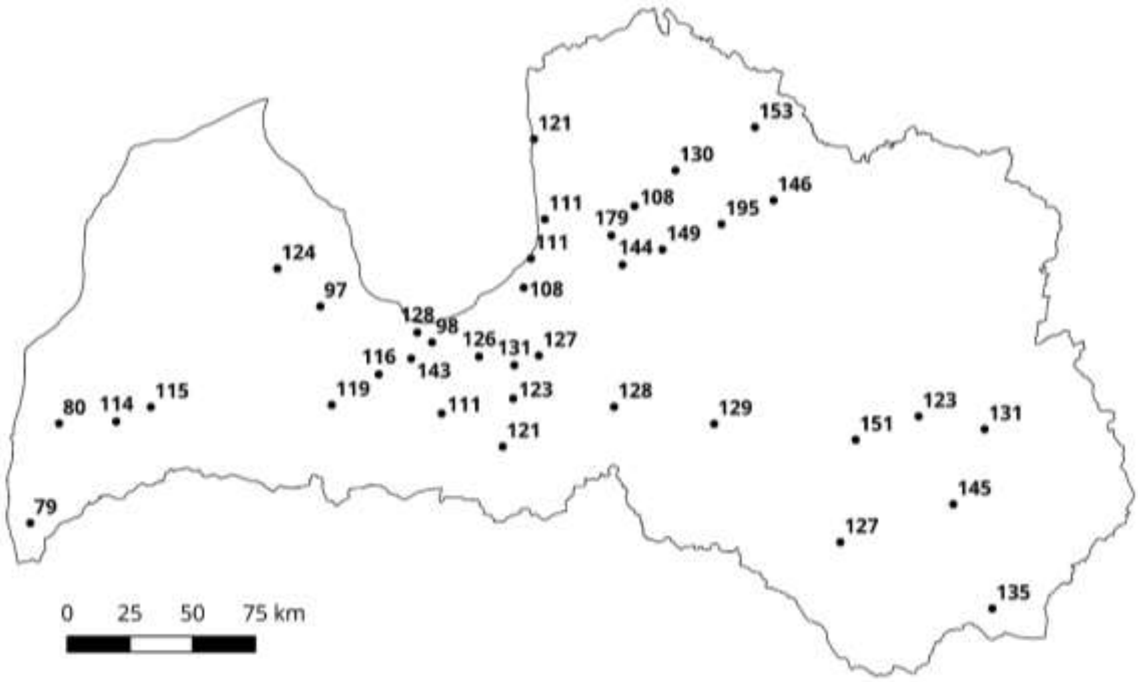

Figure 3.12. Average number of days in Frost season in the period 2001 – 2018, according to the Latvian RWS data.

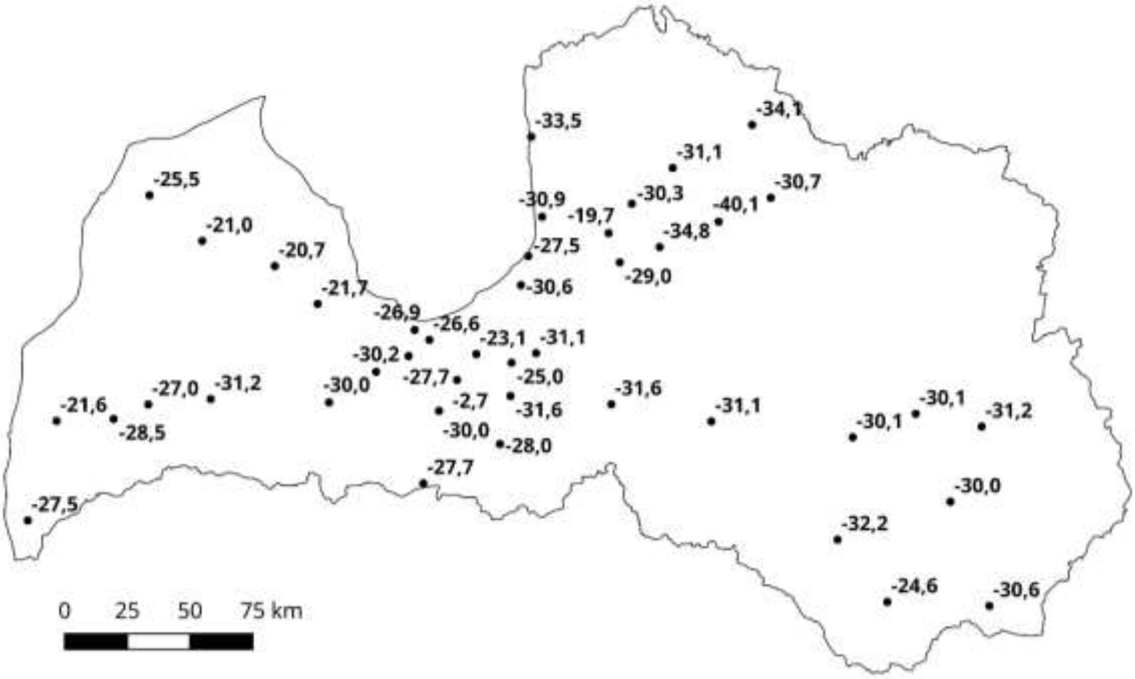

Figure 3.13. Minimum air temperature (°C) in Latvian RWS during the period 2001 – 2018.

Very low minimum air temperature is charaterestic mainly in Latgale, Northeast Vidzeme and in Central Latvia (Figure 3.13)

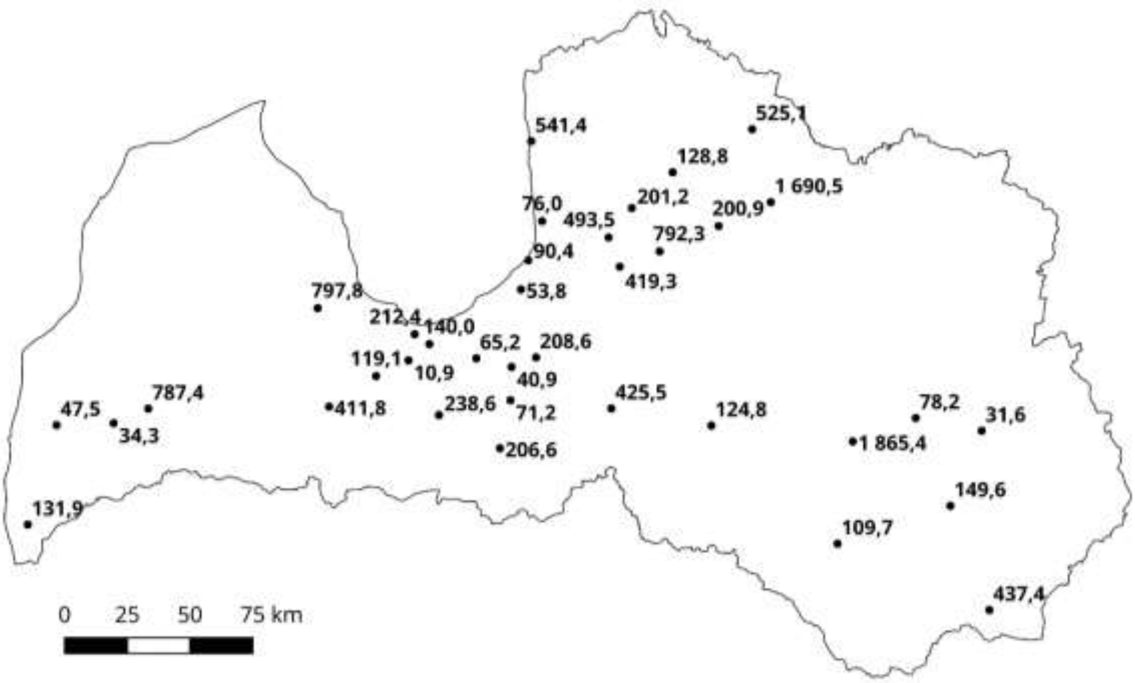

Figure 3.14. Average amount of precipitation (mm) during the Cold season in Latvian RWS during the period 2001 – 2018.

Average amount of precipitation and the average number of days with precipitation during the Cold season is greater in Latgale upland, Vidzeme upland and near coastline of the Baltic sea (Figure 3.14)

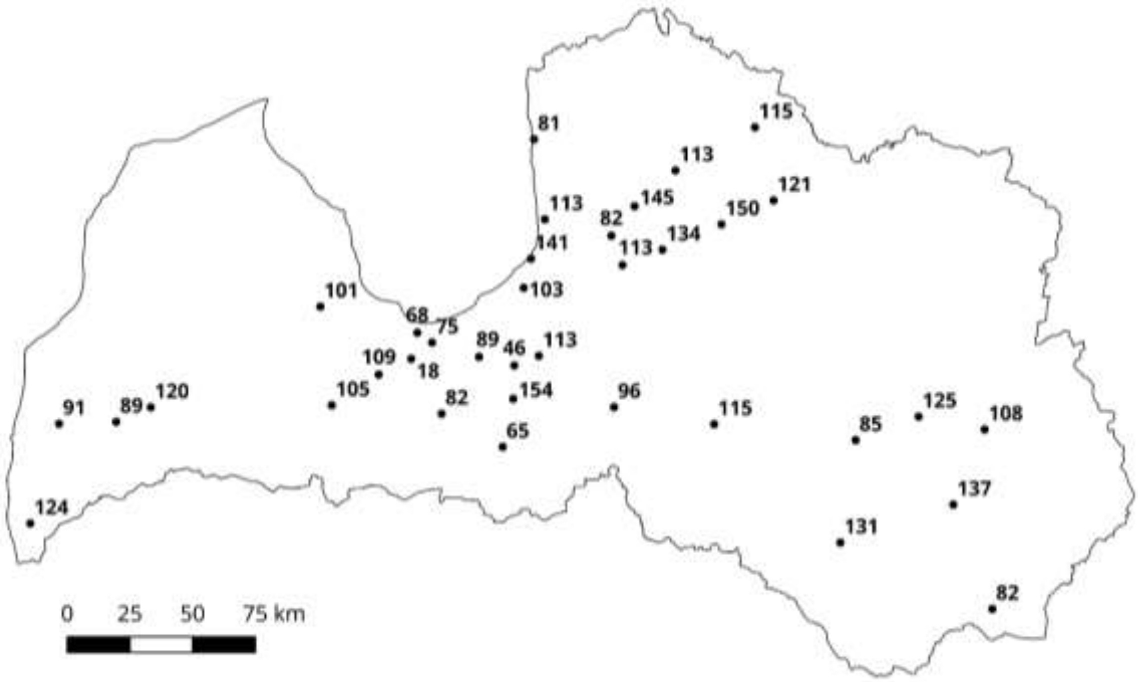

Figure 3.15. Average number of days with precipitation in the Cold season in Latvian RWS during the period 2001 – 2018.

4. SOIL SAMPLING AND LABORATORY ANALYSES

4.1. Selection of soil samples

The selection of soil samples for the realisation of the research was performed by obtaining the necessary soil samples covering the typical soil spectrum found in Latvia, from the deposits (quarries), as well as from different sites of soil dislocation in nature.

Boreholes has been done, to identify and select soil sampling sites. See boreholes dislocation scheme. Two deposit sites were selected as well (abandoned quarry near Baldone, and a quarry ″Āne″ near Jelgava), where soil samples were taken.

In general 7 samples from boreholes, 3 samples from quarrys and one specialy prepared sample (in total, 11 different types of soil samples) were taken and laboratory tests were performed.

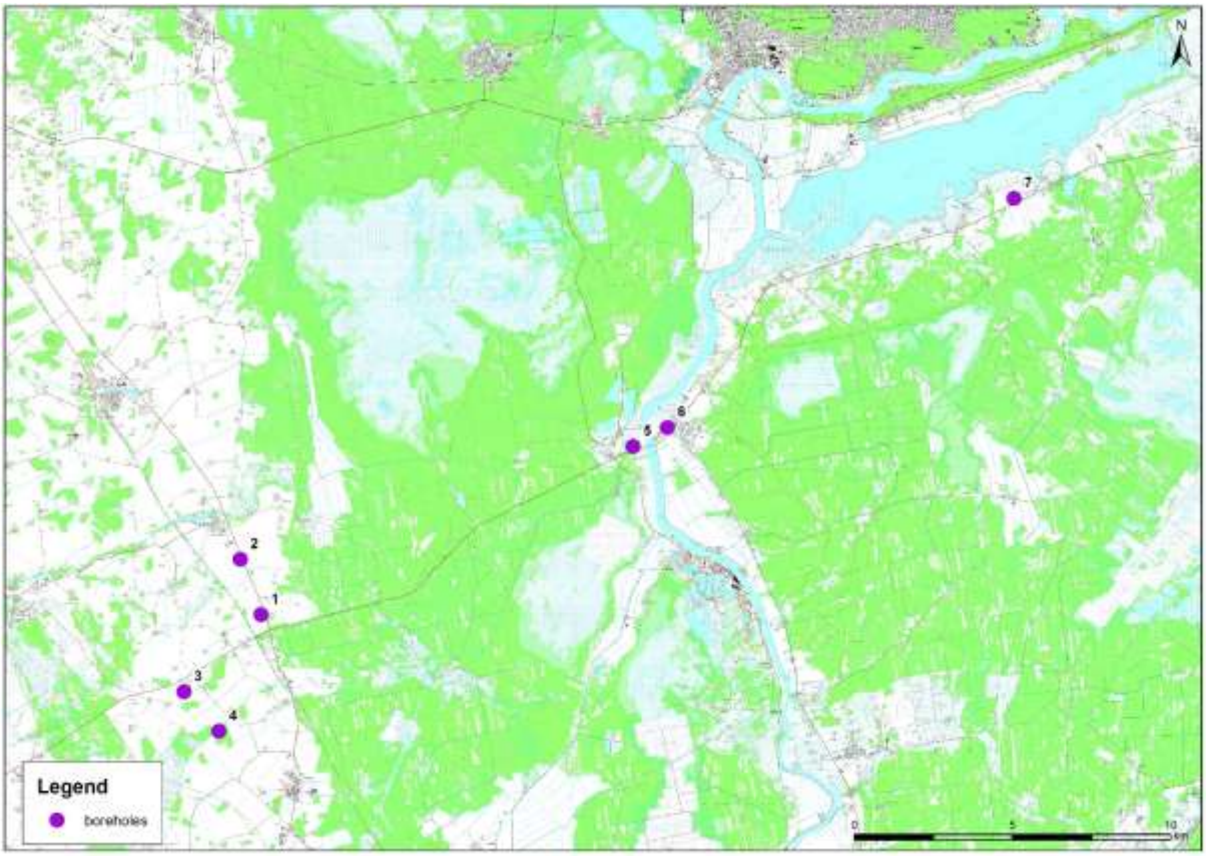

Figure 4.1. Location of the boreholes.

Table 4.1. Description of the boreholes:

Borehole No 1

Soil code	Top of the layer	Bottom of the layer	Layer thicknes	Name of the soil	Soil description	Gound-water	Genesis
	0	0,27	0,27	organic soil			elQ4
siMSa	0,27	0,6	0,33	dusty moderate coarse sand			glQ3
clsiFSa	0,6	0,7	0,1	clay, dusty fine sand	clayy, dusty fine sand with a slight mean gravel growth		glQ4
clsiFSa	0,7	1	0,3	clay, dusty fine sand	clay, dusty fine sand, brownish-red		glQ5
clSi	1	1,4	0,4	clay dust	clay dust		glQ6
clSi	1,4	1,6	0,2	clay dust	clay dust, brownish-red		glQ7
clSi	1,6	1,8	0,2	clay dust	clay dust, brownish-red, clay fractions more than the previous layer		glQ8
Si/FSa	1,8	1,9	0,1	Dust and fine sand	Dust and fine sand, light brown		
Part of the Glacial Lake							

Borehole No 2

Soil code	Top of the layer	Bottom of the layer	Layer thicknes	Name of the soil	Soil description	Gound-water	Genesis
	0	0,7	0,7	organic soil	sandy loan with organic		elQ4
siclSa	0,7	0,9	0,2	sandy loan with gravel grain	sandy loan with 1,2 cm gravel grain		gQ3
siclSa	0,9	1,1	0,2	sandy loan	sandy loan reddish-brown, semi-hard with thin, dusty, gray stripes		gQ4
siclSa	1,1	1,3	0,2	sandy loan	sandy loan reddish brown, plastic with thin, dusty, gray stripes		gQ5
clsiSa + O	1,3	1,8	0,5	sandy loan	sandy loam with a small amount of organic matter, brown-gray, moist		gQ6
The top of the slope of the low hill							

Borehole No 3

Soil code	Top of the layer	Bottom of the layer	Layer thicknes	Name of the soil	Soil description	Gound-water	Genesis
	0	0,2	0,2	organic soil	dusty clay with the organic		elQ4
CL/Si	0,2	0,47	0,27	clay dust	clay dust, starch, gray-brown		glQ3
siFSa	0,47	1,45	0,98	dusty fine sand	dusty fine sand with little clay admixture or interlayer, hard, reddish-brown with gray marbles		glQ3
siclSa	1,45	1,7	0,25	sandy loam	sandy loam with rare carbonate pebbles, hard, reddish-brown		gQ3
North of Glacial Lake							

Borehole No 4

Soil code	Top of the layer	Bottom of the layer	Layer thicknes	Name of the soil	Soil description	Gound-water	Genesis
	0	0,6	0,6	organic soil	dusty clay with the organic		elQ4
Si/Cl	0,6	0,75	0,15	dusty clay	dusty clay, grayish-brown with pieces of organic soil		glQ3
CL/SI	0,75	1,1	0,35	clay dust	clay dust, gray-red-brown		glQ3
siCl	1,1	1,6	0,5	dusty clay	dusty clay, solid with gray interlayers		glQ3
clSifsa	1,6	1,95	0,35	clay dust with sand	clay dust with fine sand admixture		glQ3
clsiSa	1,95	2,05	0,1	sandy loam	sandy loam with moderate coarse sand small admixture, reddish-brown		gQ3
The central northern part of the Glacial Lake, behind the ditch, in the glaciolymnic plain							

Borehole No 5

Soil code	Top of the layer	Bottom of the layer	Layer thickness	Name of the soil	Soil description	Gound-water	Genesis
	0	0,47	0,47	organic soil	dusty fine sand with organic		elQ4
siFSa	0,47	0,75	0,28	dusty fine sand	dusty fine sand with little organic impurity		alQ4 vai mQ4lit
siFSa	0,75	1,2	0,45	dusty fine sand	dusty fine sand, muzzle, yellowish-brown, dusty admixture pretty big		alQ4 vai mQ4lit
siFSa	1,2	1,8	0,6	dusty fine sand	dusty fine sand, muzzle, 1.6 m wet, waxy, yellowish-brown, dust admixture pretty large, under underground water grayish-brown	1,6	alQ4 vai mQ4lit
Behind the Lielupe bridge, according the geological map - the littoral sea plain, although there may also be a Lielupe upper floods terrace							

Borehole No 6

Soil code	Top of the layer	Bottom of the layer	Layer thickness	Name of the soil	Soil description	Gound-water	Genesis
	0	0,38	0,38	organic soil	fine sand with organic		elQ4
Fsa	0,38	0,95	0,57	fine sand	fine sand with a small amount of organic admixture, light tan		eQ4
FSa	0,95	1,6	0,65	fine sand	fine sand brownish-yellow		glQ3ble
The dunes are blown up by the Baltic iceberg plain							

Borehole No 7

Soil code	Top of the layer	Bottom of the layer	Layer thickness	Name of the soil	Soil description	Gound-water	Genesis
	0	0,5	0,5	organic soil	dusty fine sand with organic		elQ4
Fsa	0,5	1,1	0,6	fine sand	fine sand with a little dust, light tan, practically white		mQ4
FSa	1,1	1,25	0,15	fine sand	fine sand with a small amount of dust, light rust yellow		mQ4

Sample of each homogeneous layer (geotechnical element) was tested with 3 different moisture contents.

4.2. Testing soil composition and parameters for frost depth and frost/thaw survey data interpretation

Within the scope of the existing contract work positions, the nature and extent of the soil test properties have been specified to interpret the test research data to achieve the set research objectives. Testing was done in two laboratories, in Ltd. Ceļu eksperts laboratory and in University of Latvia laboratory.

Identification of soil classifications (DIN18196; ISO 14688; GOST 25100) and characteristics was performed by the following laboratory tests:

- granulometric composition in compliance with LVS EN 933-1 (or, if necessary, in compliance with LVS CEN ISO / TS 17892-4 (sieving and pipette method if necessary), also determining fine particle distribution below 0.063 mm mesh;
- plasticity limit in compliance with LVS CEN ISO/TS 17892-12 (for clay soils);
- natural moisture content in compliance with LVS CEN ISO/TS 17892-1;
- natural density in compliance with LVS CEN ISO/TS 17892-2 (if necessary);
- soil particle density LVS CEN ISO/TS 17892-3.
- Filtration coefficient in compliance with *Road specifications 2019* p.12.3 (for sandy soils);
- pH level according to *Road Specifications 2019* p.12.10;
- organic matter content according to *Road Specifications 2019* p.12.5 (as required);
- where possible, determination of the actual density and humidity of soils was done on site where the sample was taken in compliance with LVS EN 1097-5 and BS 1377-9.

The frost-heaving properties of the selected soil samples were tested in the laboratory. Selected samples were prepared with various moisture content levels. The following properties were tested:

- Proctor volumetric weight and optimal moisture content (LVS EN 13286-2);
- Immediate bearing index at 3 different moisture content levels (LVS EN 13286-47);
- California bearing ratio (CBR) at 3 different moisture content levels (LVS EN 13286-47);
- Elasticity module at 3 different moisture content levels (VSN 46-83);
- Frost-heave 3 cycles (GOST 28622-90):
    - soil at optimal moisture content, at 100% compaction;

- soil with increased moisture content above the optimum moisture content level at around 90% to 95% degree of compaction;
- soil with a reduced moisture content below the optimum moisture content level at around 90% to 95% degree of compaction.

Three freezing / thawing cycles were performed within the research. During the test, data on movement and temperature changes of the upper part of the sample were continuously recorded. Identification of samples:

Table 4.1. Identification of samples:

No.	Soil	Sample dislocation
1	1281-1 silty fine Sand (sifSa)	from quarry ″Baldone″
2	1281-2 fine/medium sandy Silt (f/msaSi)	from quarry ″Baldone″
3	1286 silty CLAY (siCl)	from quarry ″Āne″
4	1414-3-1 silty CLAY (fsasiSa)	from borehole 3
5	1414-3-2 fine sandy, clayed SILT (fsaclSi)	from borehole 3
6	1414-4-1 clayed, fine sandy SILT (clfsaSi)	from borehole 4
7	1414-4-2 silty CLAY (siCl)	from borehole 4
8	1414-5-1 slightly silty fine SAND (sifSa)	from borehole 5
9	1414-6-1 slightly medium, fine SAND (mfSa)	from borehole 6
10	clayed SILT (clSi)	from quarry ″Cemex″
11	slightly sandy, clayed SILT (saclSi)	prepaered by ″Ceplis″

4.3. Test results

Table 4.2. Proctor density and optimal moister:

No.	Soil	Proctor	
		Dry density, mg/m^3	Optimal moisture, %
1	1281-1 silty fine Sand (sifSa)	2,057	9,3
2	1281-2 fine/medium sandy Silt (f/msaSi)	2,016	10,2
3	1286 silty CLAY (siCl)	1,710	18,4
4	1414-3-1 silty CLAY (fsasiSa)	1,702	16,7
5	1414-3-2 fine sandy, clayed SILT (fsaclSi)	1,823	13,4
6	1414-4-1 clayed, fine sandy SILT (clfsaSi)	1,977	9,8
7	1414-4-2 silty CLAY (siCl)	1,451	25,4
8	1414-5-1 slightly silty fine SAND (sifSa)	1,666	16,7
9	1414-6-1 slightly medium, fine SAND (mfSa)	1,559	17,7
10	clayed SILT (clSi)	1,732	17,9
11	slightly sandy, clayed SILT (saclSi)	1,774	13,4

Table 4.3. Granulometry:

No.	Soil	**Sieve size (mm)**												
		0,063	**0,125**	**0,250**	**0,5**	**1,0**	**2,0**	**4,0**	**5,6**	**8,0**	**11,2**	**16,0**	**22,4**	**31,5**
1	1281-1 silty fine Sand (sifSa)	48,1	68,3	83,3	89,6	92,4	94,5	96,2	97,1	98,3	99,1	100	100	100
2	1281-2 fine/medium sandy Silt (f/msaSi)	39,7	53,5	66,7	77,7	85,1	89,7	92,7	93,9	95,7	96,5	96,5	96,5	100
3	1286 silty CLAY (siCl)	99,0	99,2	99,7	100	100	100	100	100	100	100	100	100	100
4	1414-3-1 silty CLAY (fsasiSa)	70,3	78,5	89,3	95,7	98,1	99,3	99,9	100	100	100	100	100	100
5	1414-3-2 fine sandy, clayed SILT (fsaclSi)	60,5	71,2	84,1	90,5	93,2	94,7	95,6	96,2	97	98,2	100	100	100
6	1414-4-1 clayed, fine sandy SILT (clfsaSi)	48,0	59,2	76,8	87,9	92,4	95	97,1	98,7	99,4	100	100	100	100
7	1414-4-2 silty CLAY (siCl)	96,7	97,4	98,2	98,8	99,3	99,9	100	100	100	100	100	100	100
8	1414-5-1 slightly silty fine SAND (sifSa)	12,5	55,2	99,4	99,8	99,9	100	100	100	100	100	100	100	100

No.	Soil	Sieve size (mm)												
		0,063	**0,125**	**0,250**	**0,5**	**1,0**	**2,0**	**4,0**	**5,6**	**8,0**	**11,2**	**16,0**	**22,4**	**31,5**
9	1414-6-1 slightly medium, fine SAND (mfSa)	0,3	11,2	99,5	99,7	99,9	100	100	100	100	100	100	100	100
10	clayed SILT (clSi)	99,4	99,8	99,9	100	100	100	100	100	100	100	100	100	100
11	slightly sandy, clayed SILT (saclSi)	79,5	89,2	97,2	99,2	99,6	99,9	100	100	100	100	100	100	100

Table 4.4. Immediate bearing index with reduced moister of the soil:

No.	Soil	Immediate bearing index – 1			
		Moisture, %	Density, Mg/m3	Compaction, %	Immediate bearing index, %
1	1281-1 silty fine Sand (sifSa)	6,8	1,948	94,7	37,4 (at 2,5 mm)
2	1281-2 fine/medium sandy Silt (f/msaSi)	7,6	1,939	96,2	35,6 (at 2,5 mm)
3	1286 silty CLAY (siCl)	15,1	1,68	98,2	25,63 (at 2,5 mm)
4	1414-3-1 silty CLAY (fsasiSa)	13	1,569	92,2	19,75 (at 2,5 mm)
5	1414-3-2 fine sandy, clayed SILT (fsaclSi)	9,1	1,713	94,0	21,1 (at 2,5 mm)
6	1414-4-1 clayed, fine sandy SILT (clfsaSi)	7,0	1,823	92,2	32,1 (at 2,5 mm)
7	1414-4-2 silty CLAY (siCl)	20,9	1,39	95,8	16,05 (at 2,5 mm)
8	1414-5-1 slightly silty fine SAND (sifSa)	12,2	1,668	100,1	34,3 (at 2,5 mm
9	1414-6-1 slightly medium, fine SAND (mfSa)	14,5	1,575	101,0	9,93 (at 2,5 mm)
10	clayed SILT (clSi)	14,9	1,695	97,9	15,0 (at 2,5 mm)
11	slightly sandy, clayed SILT (saclSi)	10,0	1,708	96,3	28,2 (at 2,5 mm)

Table 4.5. Immediate bearing index with optimal moister of the soil::

No.	Soil	Immediate bearing index – 2			
		Moisture, %	Density, Mg/m3	Compaction, %	Immediate bearing index, %
1	1281-1 silty fine Sand (sifSa)	9,4	2,042	99,3	35,65 (at 5,0 mm)
2	1281-2 fine/medium sandy Silt (f/msaSi)	10,5	2,017	100,0	25,73 (at 5,0 mm)
3	1286 silty CLAY (siCl)	18,2	1,733	101,3	12,69 (at 5,0 mm)
4	1414-3-1 silty CLAY (fsasiSa)	16	1,69	99,3	15,36 (at 2,5 mm)
5	1414-3-2 fine sandy, clayed SILT (fsaclSi)	12,2	1,788	98,1	16,2 (at 2,5 mm)
6	1414-4-1 clayed, fine sandy SILT (clfsaSi)	9,2	1,986	100,5	24,7 (at 5,0 mm)
7	1414-4-2 silty CLAY (siCl)	23,6	1,478	101,9	14,51 (at 2,5 mm)
8	1414-5-1 slightly silty fine SAND (sifSa)	15,1	1,686	101,2	27,1 (at 2,5 mm)
9	1414-6-1 slightly medium, fine SAND (mfSa)	16,9	1,58	101,3	10,43 (at 2,5 mm)
10	clayed SILT (clSi)	18,2	1,763	101,8	6,3 (at 5,0 mm)
11	slightly sandy, clayed SILT (saclSi)	12,6	1,791	101,0	14,32 (at 2,5 mm)

Table 4.6. Immediate bearing index with increased moister of the soil:

No.	Soil	Immediate bearing index – 3			
		Moisture, %	Density, Mg/m3	Compaction, %	Immediate bearing index, %
1	1281-1 silty fine Sand (sifSa)	12,3	1,935	94,1	0,92 (at 5,0 mm)
2	1281-2 fine/medium sandy Silt (f/msaSi)	13,1	1,927	95,6	0,89 (at 2,5 mm)
3	1286 silty CLAY (siCl)	22,4	1,634	95,6	0,42 (at 5,0 mm)
4	1414-3-1 silty CLAY (fsasiSa)	19,2	1,712	100,6	8,97 (at 5,0 mm)
5	1414-3-2 fine sandy, clayed SILT (fsaclSi)	16,4	1,813	99,5	5,4 (at 2,5 mm)
6	1414-4-1 clayed, fine sandy SILT (clfsaSi)	11,5	2,005	101,4	4,0 (at 5,0 mm)
7	1414-4-2 silty CLAY (siCl)	26,5	1,501	103,4	9,64 (at 2,5 mm)
8	1414-5-1 slightly silty fine SAND (sifSa)	18,1	1,616	97,0	4,86 (at 5,0 mm)
9	1414-6-1 slightly medium, fine SAND (mfSa)	18,3	1,562	100,2	7,47 (at 5,0 mm)
10	clayed SILT (clSi)	21,7	1,701	98,2	1,44 (at 5,0 mm)
11	slightly sandy, clayed SILT (saclSi)	15,9	1,829	103,1	4,87 (at 5,0 mm)

Table 4.7. CBR with different moisture of the soil:

No.	Soil	CBR opt. -3%, preload 2kg		CBR opt. moisture, preload 2kg		CBR opt. +3%, preload 2kg	
		Swelling, mm	CBR	Swelling, mm	CBR	Swelling, mm	CBR
1	1281-1 silty fine Sand (sifSa)	+1,50	3,96 (at 2,5 mm)	+0,18	15,09 (at 5,0 mm)	-0,17	0,58 (at 5,0 mm)
2	1281-2 fine/medium sandy Silt (f/msaSi)	+0,56	10,14 (at 2,5 mm)	+0,43	14,59 (at 5,0 mm)	-0,63	0,39 (at 5,0 mm)
3	1286 silty CLAY (siCl)	+6,70	0,56 (at 5,0 mm)	+4,30	0,83 (at 5,0 mm)		
4	1414-3-1 silty CLAY (fsasiSa)	+8,91	0,48 (at 5,0 mm)	+8,29	0,60 (at 2,5 mm)	+0,47	2,18 (at 2,5 mm)

No.	Soil	CBR opt. -3%, preload 2kg		CBR opt. moisture, preload 2kg		CBR opt. +3%, preload 2kg	
		Swelling, mm	CBR	Swelling, mm	CBR	Swelling, mm	CBR
5	1414-3-2 fine sandy, clayed SILT (fsaclSi)	+7,05	0,44 (at 5,0 mm)	+4,33	1,06 (at 5,0 mm)		
6	1414-4-1 clayed, fine sandy SILT (clfsaSi)	+3,79	0,66 (at 2,5 mm)	+2,15	1,67 (at 2,5 mm)		
7	1414-4-2 silty CLAY (siCl)	+13,70	0,37 (at 2,5 mm)	+10,84	0,46 (at 2,5 mm)		
8	1414-5-1 slightly silty fine SAND (sifSa)	+0,15	44,0 (at 5,0 mm)	0	7,81 (at 5,0 mm)	-0,38	1,80 (at 5,0 mm)
9	1414-6-1 slightly medium, fine SAND (mfSa)	-0,10	8,12 (at 5,0 mm)	0	12,47 (at 5,0 mm)	-0,01	4,83 (at 5,0 mm)
10	clayed SILT (clSi)	+7,00	0,37 (at 5,0 mm)	+2,06	2,12 (at 5,0 mm)	-0,02	1,78 (at 5,0 mm)
11	slightly sandy, clayed SILT (saclSi)	+6,17	0,33(at 2,5 mm)	+1,56	3,88 (at 2,5 mm)	+4,98	0,65 (at 2,5 mm)

Table 4.8. Elasticity modulus of the soil:

No.	Soil	E-mod					
		Moisture	E-mod1, Mpa	Moisture	E-mod2, Mpa	Moisture	E-mod3, Mpa
1	1281-1 silty fine Sand (sifSa)	6,8	185,0	9,4	99,4	12,3	7,3
2	1281-2 fine/medium sandy Silt (f/msaSi)	7,6	186,4	10,5	53,0	13,1	15,2
3	1286 silty CLAY (siCl)	15,1	71,6	18,2	32,6	22,4	4,2
4	1414-3-1 silty CLAY (fsasiSa)	13,0	109,4	16,0	67,8	19,2	41,9
5	1414-3-2 fine sandy, clayed SILT (fsaclSi)	9,1	100,5	12,2	53,0	16,4	27,1
6	1414-4-1 clayed, fine sandy SILT (clfsaSi)	7,0	158,2	9,2	109,4	11,5	24,6
7	1414-4-2 silty CLAY (siCl)	20,9	62,5	23,6	46,9	26,5	31,6
8	1414-5-1 slightly silty fine SAND (sifSa)	12,2	106,7	15,1	84,3	18,1	28,4

No.	Soil	E-mod					
		Moisture	E-mod1, Mpa	Moisture	E-mod2, Mpa	Moisture	E-mod3, Mpa
9	1414-6-1 slightly medium, fine SAND (mfSa)	14,9	83,2	17,3	73,7	18,7	54,5
10	clayed SILT (clSi)	14,9	54,2	18,2	21	21,7	16,9
11	slightly sandy, clayed SILT (saclSi)	10	119,1	12,6	71,1	15,9	25,8

Table 4.9. Filtration, organic matters, natural density and moisture:

No.	Soil	Filtration coefficient			Organic matter, %	Natural density and moisture (sampling with ring)	
		Dray Proctor density, Mg/m3	Optimal moisture, %	Filtration coefficient, m/day		Dray density, Mg/m3	Moisture, %
1	1281-1 silty fine Sand (sifSa)	-	-	-	0,6	-	-
2	1281-2 fine/medium sandy Silt (f/msaSi)	-	-	-	0,9	-	-
3	1286 silty CLAY (siCl)	-	-	-	4,0	-	-
4	1414-3-1 silty CLAY (fsasiSa)	-	-	-	3,7	1,665	20,2
5	1414-3-2 fine sandy, clayed SILT (fsaclSi)	-	-	-	2,4	-	-
6	1414-4-1 clayed, fine sandy SILT (clfsaSi)	-	-	-	2,7	1,758	8,5
7	1414-4-2 silty CLAY (siCl)	-	-	-	5,2	1,438	29,5
8	1414-5-1 slightly silty fine SAND (sifSa)	1,728	13,8	0,02	0,9	1,634	18,2
9	1414-6-1 slightly medium, fine SAND (mfSa)	1,602	15,5	2,50	0,1	1,563	6,2
10	clayed SILT (clSi)	-	-	-	3,4	-	-
11	slightly sandy, clayed SILT (saclSi)	-	-	-	2,5	-	-

Table 4.10. Plasticity of the soils and pH:

No	Soil	**Atterberg limits** *LVS EN CEN ISO/TS 17892-12:2005 (60g/60°)*				pH (RoadSpec. 2019. p.12.10.)
		Plasticity **Wp, %**	Flowing **W_L** (60g/60°), **%**	Plasticity index **Ip**	Flowing indexs **I_L**	
1	1281-1 silty fine Sand (sifSa)	13	18	5	-	8,77
2	1281-2 fine/medium sandy Silt (f/msaSi)	13	20	7	-	8,60
3	1286 silty CLAY (siCl)	19	40	21	-	8,50
4	1414-3-1 silty CLAY (fsasiSa)	18	46	28	0,08	8,01
5	1414-3-2 fine sandy, clayed SILT (fsaclSi)	16	36	20	-	8,43
6	1414-4-1 clayed, fine sandy SILT (clfsaSi)	12	25	13	-0,27	8,45
7	1414-4-2 silty CLAY (siCl)	29	79	50	0,01	7,93
8	1414-5-1 slightly silty fine SAND (sifSa)	-	-	-	-	8,11
9	1414-6-1 slightly medium, fine SAND (mfSa)	-	-	-	-	7,98
10	clayed SILT (clSi)	19	42	23	-	8,44
11	slightly sandy, clayed SILT (saclSi)	15	36	20	-	8,55

Table 4.11. Freezing – 1 cycle:

		1. freezing					
No	Soil	Data from equipment			Data from laser measuring device, mm		
		Average temperature during freezing, ^{o}C	Preload Mpa	Frost heave, mm	Before freezing 12h	Frost heave, mm	Thawing comper with beginning
1-1	1281-1 silty fine Sand (sifSa)	-5,4	0,022	0,60	0,2	0,6	-0,4
1-2	1281-1 silty fine Sand (sifSa)	-6,3	0,019	1,28	-0,8	0,8	-3
1-3	1281-1 silty fine Sand (sifSa)	-5,0	0,022	1,09	0,4	1,2	0,4
2-1	1281-2 fine/medium sandy Silt (f/msaSi)	-5,8	0,021	0,10	0,4	0,4 (1,4)	0
2-2	1281-2 fine/medium sandy Silt (f/msaSi)	-5,4	0,018	1,01	-1,0	0,6	-4,2
2-3	1281-2 fine/medium sandy Silt (f/msaSi)	-4,6	0,022	0,32	0,6	(-2,6)	0,4
3-1	1286 silty CLAY (siCl)	-6,8	0,022	0,01	0,6	0,4 (1,2)	0,8
3-2	1286 silty CLAY (siCl)	-6,4	0,020	3,99	0,0	2,8	-2,4
4-1	1414-3-1 silty CLAY (fsasiSa)	-7,6	0,022	1,17	1,0	0,6	1,2
4-2	1414-3-1 silty CLAY (fsasiSa)	-6,8	0,022	2,01	0,2	1,8	2,2
5-1	1414-3-2 fine sandy, clayed SILT (fsaclSi)	-6,9	0,021	0,31	0,8	0,2	0,6
5-2	1414-3-2 fine sandy, clayed SILT (fsaclSi)	-6,4	0,022	1,44	0,2	1,2	-0,6
6-1	1414-4-1 clayed, fine sandy SILT (clfsaSi)	-7,0	0,022	0,02	0,4	0 (0,4)	0,6
6-2	1414-4-1 clayed, fine sandy SILT (clfsaSi)	-6,1	0,021	0,43	0	0,2	-1,8
7-1	1414-4-2 silty CLAY (siCl)	-7,6	0,021	0	0,6	0,4	0
7-2	1414-4-2 silty CLAY (siCl)	-6,4	0,021	3,05	0,2	3,0	1,2
8-1	1414-5-1 slightly silty fine SAND (sifSa)	-4,5	0,022	0,29	0,2	0,4	0,2

		1. freezing					
No	Soil	Data from equipment			Data from laser measuring device, mm		
		Average temperature during freezing, ºC	Preload Mpa	Frost heave, mm	Before freezing 12h	Frost heave, mm	Thawing comper with beginning
8-2	1414-5-1 slightly silty fine SAND (sifSa)	-5,6	0,022	1,47	0,2	1,4	-0,2
9-1	1414-6-1 slightly medium, fine SAND (mfSa)	-4,7	0,022	0,03	0,2	0,2	-0,4
9-2	1414-6-1 slightly medium, fine SAND (mfSa)	-5,3	0,021	0,72	0,4	0,8	0
10-1	clayed SILT (clSi)	-6,2	0,022	1,83	0,4	1,6	0,80
10-2	clayed SILT (clSi)	-6,0	0,021	1,97	0,0	1,8	-0,8
11-1	slightly sandy, clayed SILT (saclSi)	-7,0	0,021	0,02	0,6	0 (0)	0,6
11-2	slightly sandy, clayed SILT (saclSi)	-4,4	0,021	0,43	0,2	0,6	-1,4

Table 4.12. Freezing – 2 cycle:

		2. freezing					
No	Soil	Data from equipment			Data from laser measuring device, mm		
		Average temperature during freezing, ºC	Preload Mpa	Frost heave, mm	Before freezing 12h	Frost heave, mm	Thawing comper with beginning
1-1	1281-1 silty fine Sand (sifSa)	-4,8	0,024	3,98	0,2	3,4	0,60
1-2	1281-1 silty fine Sand (sifSa)	-5,4	0,021	4,70	0,2	4,2	-0,40
1-3	1281-1 silty fine Sand (sifSa)	-5,1	0,024	3,11	0,4	2,6	0,20
2-1	1281-2 fine/medium sandy Silt (f/msaSi)	-4,7	0,023	0,96	0,6	1,2 (3,2)	0,4
2-2	1281-2 fine/medium sandy Silt (f/msaSi)	-5,2	0,019	2,45	0,4	2,6	-0,8

		2. freezing					
No	Soil	Data from equipment			Data from laser measuring device, mm		
		Average temperature during freezing, °C	Preload Mpa	Frost heave, mm	Before freezing 12h	Frost heave, mm	Thawing comper with beginnin g
2-3	1281-2 fine/medium sandy Silt (f/msaSi)	-4,1	0,022	0,81	0,4	(-3,6)	0,4
3-1	1286 silty CLAY (siCl)	-6,2	0,022	0,71	0,4	0,8 (3,0)	0,8
3-2	1286 silty CLAY (siCl)	-6,3	0,024	3,71	0,0	3,2	-1,0
4-1	1414-3-1 silty CLAY (fsasiSa)	-6,5	0,022	2,57	0,6	2,4	0,2
4-2	1414-3-1 silty CLAY (fsasiSa)	-6,6	0,024	1,59	0,2	1,4	-0,4
5-1	1414-3-2 fine sandy, clayed SILT (fsaclSi)	-7,1	0,022	1,04	0,4	1,0	0,4
5-2	1414-3-2 fine sandy, clayed SILT (fsaclSi)	-6,1	0,024	1,41	0,2	1,6	0,4
6-1	1414-4-1 clayed, fine sandy SILT (clfsaSi)	-5,9	0,022	0,19	0,2	0,2 (1,0)	0,4
6-2	1414-4-1 clayed, fine sandy SILT (clfsaSi)	-5,7	0,022	0,78	0,2	0,8	-0,4
7-1	1414-4-2 silty CLAY (siCl)	-6,5	0,021	0,13	0,4	0,2	0,2
7-2	1414-4-2 silty CLAY (siCl)	-6,8	0,027	2,70	0,2	2,4	-0,6
8-1	1414-5-1 slightly silty fine SAND (sifSa)	-4,9	0,022	0,23	0,2	0,4	-0,2
8-2	1414-5-1 slightly silty fine SAND (sifSa)	-5,5	0,024	0,67	0,6	0,6	0,2
9-1	1414-6-1 slightly medium, fine SAND (mfSa)	-5,0	0,022	0,68	0,4	0,4	0,4
9-2	1414-6-1 slightly medium, fine SAND (mfSa)	-5,3	0,023	0,29	0,6	0,2	0,4
10-1	clayed SILT (clSi)	-6,7	0,023	2,96	0,2	2,4	0
10-2	clayed SILT (clSi)	-6,2	0,024	4,31	0,4	3,6	-0,6
11-1	slightly sandy, clayed SILT (saclSi)	-7,0	0,021	0,02	0,6	0 (0)	0,6

No	Soil	2. freezing					
		Data from equipment			Data from laser measuring device, mm		
		Average temperature during freezing, °C	Preload Mpa	Frost heave, mm	Before freezing 12h	Frost heave, mm	Thawing comper with beginning
11-2	slightly sandy, clayed SILT (saclSi)	-6,2	0,023	1,61	0,4	1,6	0

Table 4.13. Freezing – 3 cycle

No	Soil	3. freezing					
		Data from equipment			Data from laser measuring device, mm		
		Average temperature during freezing, °C	Preload Mpa	Frost heave, mm	Before freezing 12h	Frost heave, mm	Thawing comper with beginning
1-1	1281-1 silty fine Sand (sifSa)	-4,96	0,026	6,69	0,2	5,6	0
1-2	1281-1 silty fine Sand (sifSa)	-5,4	0,023	6,06	0,4	5,4	0
1-3	1281-1 silty fine Sand (sifSa)	-5,2	0,026	3,91	0,4	3,4	-0,2
2-1	1281-2 fine/medium sandy Silt (f/msaSi)	-4,3	0,025	1,51	0,4	1,8 (5,2)	0
2-2	1281-2 fine/medium sandy Silt (f/msaSi)	-5,8	0,021	1,6	0,4	2,2	-0,6
2-3	1281-2 fine/medium sandy Silt (f/msaSi)	-5,3	0,022	1,66	0,6	(-4,2)	-0,2
3-1	1286 silty CLAY (siCl)	-6,5	0,024	1,46	0,4	1,4 (4,2)	0,2
3-2	1286 silty CLAY (siCl)	-6,2	0,025	3,91	0,4	3,0	-1,2
4-1	1414-3-1 silty CLAY (fsasiSa)	-6,1	0,022	3,29	0,4	3,00	-0,4
4-2	1414-3-1 silty CLAY (fsasiSa)	-5,9	0,024	1,60	0,2	1,60	0,2
5-1	1414-3-2 fine sandy, clayed SILT (fsaclSi)	-6,6	0,023	1,85	0,6	1,6	0,4

		3. freezing					
No	Soil	Data from equipment			Data from laser measuring device, mm		
		Average temperature during freezing, ºC	Preload Mpa	Frost heave, mm	Before freezing 12h	Frost heave, mm	Thawing comper with beginning
5-2	1414-3-2 fine sandy, clayed SILT (fsaclSi)	-6,9	0,025	1,6	0,4	1,4	-0,2
6-1	1414-4-1 clayed, fine sandy SILT (clfsaSi)	-5,4	0,023	0,83	0	0,8 (2,4)	0,2
6-2	1414-4-1 clayed, fine sandy SILT (clfsaSi)	-6,0	0,023	1,08	0,2	1,0	-0,4
7-1	1414-4-2 silty CLAY (siCl)	-6,7	0,021	0,06	0,4	1,4	0
7-2	1414-4-2 silty CLAY (siCl)	-6,8	0,026	2,67	0,4	2,2	0,2
8-1	1414-5-1 slightly silty fine SAND (sifSa)	-4,9	0,022	0,25	0,2	0,4	-0,2
8-2	1414-5-1 slightly silty fine SAND (sifSa)	-5,7	0,028	0,5	0,2	0,6	-0,2
9-1	1414-6-1 slightly medium, fine SAND (mfSa)	-5,2	0,022	0,32	0,2	0,4	0
9-2	1414-6-1 slightly medium, fine SAND (mfSa)	-4,2	0,025	0,04	0,2	0,2 (2,2)	-0,4
10-1	clayed SILT (clSi)	-6,7	0,024	3,50	0,2	2,8	0
10-2	clayed SILT (clSi)	-6,4	0,022	3,88	0,4	3,2	-0,4
11-1	slightly sandy, clayed SILT (saclSi)	-7,0	0,021	0,02	0,6	0 (0)	0,6
11-2	slightly sandy, clayed SILT (saclSi)	-6,0	0,023	1,41	0,6	0,8	-1,0

Table 4.14. Soil sample density and moisture change during sample freezing (all cycles in total):

No.	Soil	Moisture, %		Dry density, Mg/m3
		At the beginning of the testing	After testing	
1	1281-1 silty fine Sand (sifSa)	9,3	12,9	1,941

No.	Soil	Moisture, %		Dry density, Mg/m3
		At the beginning of the testing	After testing	
2-1	1281-2 fine/medium sandy Silt (f/msaSi)	10,2	12,7	1,958
2-2	1281-2 fine/medium sandy Silt (f/msaSi)	12,7	11,6	1,928
3	1286 silty CLAY (siCl)	19,3	26,3	1,593
4-1	1414-3-1 silty CLAY (fsasiSa)	16,7	25,6	1,582
4-2	1414-3-1 silty CLAY (fsasiSa)			
5-1	1414-3-2 fine sandy, clayed SILT (fsaclSi)	13,7	18,4	1,725
5-2	1414-3-2 fine sandy, clayed SILT (fsaclSi)			
6-1	1414-4-1 clayed, fine sandy SILT (clfsaSi)	9,5	14,9	1,893
6-2	1414-4-1 clayed, fine sandy SILT (clfsaSi)	12,2	12,4	1,951
7	1414-4-2 silty CLAY (siCl)	22,8	28,9	1,351
8	1414-5-1 slightly silty fine SAND (sifSa)	16,7	20,1	1,609
9	1414-6-1 slightly medium, fine SAND (mfSa)	17,0	22,4	1,52
10	clayed SILT (clSi)	18,8	22,3	1,659
11	slightly sandy, clayed SILT (saclSi)	11,9	14,2	1,777

Table 4.15. LU analysis results - granulometric content

No.	Soil	**Sieve size (mm)**												
		0,063	***0,125***	***0,250***	***0,5***	***1,0***	***2,0***	***4,0***	***5,6***	***8,0***	***11,2***	***16,0***	***22,4***	***31,5***
1	1281-1 silty fine Sand (sifSa)	48.7	68.3	82.6	88.1	90.7	92.7	95.6	97.2	98.5	99.3	100.0	100.0	100.0
2	1281-2 fine/medium sandy Silt (f/msaSi)	48.7	58.3	68.6	76.5	81.9	85.5	88.7	91.2	93.2	94.7	98.4	100.0	100.0
3	1414-3-1 silty CLAY (fsasiSa)	80.3	86.4	94.1	97.5	98.4	99.1	99.6	99.8	99.9	100.0	100.0	100.0	100.0
4	1414-3-2 fine sandy, clayed SILT (fsaclSi)	69.9	78.7	90.2	94.7	96.0	96.6	97.1	97.4	98.1	98.8	100.0	100.0	100.0
5	1414-4-1 clayed, fine sandy SILT (clfsaSi)	56.8	66.5	80.6	87.4	89.9	91.8	94.3	95.4	96.3	97.5	100.0	100.0	100.0
6	1414-5-1 slightly silty fine SAND (sifSa)	13.1	69.0	99.0	99.5	99.7	100.0	100.0	100.0	100.0	100.0	100.0	100.0	100.0
7	1414-6-1 slightly medium, fine SAND (mfSa)	2.9	15.9	99.6	99.7	99.8	99.9	100.0	100.0	100.0	100.0	100.0	100.0	100.0
8	slightly sandy, clayed SILT (saclSi)	80.3	88.6	96.8	99.3	99.7	99.9	100.0	100.0	100.0	100.0	100.0	100.0	100.0

Table 4.16. LU analysis results - fines granulometric content

No.	Soil	Sieve size (mm)							
		0,002	***0,004***	***0,008***	***0,016***	***0,02***	***0,025***	***0,038***	***0,063***
1	1281-1 silty fine Sand (sifSa)	9,2	12,8	17,4	21,1	22,1	23,1	24	48,7
2	1281-2 fine/medium sandy Silt (f/msaSi)	8,7	13,1	19,4	27,8	30,6	34,1	40,3	48,7
3	1286 silty CLAY (siCl)	72,2	83,7	90,6	93,7	95,7	97,7	97,7	97,7
4	1414-3-1 silty CLAY (fsasiSa)	53,7	55,9	57,2	62,9	64,3	67,9	72,1	80,3
5	1414-3-2 fine sandy, clayed SILT (fsaclSi)	30,9	39	50,1	56,8	58,1	61,8	67,1	69,9
6	1414-4-1 clayed, fine sandy SILT (clfsaSi)	18,8	24,3	30,6	39,8	40,6	44,8	48,3	56,8
7	1414-4-2 silty CLAY (siCl)	71,2	77,4	85,0	91,6	92,9	96,3	99,2	98,3
8	1414-5-1 slightly silty fine SAND (sifSa)	4,1	4,9	6,0	7,1	7,5	8,2	9,2	13,1
9	1414-6-1 slightly medium, fine SAND (mfSa)	0,5	0,6	0,7	0,7	0,8	0,8	0,9	2,9
10	clayed SILT (clSi)	46,7	62,0	77,9	90,0	92,4	95,7	99,4	99,4
11	slightly sandy, clayed SILT (saclSi)	32,4	41,3	52,1	61,5	66,1	70,7	76,9	80,3

Table 4.17. LU analysis results: Atterberg limits determination.

No.	Soil	**Atterberg limits** *LVS EN CEN ISO/TS 17892-12:2005 (60g/60º)*			
		Plasticity **Wp, %**	Flowing **W_L** (60g/60º), **%**	Plasticity index **Ip**	
1	1281-1 silty fine Sand (sifSa)	13	19	6	
2	1281-2 fine/medium sandy Silt (f/msaSi)	13	20	7	
3	1286 silty CLAY (siCl)	27	68	41	
4	1414-3-1 silty CLAY (fsasiSa)	19	47	28	
5	1414-3-2 fine sandy, clayed SILT (fsaclSi)	16	39	23	
6	1414-4-1 clayed, fine sandy SILT (clfsaSi)	13	28	15	
7	1414-4-2 silty CLAY (siCl)	28	83	55	
8	clayed SILT (clSi)	19	41	22	
9	slightly sandy, clayed SILT (saclSi)	15	36	21	

Table 4.18. Density of soil particles

Soil	Density (g/cm3)

1281-1 silty fine Sand (sifSa)	2.704
1414-5-1 slightly silty fine SAND (sifSa)	2.644
1281-2 fine/medium sandy Silt (f/msaSi)	2.695
1414-3-2 fine sandy, clayed SILT (fsaclSi)	2.719
1414-6-1 slightly medium, fine SAND (mfSa)	2.646
1414-4-2 silty CLAY (siCl)	2.793
1286 silty CLAY (siCl)	2.803
clayed SILT (clSi)	2.778
1414-3-1 silty CLAY (fsasiSa)	2.750
1414-4-1 clayed, fine sandy SILT (clfsaSi)	2.721
slightly sandy, clayed SILT (saclSi)	2.743

4.4. Analysis of test results

Frost heave dependence of typical soil parameters

Several typical soil properties were determined during the project (4.2., 4.3. sections). Attempts were made to correlate those parameters with the frost heave determined in laboratory.

Tested soil samples show weak to moderate frost susceptibility according to GOST 28622-90 standard that is rather surprising considering the fact that part of collected soil samples could be highly susceptible to frost heave (Table 1.6.; 1.7 section).

Table 4.19. Soil frost susceptibility class of tested samples according to DIN

Sample No.	Soil type* ISO	Frost group
1281-1 Red-brown clay, quarry "Baldone"	silty fine Sand (sifSa)	F3
1281-2 Gray clay, quarry "Baldone"	fine/medium sandy Silt (f/msaSi)	F3
1286 Gryish clay, quary "Āne"	silty CLAY (siCl)	F2
1414-3-1 Clay dust, from A9 (SP-1)	silty CLAY (fsasiSa)	F3
1414-3-2 Sandy loan, from A9 (SP-2)	Fine sandy, clayed SILT (fsaclSi)	F3
1414-4-1 Clay dust No. 1, from A9 (SP-3)	clayed, fine sandy SILT (clfsaSi)	F3
1414-4-2 Clay dust No. 2, from A9 (SP4)	silty CLAY (siCl)	F2
1414-5-1 Dusty fine sand, from A9 (SP-5)	slightly silty fine SAND (sifSa)	F2
1414-6-1 Smalka smilts, from A9 (SP-6)	slightly medium, fine SAND (mfSa)	F1
Clay, quarry ″CEMEX″	clayed SILT (clSi)	F3
Clay prepared by ″Ceplis″	slightly sandy, clayed SILT (saclSi)	F3

Obtained soil parameters were correlated with first, second and third cycle frost heave results (4.3. section) and it was concluded that data correlation is not dependent of the number of freezing cycles of the test. During analysis of obtained data, it was obvious that correlation of any determined parameter with the determined frost heave is weak or is not present at all. For example, there were no correlation between moisture and frost heave (Figure 4.2.)

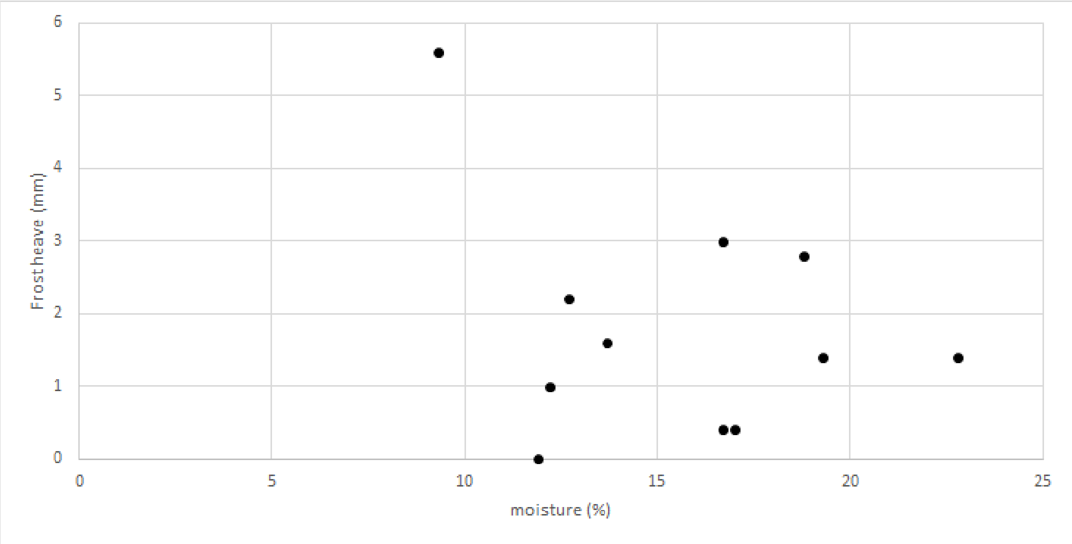

Figure 4.2. Frost heave dependence on moisture content

The only soil parameter with weak correlation is the content of fines (Figure 4.3).

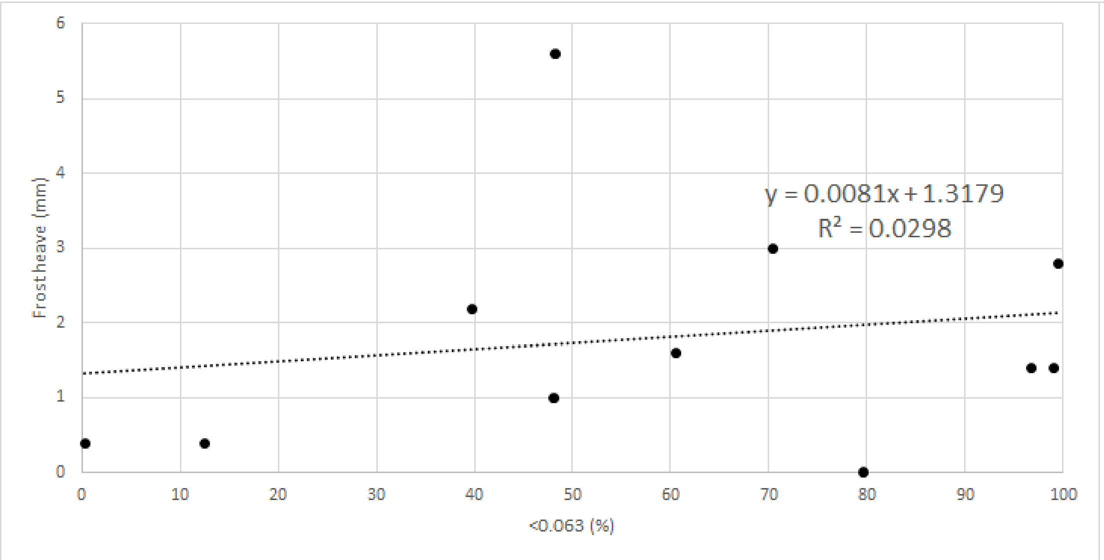

Figure 4.3. Frost heave dependence on percentage of fines

Obtained results show that it is not possible to determine frost heave simply by using some of frequently determined soil parameters and it is necessary to perform direct soil frost heave tests. It is rather surprising that there is almost no correlation between moisture content and frost heave but that can be explained by the fact that currently frost heave was determined in the laboratory and not on the field. The same can be stated also when remaining of determined parameters are discussed.

Before some general conclusions can be drawn, in situ frost heave measurements must be done. Firstly, it is not clear how well laboratory frost heave tests represent frost heave that is happening in the field and secondly some of the determined parameters my not influence frost heave in small scale laboratory samples while they could play significant role when field conditions are considered.

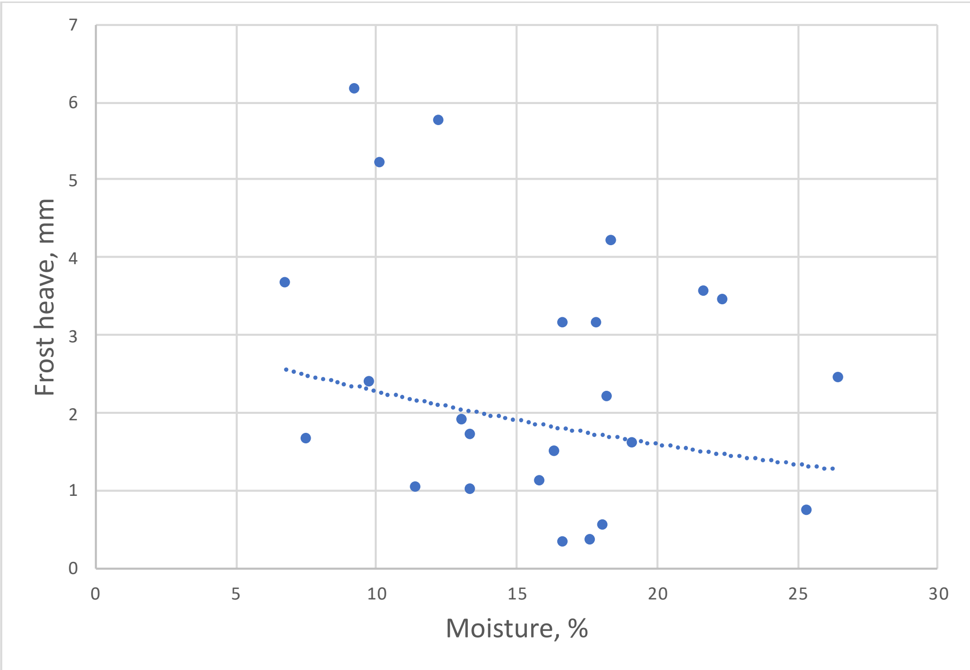

Figure 4.4. Relationship between frost heave and moisture of soil samples.

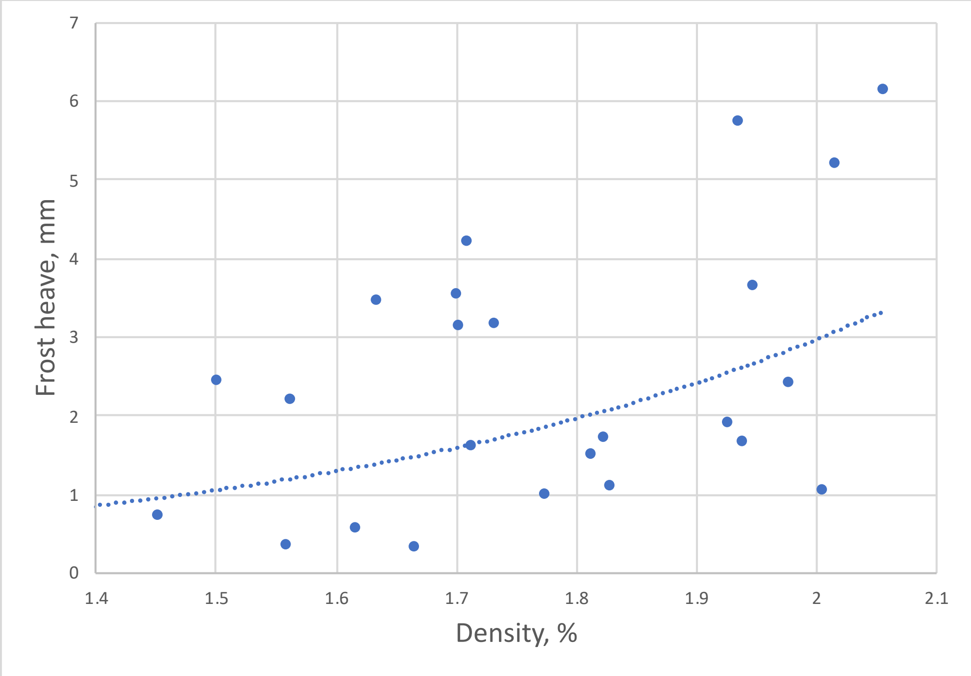

Figure 4.5. Relationship between frost heave and density of soil samples

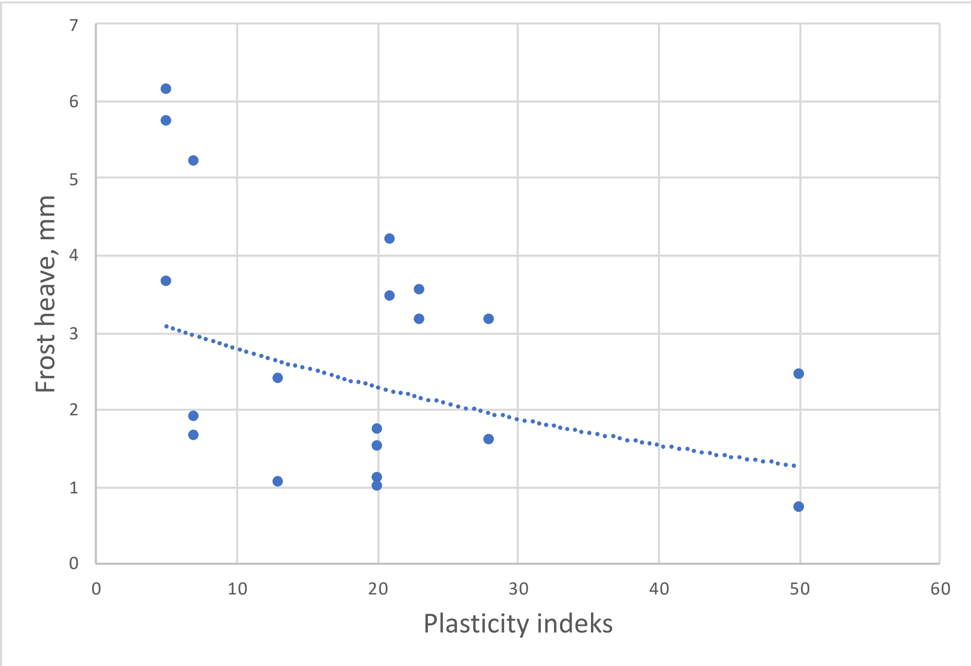

Figure 4.6. Relationship between frost heave and plasticity index

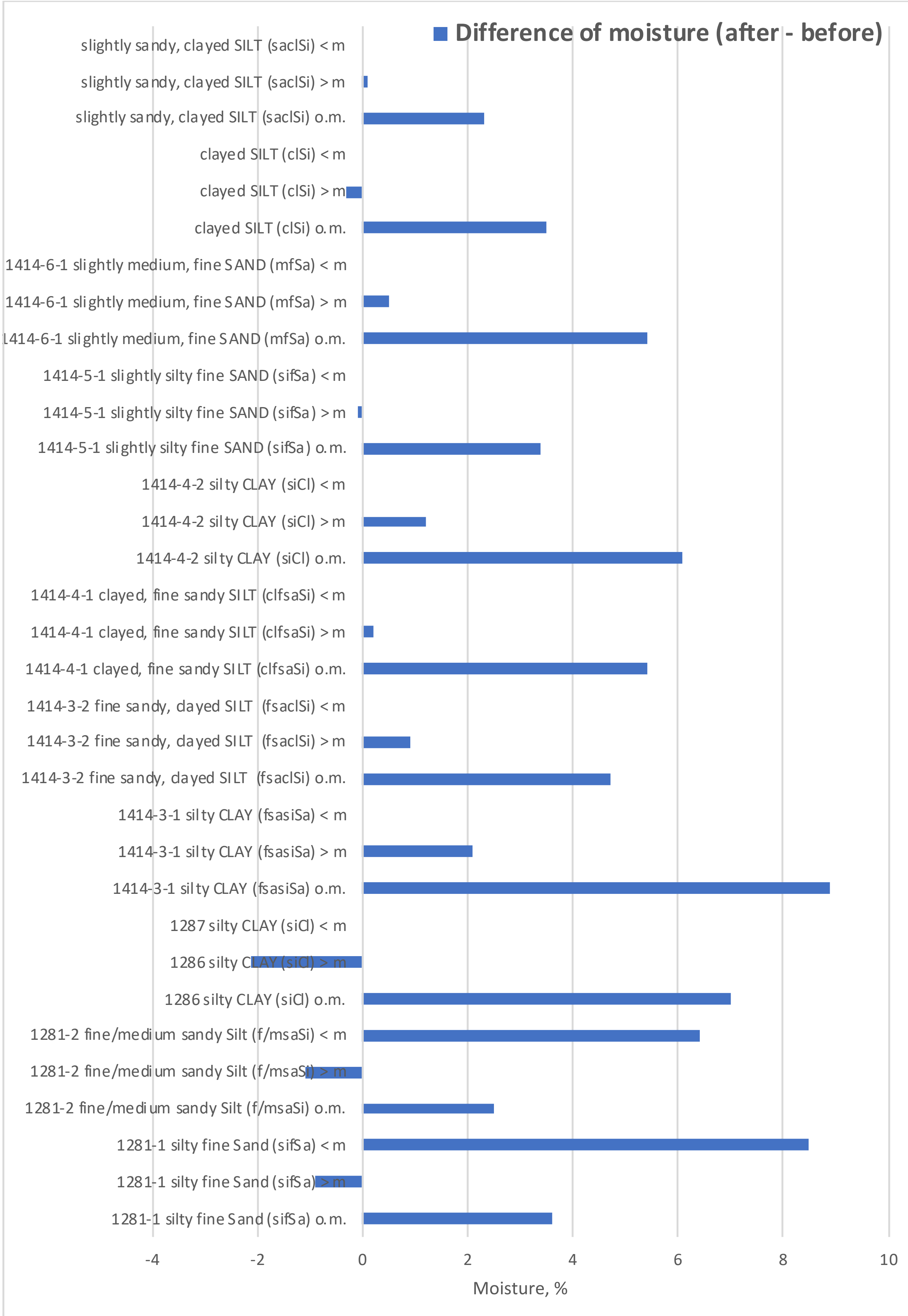

Figure 4.7. Changes in moisture content during freezing and thawing of samples (3 cycles)

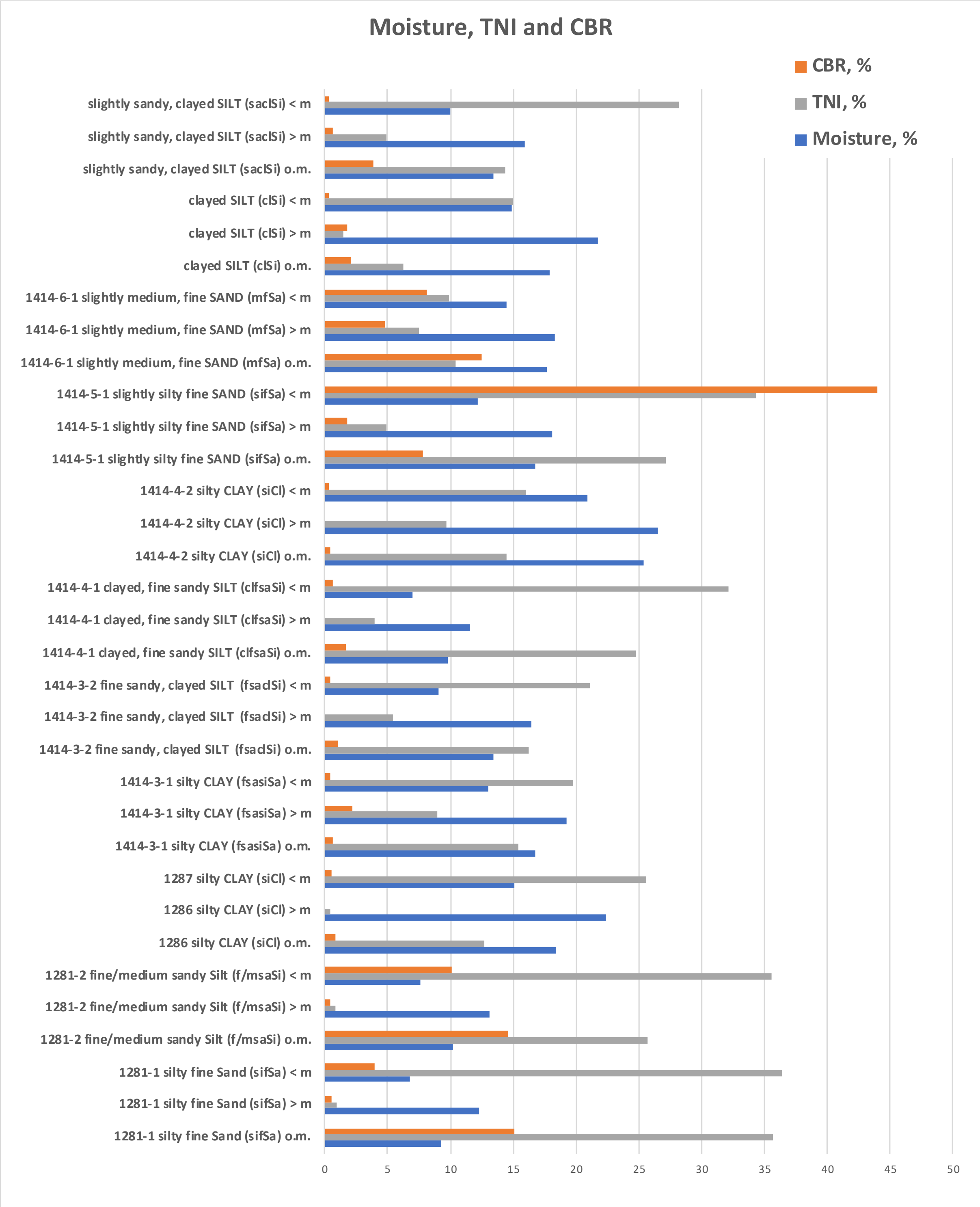

> m – increased moisture content; o.m. – optimum moisture content; < m – decreased moisture content.

Figure 4.8. Changes in Immediate Bearing Index and Californian Bearing Rate depending on moisture for different soils

5. DEVELOPMENT OF MONITORING PROGRAMME

5.1. Satellites as a monitoring option

Satellite data can be effectively used to observe the meteorological phenomena on the Earth from afar. Various satellites measure multiple parameters globally and regionally. This chapter focuses primarily on land surface temperature, snowfall rate and snow cover extent.

5.1.1. Land surface temperature (LST)

Satellite land surface temperature measurements (LST) are usually derived mathematically from radiance sensors in various wavelength bands (Uddstrom, 1988; LSA, 2015) In such case calculated LST might differ depending on the institution doing the data analysis. LST parameter quality is heavily dependent on cloudiness as well as various lower atmosphere and soil parameters. Usually higher cloudiness level significantly lowers the accuracy of the measurements. For this reason, all the data providers below, besides German Aerospace Center, offer “quality control grids” which allow the user to estimate the accuracy and precision of given measurements.

Much of the European land surface meteorological analysis regarding satellite data is done by European Organisation for the Exploitation of Meteorological Satellites (EUMETSAT) Land monitoring satellite application facility (LSA SAF). Their products include various LST datasets derived from two radiation sensors in top of multiple satellites – SEVIRI and AVHRR. Products differ in their spatial and temporal resolution as well as represented time period. Short description of all LST products including LSA SAF data can be found in the table 5.1 below. Datasets are available in compressed binary formats, however LSA SAF provides Meteosat Second Generation (MSG) toolbox (MSG tooblox, 2018) for extracting data for use in GIS software (LSA, 2019).

Various LST datasets are also provided by European Union’s Earth Observation Programme (Copernicus). Copernicus LSTs are estimated from infrared spectral channels of three geostationary satellites – MSG, GOES and MTSAT/Himwari. Estimation is highly dependent on surface albedo, vegetation cover and soil moisture. Copernicus provides three different global LST products (Coppernicus, 2019), which are all freely downloadable.

Since 1972 United States Geological Survey (USGS) in cooperation with National Aeronautics and Space Administration (NASA) has been remotely monitoring various land surface parameters. One such satellite sensor is Moderate Resolution Imaging Spectrometer (MODIS) which in combination with different meteorological and geographical parameters estimates land surface temperature. NASA and USGS provide daily MODIS land surface temperature calculations globally. LST datasets are available with multiple temporal resolutions and spatial resolutions, of which the highest available are listed in table 5.1 (Wan et al, 2015).

Another possible source of LST data can be Advanced Very High Resolution Radiometer (AVHRR) sensors on top of multiple satellites. AVHRR sensors are found on various National Oceanic and Atmospheric Administration (NOAA) satellites as well as on EUMETSAT MetOp satellites. NOAA satellites provide information in multiple spectral bands, however no processed LST product is freely available, and user has to do the calculations himself. However, for the European territory LST datasets are provided by German Aerospace Center. Metadata about this specific dataset are provided in the table 5.1.

Land surface temperature can be calculated from various other high resolution satellite mission data, such as Landsat (USGS, 2019) or Sentinel-3 (ESA, 2019). While these missions can provide comparably extremely high spatial resolution (even below 50 meter pixel size), they provide irregular temporal coverage of multiple days. Measurements from these satellites are dependent on satellite trajectory, so relative pixel locations changes for each overflight (in other words – pixels never represent the same area). For these reasons, missions can be used to estimate LST in singular point in time; however, they are not as useful for monitoring purposes, and were not described in detail.

Table 5.1 Land surface temperatures satellite datasets

Product	Satellite	Sensor	Temporal resolution	Spatial resolution	Spatial extent	Time period	Data format	Error	Available
LSA-001 (MLST)	EUMETSAT satellite MSG	SEVIRI	15 min	3.1 x 3.1 km	Europe, Africa, South America	2005-2019	HFD5	Average 3K, never above 4K	https:// landsaf.ipma.pt/ en/products/land-surface-temperature/
LSA-002 (EDLST)	EUMETSAT MetOp, NOAA POES	AVHRR	12 hours	1.1 x 1.1 km	Global	2015-2019	HFD5	Varying, never above 4K	https:// landsaf.ipma.pt/ en/products/land-surface-temperature/
LSA-003 (DLST)	EUMETSAT satellite MSG	SEVIRI	Derived 10 day composite (median, maximum)	3.1 x 3.1 km	Europe, Africa, South America	2015-201	HFD5	Average 3K, never above 4K	https:// landsaf.ipma.pt/ en/products/land-surface-temperature/
Coppernicus Hourly LST	MSG, GOES East, MTSAT	SEVIRI, MTSAT, Himawari	Hourly	5 x 5 km	Global, -60°/70° latitude range	2010-2019	NetCDF4	Average about 3K	https:// land.copernicus.eu/global/ products/lst
Coppernicus 10-day LST Daily Cycle	MSG, GOES East, MTSAT	SEVIRI, MTSAT, Himawari	10 days minimum, median and maximum	5 x 5 km	Global, -60°/70° latitude range	2017-2019	NetCDF4	2– 6K, median 3K	https:// land.copernicus.eu/global/ products/lst
MODIS	Terra, Aqua	MODIS	Daily	1 x 1 km	Global	2000-2019	HDF-EOS	Usually below 2K, maximum of 4.2K	https:// modis.gsfc.nasa.gov/data/ dataprod/ mod11.php
AVHRR LST	NOAA POES	AVHRR	Daily	1.1 x 1.1 km	Europe	1998-2019	No information	Up to 3K (Dech et al, 1998)	https:// www.europeandataportal.eu/data/ en/dataset/ b673f41b-d934-49e4-af6b-44bbdf164367

5.1.2. Snowfall and snow cover

Satellite data can be used to determine precipitation intensity and location. Multiple satellites such as Global precipitation measurement (GPM) or Tropical rainfall measuring mission (TRMM) measure precipitation (NASA, 2019). Precipitation from satellites is determined by imaging microwave reflections. For example, GPM mission measures two microwave frequencies, which correspond with precipitation – 13,6 GHz and 35,5 GHz (NASA, 2019). While precipitation satellites can be used to determine strong rainfall quite accurately, precipitation types such as snowfall and light rainfall are often missed and underestimated (Wen et al., 2016).

Recently, however, various developments have been made to determine the snowfall rates from passive microwave sensors on top of NOAA-18, NOAA-19, Meteop-A, Meteotop-B and Suomi-NPP satellites. Snowfall rates are extracted according to algorithm in (Meng et al, 2017). Data are available globally, almost immediately after measurements, however, only visualized as PNG format. To access raw data, user has to contact NOAA. Metadata about the product can be seen in the table 5.2 below.

There have been efforts to extract the snowfall rate from precipitation data, especially with the relatively recent improvements in Goddart Profiling Algorithm (GPROF) that is expected to show improved accuracy in measurements of snowfall and light rainfall (Kummerow et al., 2015). The recent validation study of the data however show very large root-mean-squared error (up to 13,55 mm/day), and authors themselves conclude that improvements have to be made before the data can effectively be used in climatological or meteorological studies (Wen et al., 2016).

Table 5.2 Snowfall rate satellite datasets

Product	Satellite	Sensor	Temporal resolution	Spatial resolution	Spatial extent	Time period	Data format	Error	Available
NOAA SFR	MeteOp, NOAA POES	Passive Microwave	Daily	1.1 x 1.1 km	Global	2012-2019	Image formats, PNG	up to 1,07 mm/h	https://www.star.nesdis.noaa.gov/corp/scsb/mspps_backup/sfr_realtime.html

There are multiple sources available of satellite information about snow cover extent. Snow cover parameter is usually derived from visible light and infra-red sensors taking into account land surface albedo changes. Various satellite sensors that monitor land surface are also used to provide products for snow coverage. As before, parameter accuracy is dependent on various factors, of which the most important is cloud cover. Metadata about all after mentioned satellite products can be found in table 5.3 below.

LSA SAF in cooperation with EUMETSAT Support to Operational Hydrology and Water Management (HSAF) provides snow cover extent information. Two snow cover products are available from two different satellite sensors – AVHRR and SEVIRI (LSA, 2019). Surface data is classified in 6 classes – non-processed, totally snow covered, partially snow covered, snow free ground, unclassified and water. All data is available in HDF5 format, along with supplementary quality control grids, which allow the user to determine the accuracy of the measurements. It is worth mentioning that HSAF along with snow cover information provides other snow parameters, such as snow water equivalent or snow wetness (HSAF, 2019).

Copernicus also provides datasets for snow cover extent. Two datasets are available in 500 x 500 m and 1 x 1 km resolution. Copernicus products are derived from MODIS sensor on Terra satellite and VIIRS sensor on POES satellites. Copernicus provides snow cover information for each pixel in percentages i.e. 80% of a pixel is covered in snow. Information is provided as a daily composite, depending on daily cloud cover over the area (Copernicus, 2019).

National Snow & Ice data Center (NSIDC) of America also provide snow cover extent products based on Terra/Aqua satellite MODIS sensors. Data are available globally on various temporal resolutions of which the shortest is every 5 minutes, and 500 x 500 meter spatial resolution. Datasets can be downloaded manually or using NSIDC provided data application-program interface (API). Snow cover extent is calculated using Normalized Difference Snow Index (NDSI) and, similarly to Coppernicus dataset, also provides information of snow cover percentage of an individual pixel area (Hall, Riggs, 2016).

Snow cover extent, as in case with LST can be easily observed at a greater spatial resolution using satellite missions such as Landsat or Sentinel. However, for the reasons mentioned above, these datasets were not described in greater detail.

Table 5.3 Snow cover extent satellite datasets

Product	Satellite	Sensor	Temporal resolution	Spatial resolution	Spatial extent	Time period	Data format	Error	Available
SC	EUMETSAT satellite MSG	SEVIRI	Daily	3.1 x 3.1 km	Europe, Africa, South America	2005-2019	HFD5	<10%	https://landsaf.ipma.pt/en/products/snow-cover/
EPS daily Snow Cover	EUMETSAT MetOp, NOAA POES	AVHRR	Daily	1.1 x 1.1 km	Global	2015-2019	HFD5	<10%	https://landsaf.ipma.pt/en/products/snow-cover/
Coppernicus SCE 500m	Terra	MODIS	Daily	0.5 x 0.5 km	Europe	2017-2019	NetCDF4	<15%	https://land.copernicus.eu/global/products/sce
Coppernicus SCE 1 km	EUMETSAT MetOp, NOAA POES	VIIRS	Daily	1 x1 km	Northern Hemisphere	2018-2019	NetCDF4	<10%	https://land.copernicus.eu/global/products/sce
NSIDC MODIS	Terra/Aqua	MODIS	Multiple, shortest 5 minutes	0.5 x 0.5 km	Global	2000-2019	HDF-EOS	Varying, about 10%	https://modis.gsfc.nasa.gov/data/dataprod/mod10.php

5.1.3. Satellite data use to determine road state

Satellite data can be used quite efficiently to monitor large scale geographical and meteorological phenomena. Satellites are extensively used for weather prediction (Ratier, S.a.), for monitoring changes of the land surface (USGS, 2019) or climate research (CMSAF, 2019) as well as various different areas or Earth and Planetary Science. While satellites are excellent at providing large scale information for regional research, spatial or temporal resolution for detailed studies is still lacking. Multiple studies have tried to use satellite data to gather information about urban climate or environmental research (Dousset and Gourmelon, 2003; Shaker and Yan, 2010) with varying degrees of success. As it is seen in tables 5.1 to 5.3, satellites usually have to sacrifice either temporal resolution to increase spatial (as with Landsat and Sentinel missions) or spatial resolution to increase temporal (as with geostationary MSG satellite). In fields such as engineering it is necessary to gather data with maximal temporal and spatial resolution. This makes it hard to use satellite data to inquire accurate information for engineering purposes.

Another important aspect for using satellites is data accuracy. Various meteorological parameters estimated from satellites are usually measured with unfavourable conditions, such as cloudy lower part of the atmosphere. This greatly reduces satellite data accuracy. In table 5.1 for example it can be seen that satellite measurement errors average at about ±2K. This error is acceptable for vegetation or climate studies, however in many engineering applications, such as estimating the freezing depth, such errors are extremely important. Error range as large as 4K might lead to improper conclusions about the physical state of the ground.

Factors mentioned above make it hard to use only satellite data in applications such as road physical state monitoring. This means that *in situ* measurements are absolutely necessary to determine precise road surface temperature, snow depth and coverage. However, the greatest asset of the satellite measurements is large homogeneous spatial coverage. By taking the best of two worlds – combining *in situ* measurements with satellite data, it might be possible to improve the resolution of road monitoring network, gaining some information for areas where no on site measurements have been done before.

Note from client: in order to thoroughly evaluate the state of the road, it should be possible to detect the vertical movements of pavement surface. Transport Infrastructure Ireland (for karst events) and Estonian company Datel http://www.datel.eu/en/ (for infrastructure monitoring) are already employing the possibilities given by Sentinel 1. The idea would be to have a “ground station” as a reference, then, coupled with the satellite data, a section of the road could be monitored over a certain period of time, giving valuable data on which sections show signs of frost susceptibility.

5.2. In-situ SENSORS AND MEASURING EQUIPMENT

5.2.1. Experience in other countries

Swedish experience

In the end of 1990-ties, Swedish National Road and Transport Research Institute (VTI) has performed frost heave measurements *in situ* with their in-house developed and assembled instrument *STÖR-96*. According to the VTI Report (Stenberg, 1997), the instrument was a plastic pipe with temperature sensors mounted at chosen intervals on its outer wall while on the inner wall water level sensors were installed to measure the groundwater level in the plastic pipe. The pipe could move vertically with respect to the caps at both ends, and movement sensors were installed in the upper and lower parts of the instrument to register this movement as a frost heave (see Figure 5.1.)

Figure 5.1. VTI team installing the *STÖR-96* instrument on January 8, 1997 in Sweden (left) and its principal scheme (right).

However, the use of this instrument discontinued and there are no new models or further alternative developments since then at VTI. The only article found on frost heave *in situ* measurements with other techniques (levelling) in Sweden refers to the same period of mid-1990-ties (Vikstrom, 1996). Moreover, since the end of experiments with *STÖR-96* no other *in situ* measurements or monitoring of frost heave have been performed in Sweden (Kalman, 2018).

Presently temperature profile on-line monitoring is carried out on Swedish roads by using again a VTI in-house build instrument *Tjälstav 2004*, which registers temperature at a 5 cm interval down to 2m depth. Figure 5.2. shows an example from two such monitoring stations in Sweden. On-line monitoring data are available at: *http://tjaldjup.trafikverket.se*

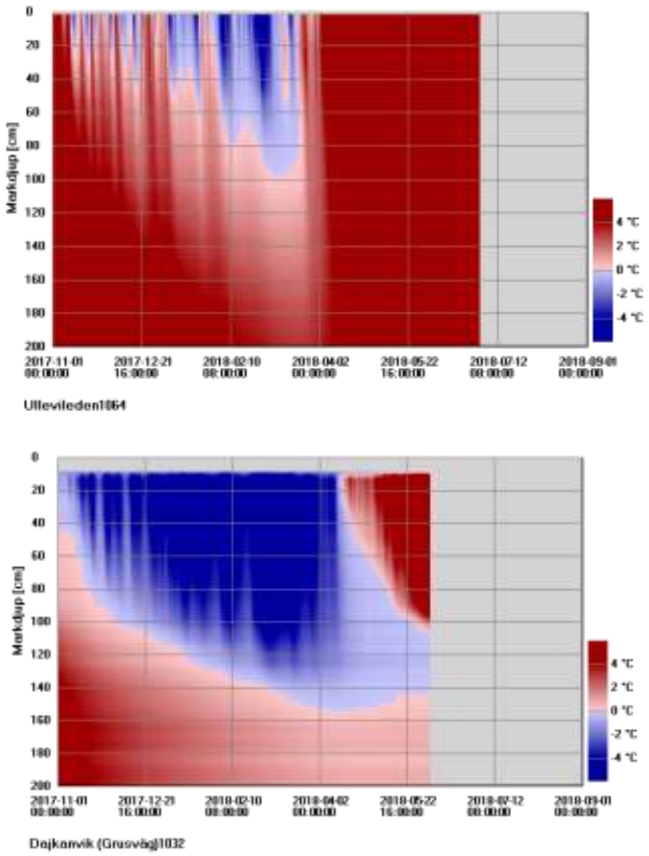

Figure 5.2. On-line temperature monitoring results (illustrative example) from Southern (above) and Northern Sweden (below) using the instrument *Tjälstav* 2004 (available at *http://tjaldjup.trafikverket.se)*

Tjälstav 2004 can be purchased from VTI at around 70 000 SEK (**6800 EUR**) ex works.

Estonian experience

A rather recent Estonian report (Kaal and Jentsen, 2011) shows installation of moisture sensors (percostations) under the pavement and temperature profile measurements off the roadway (Figure 5.3.)

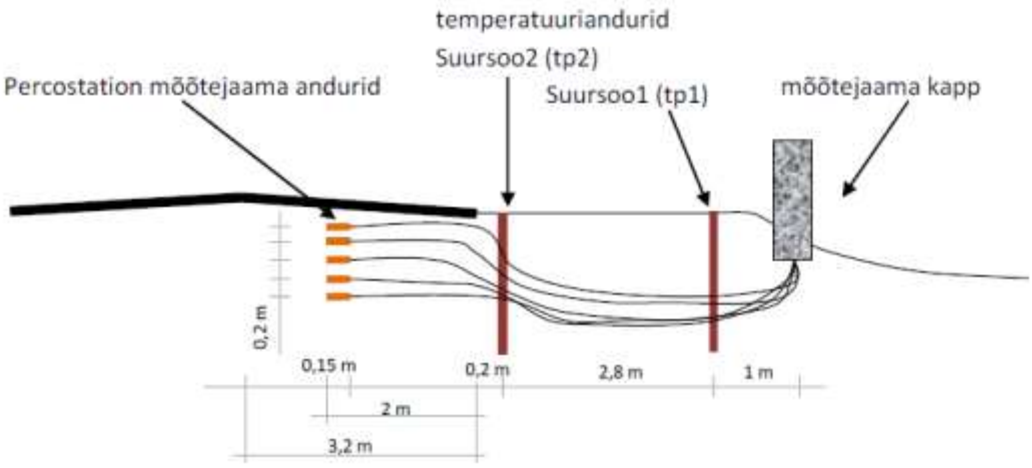

Skeem 1. Percostation mõõtejaama, jaama toruandurite ning vertikaalsete temperatuuriandurite paigalduse skeem

Figure 5.3. Scheme of monitoring installation of moisture sensors (percostations) under the pavement and temperature profile monitoring off the roadway in Estonia.

The report is in Estonian and rich in pictures and description of sensor installation procedures, However, no frost heave *in situ* measuring sensor installation is reported there. Neither there is evidence for other frost heave *in situ* measurements in Estonia.

Lithuanian experience

In Lithuania road weather stations (RWS) are equipped with temperature sensors at different pavement depths and surface conditions. These data allowed for calculation of the thickness of frost resistant pavement structure and to correct according to the specific local conditions (Vaitkus et al, 2016). After performing statistical analysis of 2012-2014 data pertaining 26 RWSs, Lithuania was divided into four regions according to the maximum frost depths, where the maximum values depending on the RWS location varied from 110,4 cm to 179,1 cm.

RWSs started to be installed in 1999 and temperature sensors were installed at pavement surface as well at different pavement depths (Figure 5.4.) In 2012 temperature sensors were installed at other depths as well and data are recorded every 15 min (Vaitkus et al, 2016).

Figure 5.4. Lithuanian RWSs temperature probe PT100 with a highly stable and accurate platinum sensing element.

Some basic characteristics of PT100 probe are:

Accuracy: +/-0.10 °C

Resolution: 0.1 °C

Measuring element: 100 Ω, α= 0.00385

Measuring depths: 0.07, 0.2, 0.5, 0.8, 1.1, 1.4, 1.7, 2m

5.2.2. Soil moisture and temperature sensors

As follows from the theoretical considerations it is necessary to measure simultaneously both soil moisture content and the soil temperature.

For soil moisture measurements (as volumetric water content - VWC) high-frequency capacitance sensors are widely used. These sensors are measuring the dielectric permittivity of the soil, thus sometimes also referred to as percometers. An example of a percometer is given in Figure 5.5 and Table 5.4.

Table 5.4. Percometer v.7, Manufacturer - *Adek* (Estonia), Roadscanners

Short Tube ProbeTFS(L=18cm)	Measured units: Er (range 1..15), electrical conductivity (range (range 0..1000 µS cm–1), temperature (range -40..+80C) Accuracy of Er measurements: +- (0.05 + 1%) Recommended applications: Laboratory tests, e.g. triaxal testing of aggregates
Short Tube ProbeTVS(L=18cm)	Measured units: Er (range 1..81), electrical conductivity (range (range 0..1000 µS cm–1), temperature (range -40..+80C) Accuracy: +- (0.25 + 2%) Recommended applications: Percostation; laboratory tests
LongTube ProbeTVL(L=100cm)	Measured units: Er (range 1..81), electrical conductivity (range (range 0..1000 µS cm–1), temperature (range -40..+80C) Accuracy: Er +- (0.25 + 2%) Recommended applications: Field measurements of soil (high Er value)
Long Tube ProbeTFL(L=100cm)	Measured units: Er (range 1..15), electrical conductivity (range (range 0..1000 µS cm–1), temperature (range -40..+80C) Accuracy: Er +- (0.05 + 1%) Recommended applications: Field measurements of low Er materials

Figure 5.5. Probes of *Adec* percometer v.7. Source: www.roadscanners.com/products/percometer/

For the temperature measurements thermistor sensors are used, which can be placed, for example, at certain distances along an electrical cable, thus forming a thermistor string. The sensor intervals and total length of such strings can vary greatly, thus allowing for a temperature profile measurements at various depths.

Several manufacturers offer also a combination of these two sensor types (for example, *METERGroup, Decagon Devices, Scanntronik, Eijkelkamp,*) in one sensor unit. An example of a combined sensor is given in Figure 5.6. The combined sensor with steel needles is shown in Figure 5.7. Such sensor has to be “plugged” into the soil.

Figure 5.6. *Scantronic* Soil analysis sensor. Dimensions 36 x 114 x 16 mm.

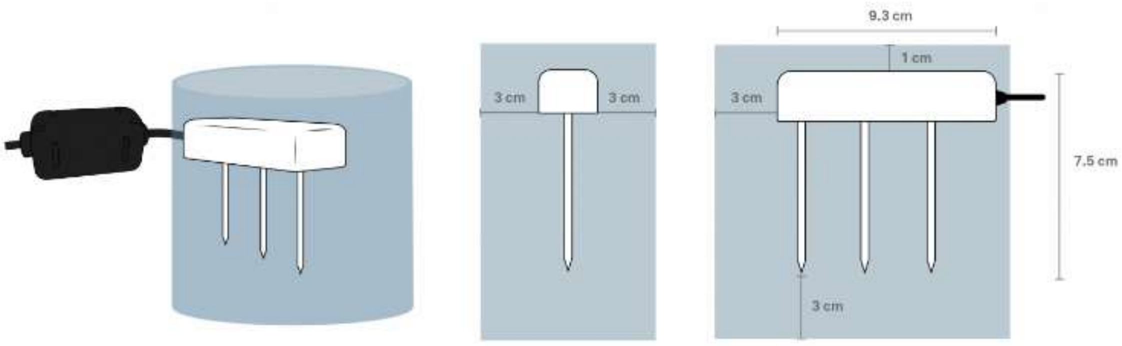

Figure 5.7. Combined sensor *TEROS 12* from the *METERGroup* and its volume of influence.

By analysing the prices of the sensors, system solutions and installation options, it appears that the best choice is the combined temperature-moisture sensors (as compared to separate systems of temperature sensing and moisture sensing). The market price of the combined moisture-temperature sensors is around 200 EUR per sensor (see Table 5.5. for comparison). In addition, a connection of each sensor to a data logger has to be ensured, possibly with data transmission option through GSM network or internet connection.

Table 5.5. Comparison of typical sensors for soil moisture and temperature determination

	MeterGroup	*MeterGroup*	*Scantronic*	*Geokon*	*VTI*
	5TM	**Teros**	**Soil Analysis Sensor**	**3810A**	**Tjalstav 2004**
Soil moisture	YES	YES	YES	No	No
Soil temperature	YES	YES	YES	YES	YES
Sensors / data logger	6	6	4	unlimited	no information
Robust needles	No	YES	No	No	No
Resolution, T °C	0.1	0.1	0.1	0.01	no information
Accuracy, T °C	±1	±1	±1	±0.5 to ±0.05 (above 0°C)	no information
Price / sensor (EUR)	186	225	231	130	180

To be able to choose the optimum number of sensors and distance between them for the long-term monitoring programme (and thus to save the costs), we propose first to install such combined sensors at a very small distance between them down to a 2 m depth in each borehole. The optimum interval for the long-term monitoring programme can be chosen irregular with the depth.

First, an option to install the sensors at a 5 cm interval was considered. However, such an arrangement has several drawbacks:

- The total number of sensors reaches 40 to 42 sensors in one 2 m deep borehole, resulting in high equipment purchase costs;
- It creates a corresponding amount of wiring to fit into the borehole, thus seriously interfering with the installation of sensors closer to the surface; (alternatively, sensors could be installed into the soil profile from an excavated pit)
- It would be rational to de-install the sensors after the test season and use them in the long term monitoring programme in an optimum way. However, de-installation is only possible by excavating the soil next to the borehole in the whole depth profile (that is down to 2 m) and carefully "unplugging" the sensors.
- It is recommended at such small interval to position the sensors in a way of winding spiral along the borehole profile so as to avoid having them one exactly above the other as they can influence each other (see volume of influence on Figure 5.7.).
- A possibility to choose the thermistor string was also considered, however, it did not reduce the costs (Table 5.5.).

Due to these restrictions, it is recommended to consider a 10 cm interval between the sensors, which results in about 18 sensors for a 2 m deep borehole as the most appropriate arrangement. The uppermost sensor shall be installed below the asphalt layer. However, it has to be taken into account that there can be mechanical problems to install ("plug in") needle sensors in a crushed stone layer just below the asphalt. Data flow can be regulated on cloud based data delivery, which simplify and speed up the process of data collection. Integrated solar charging panel means there's hardly any power maintenance required, and data loggers can store 8MB (40,000 to 80,000+ records), depending on sensor configuration. Sensors need to be designed in a rugged casing with stainless steel needles for insertion in the soil. Special borehole installation instrument depicted on Figure 5.8. can be used to insert the sensors perpendicularly into the soil in a borehole.

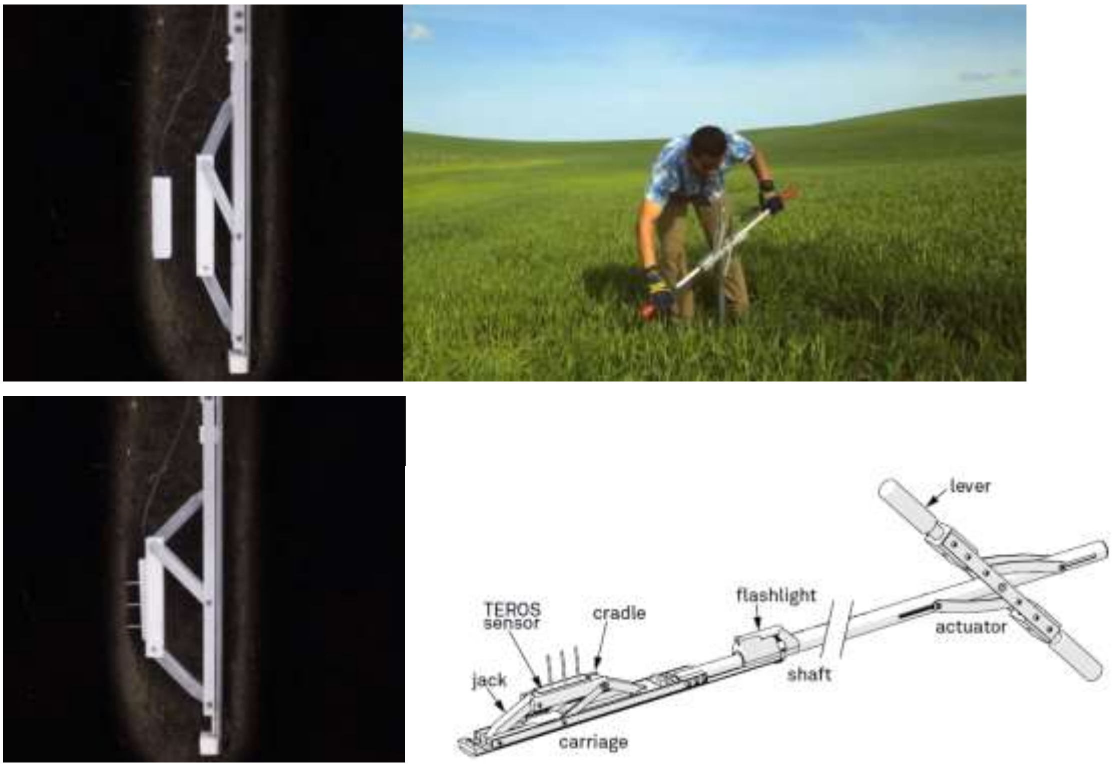

Figure 5.8. *TEROS* installation instrument. Works similar to a bottle corker, but at a 90 degree angle

These sensors can be left permanently in the borehole to later form a part of a long-term monitoring programme.

No other maintenance is necessary except changing the batteries in the data loggers. It is difficult to exactly predict the battery life as that is determined by several factors, including total log-in time, GPS network strength, sunlight availability and others. However, a rough estimate is to consider at least 2 visits per year to monitoring sites; the remaining battery capacity can be monitored remotely (Figure 5.9.).

Figure 5.9. A web-based communication interface screen, including remaining battery capacity status

Data loggers may have an inclined built-in solar panel but in case there is no or not enough sunlight there is an option to use regular alkaline batteries. As an example, from the manufacturer, if the solar panel is covered with snow the battery life decreases but it will still last for a couple of months. So, it is possible that data collection can be done through the frost monitoring season without any or only one maintenance (battery change) visit.

5.2.3. Frost heave sensors

Manufacturers

In contrast to soil temperature and moisture sensors, there seems to be no specialised frost heave *in situ* measurement instruments on the market. For example, the well known geotechnical measurement instruments manufacturer *Geokon* suggested a *Vibrating Wire Deformation meter 4430* for frost heave determination. However, not as a ready solution, but only as a sensor and measuring principle which further needs to be adapted for installation and frost heave measurements.

Also, various other sensing techniques for *in situ* measurements were considered, including laser sensors and ultrasound. However, the laser technique (*LAP GmbH, www.lap-laser.com*) was not recommended for freezing temperatures and neither there was a ready instrument for *in situ* measurements. Similarly, ultrasound technique was neither adapted for *in situ* measurements (*Omni instruments, www.omniinstruments.co.uk*).

Vibrating Wire technique is applied in extensometer sensors, which are available on the market for various geological investigations. From the manufacturer *RST instruments*, which is partly specialised in road construction measurements there is available a specialised Road Extensometer with a vibrating wire displacement transducer which is intended for measurements of settlement and heave of foundations under roadways. However, after a direct communication with the manufacturer a proposal was received to use the *Inline Extensometer 1100* instrument. For this instrument the frost heave measurement range is 10 cm and the data loggers can store sufficient amount of data throughout the monitoring season so that the data transmission option is not necessary, and data can be downloaded via USB at a visit to the monitoring site. Since at least one visit per year to the site is expected due to battery change for temperature-moisture sensors data logger, it is a reasonable solution to save 3000 - 4000 EUR per data logger (by not choosing a data transmission option and during the visit download frost heave data). Single Channel Vibrating Data Logger is a low-cost solution and ideal for remote locations, battery powered and unattended monitoring of a single vibration sensor. It is possible to store 4MB (up to 600, 000 records) memory in Data Logger which is enough for one visit per year for data download (see recording frequency in next chapter 5.3.)

A Vibrating Wire Inline Extensometer has an advantage that it has no electrical head sprouting out of the borehole. The Inline Extensometer is installed flush with the borehole collar or ground surface and measures movement at different depths in the borehole. It can be installed in at least 76,2 mm diameter boreholes. The appropriate anchor type would be groutable anchor with spring legs because of use in a groutable installation in loose soil and it is necessary to have the bottom anchor firmly fixed below the maximum frost depth. The anchor depth can be chosen at 0.5 m increments as the minimum extension rod length is 0.5 m. Thus, the optimum anchor depth is at 2,5 m. Spring legs on both the bottom anchor and the sensor assembly itself will keep the sensor fixed until the borehole is grouted (cement/bentonite grout mix). The mechanically activated spring legs provide extra connection to the borehole wall. Rods are sheathed in individual PVC protective pipe to minimize frictional effects between different rods and between rods and borehole wall (Figure 5.10. and Figure 5.11.).

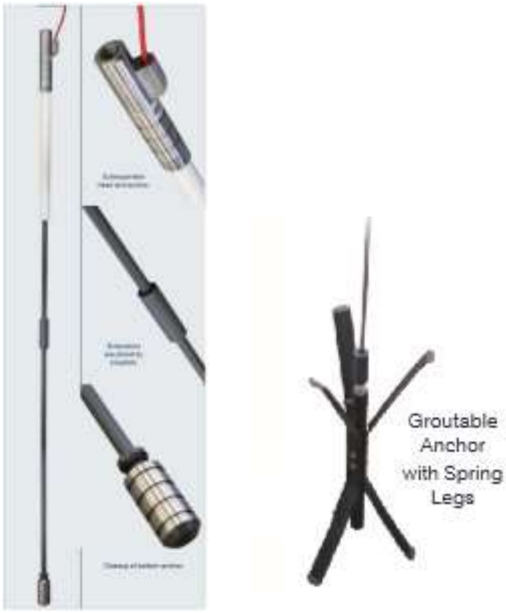

Figure 5.10. RST Vibrating Wire Inline Extensometer and anchor

Figure 5.11. Installation of a Vibrating Wire Inline Extensometer and *Single Channel Vibration Wire Data Logger*

5.3. Monitoring programme design

5.3.1. Monitoring site

In order to assess the frost heave properties both under the road structure and in the natural soil conditions and to be able to compare them, it is proposed to install sensors both under the road pavement and in a direct proximity off the road at each monitoring site. Thus, under the road structure in one borehole temperature-moisture sensors shall be installed and in a second borehole frost heave sensor. In the same manner sensors shall be installed in two boreholes off the road – temperature-moisture sensors in one borehole and frost heave in the second borehole. See table 5.6. and Figure 5.12. for monitoring site parameters and layout.

Table 5.6. Monitoring site parameters

No	Parameter	Value
1	Number of boreholes under the road pavement	2
2	Number of boreholes off the road	2
3	Total number of temperature-moisture sensors	Up to 36
4	Total number of frost heave sensors	2
5	Lowermost temperature- moisture sensor	2 m
6	Lowermost position (anchor) of frost heave sensor	2.5 m
7	temperature- moisture sensor vertical interval	10 cm
8	Number of temperature- moisture sensors in one borehole	Up to 18
9	Number of frost heave sensors in one borehole	1
10	Frost heave data acquisition	Data loggers – USB download
11	Temperature- moisture data acquisition	Data loggers – transmission through mobile network
12	Data readout interval	15 min

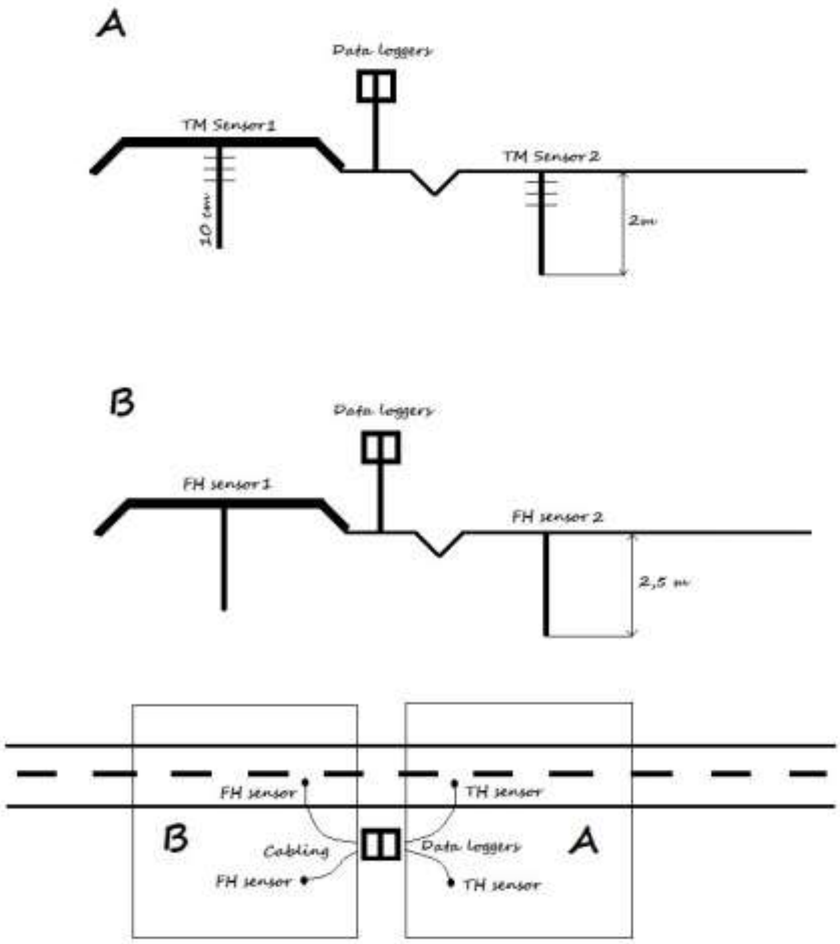

Figure 5.12. Principal placement of frost heave (FH) and temperature- moisture (TH) sensors as well as data-loggers at a monitoring site location.

A metallic pole with electrical grounding has to be installed at roadside close to the boreholes to fix to it data loggers and small trenches have to be made from each borehole to the data logger pole for cabling. All boreholes after installations have to be backfilled with a grout mixture and those on the road also with an asphalt layer.

Lowermost moisture -temperature sensor has to be installed at the 2 m depth, with next sensors installed at a 10 cm interval up to just below the asphalt layer. Recommended data measurement interval for both moisture, temperature sensors and for frost heave sensors is 15 minutes as this allows for analysis of soil frost heave behaviour and temperature dynamics, in the same time not overloading the system with too heavy data amount.

It is proposed first to equip up to three such monitoring sites, to test the system performance. For extension of the monitoring programme the vertical interval and thus the number of temperature- moisture sensors can be possibly optimised and reduced.

5.3.2. Locations of monitoring sites

For further frost penetration depth and frost heave studies, real *in situ* measurements are necessary. During this project, information about possible technical solutions of previously mentioned studies (5.2. section), theoretical aspects of frost heave (1. section) and climate conditions of Latvia (3. section) were analysed. All those aspects were considered in the process of selection of possible monitoring stations.

In order to select possible monitoring stations several major factors were taken into account:

- Monitoring stations must be located on soils that are susceptible to frost heave. (During analysis of this parameter Map of Quaternary sediments of Latvia (Scale 1:50000) and laboratory test results were used);
- Monitoring stations should be located close to weather monitoring stations.
- Monitoring stations should be located on places were Freezing season and also cold season is the longest (section 3.4.);
- Monitoring station should be located in places where vegetation cover could not significantly affect results (During analysis of this parameter orthophoto map of Latvia were used);

As a result of data analysis 5 possible monitoring sites were selected (Table 5.7.; Figures 5.13. up to 5.11)

Figure 5.13. Monitoring stations

Table 5.7. Possible monitoring stations

Nr.	Station	Coordinates (LKS-92)		Soil type	Freezing period	Cold period
1	LV02	558400	336527,4	Till	144	208
2	LV50	597860,3	352776,5	Till	195	230
3	LV49	645322	226015	Glaciolimnic	127	207
4	LV46	676491	276173	Glaciolimnic	123	218
5	LV04	515235	296520	Till	131	211

Figure 5.14. Monitoring station 1. Legend: Green dot – monitoring station; Red dot – weather monitoring station.

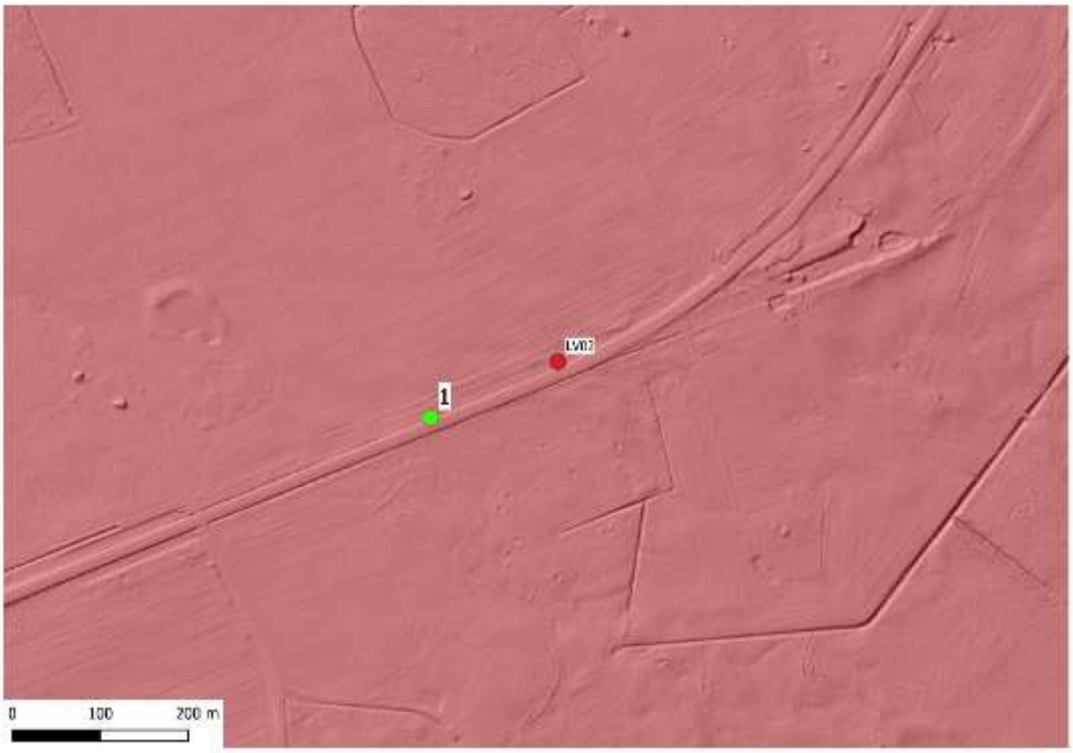

Figure 5.15. Monitoring station 1. Legend: Green dot – monitoring station; Red dot – weather monitoring station; brownish red colour represents glacigenic sediments (LIDAR DEM base map).

Figure 5.16. Monitoring station 2. Legend: Green dot – monitoring station; Red dot – weather monitoring station.

Figure 5.17. Monitoring station 2. Legend: Green dot – monitoring station; Red dot – weather monitoring station; brownish red colour represents glacigenic sediments (Ortho photo mosaic base map).

Figure 5.18. Monitoring station 3. Legend: Green dot – monitoring station; Red dot – weather monitoring station.

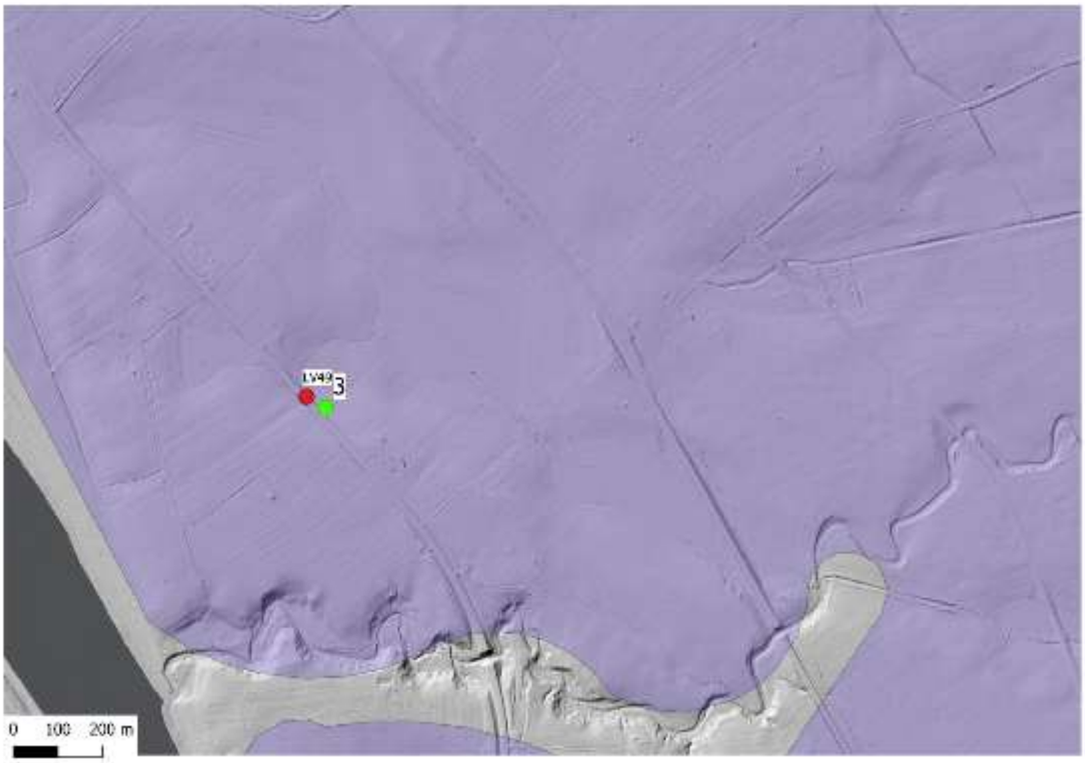

Figure 5.19. Monitoring station 3. Legend: Green dot – monitoring station; Red dot – weather monitoring station; purple colour represents glaciolimnic sediments (LIDAR DEM base map).

Figure 5.20. Monitoring station 4. Legend: Green dot – monitoring station; Red dot – weather monitoring station.

Figure 5.21. Monitoring station 4. Legend: Green dot – monitoring station; Red dot – weather monitoring station; brownish red colour represents glacigenic sediments, purple colour represents glaciolimnic sediments (Ortho photo mosaic base map).

Figure 5.22. Monitoring station 5. Legend: Green dot – monitoring station; Red dot – weather monitoring station.

Figure 5.23. Monitoring station 5. Legend: Green dot – monitoring station; Red dot – weather monitoring station; brownish red colour represents glacigenic sediments (LIDAR DEM base map).

Selected station should be viewed as initial step of possible wider monitoring network of frost heave studies of Latvia. During this study it was found that there is no reliable information about frost heave in Latvia so selected stations could serve as basis for further reliable studies. As up till now conducted laboratory analysis of frost heave gave just insight of frost susceptibility of soils that are present in Latvia, without such in-situ monitoring stations it is not possible to give wider conclusions about possible frost heave in Latvia.

5.4. Specifications and costs

Table 5.8. Combined temperature-moisture sensor specifications

Volumetric Water Content (VWC)	
Range Mineral soil calibration	0.00–0.70 m3/m3
Soilless media calibration	0.0–1.0 m3/m3
Apparent dielectric permittivity (ε_a)	1 (air) to 80 (water)
Dielectric measurement frequency	70 MHz
Resolution	0.001 m3/m3
Generic calibration	±0.03 m3/m3 typical in mineral soils that have solution EC <8 dS/m
Medium specific calibration	±0.01–0.02 m3/m3 in any porous medium
Apparent dielectric permittivity (ε_a)	1–40 (soil range), ±1 ε_a (unitless) 40–80, 15% of measurement
Temperature	
Range	−40 to 60 °C
Resolution	0.1 °C
Accuracy	±1 °C
Output	
DDI serial or SDI-12 communications protocol	
Data Logger Compatibility	
Any data acquisition system capable of 4.0- to 15-VDC power and serial or SDI-12 communication	
PHYSICAL SPECIFICATIONS	
Suitable for installation in 10 cm diam boreholes (tool, wire connections protruding perpendicular, robust casing and needles)	
Needle Length at least 5.5 cm	

Table 5.9. Specifications for data logger for temperature-moisture sensors

Sensor Input Ports	6 (supports METER analog, digital, or pulse sensors)
Sensor Port Type	3.5-mm stereo plug connector
Logging Interval	5 min to 12 h
Reporting Interval	Hourly with additional charges for more frequent reporting
Data Storage	8 MB (40,000 to 80,000+ records depending on configuration)
Memory Type	Nonvolatile flash, full data retention with loss of power
Global Position	Integrated 56-channel GPS/QZSS receiver
GPS Position Update	Daily (automatic) and on-demand (manual)
GPS Position Accuracy	±3 m, with good sky view
Timekeeping	Synchronize automatically and on-demand;
	GPS system, cellular, or software
Battery Capacity	6 AA NiMH or alkaline batteries
NiMH Battery Charging	Solar energy harvesting or USB
NiMH Battery Life	3+ years with unobstructed view of sun
Alkaline Battery Life	3–12 months depending on configuration
Computer Communication	Standard USB cable, USB A to micro-B
Cellular Specifications	UMTS 3G 5-band Cellular Module with 2G fallback
Cellular Coverage	AT&T® and T-Mobile® in USA, 200+ global partner carriers.
	Cellular and data hosting service provided by METER.
Internet Downloads	SSL/TLS encrypted
Enclosure	Weather-, impact-, and UV-resistant polymer
Enclosure Rating	IP56, NEMA 3R
Enclosure Size	14.9 cm × 25 cm × 6.3 cm (5.9 in × 9.9 in × 2.5 in)
Enclosure Access	Hinged door with latches and eyelets for lock or zip tie
Operating Environment	–40 to +60 °C (0%–100% relative humidity)
Compliance	Manufactured under ISO 9001:2015 EM ISO/IEC 17050:2010 (CE Mark)

Table 5.10. Specification for frost heave *in situ* measuring extensiometer

ITEM	**DESCRIPTION**
Measurement Range	At least 100 mm
Accuracy	+/- 0.25 % FSR
Resolution	0,02 FSR
Linearity	0,25 FSR
Thermal Zero Shift	< 0,05 % FSR/°C
Operating temperature	–20 °C to 80 °C
Extensometer Head max/min Diameter	63,5 mm/42,5 mm
Signal Cable	Two twisted pair cable with polyurethane jacket (one cable per measurement point)

Table.5.11. Specifications for data logger for frost heave *in situ* measuring extensiometer

ITEM	**SPECIFICATION**
Frequency Accuracy	0,01 % Full Scale
Resolution	1 part in 65,000
Memory Records	Up to 600,000 records including: time, frequency, temperature
Power source	Lithium ‘C’ or ‘D’ cell battery
Battery life	Up to 7 years (assuming 1 hour reading frequency)/4 memory fills depending on temperature
Communication	USB Type B connector (radio optional)
Dimensions	185 x 75 x 55 mm (7,28 x 2,95 x 2,17 in)
Temperature Range	–40 °C to 60 °C
Enclosure	NEMA 4x (IP65)
MEMORY	
Memory size	4MB
Data Transfer	2,300 data points per second
Interval Mode	2 seconds to 1 day
Variable Rate Mode	16 user programmable sampling rates
Time Format	Month/day/year Hour/minute/second
Memory Full Behavior	“Wrap around” or “fill&stop”option

References

Aldrich, H.P.Jr., Paynter, H.M. 1966. *Depth of Frost Penetration in Non-uniform Soil.* U. S. Army Cold Reg. Res. Eng. Lab. Spec. Rep. 104.

Andersland, O.B., Ladanyi, B. 1994. Introduction to frozen ground engineering. Springer. 363 pp.

Andersland, O.B., Ladanyi, B. 2003. Introduction to frozen ground engineering. Second edition. John Wiley & Sons, Inc. 384 pp.

Anderson, D.M., Tice, A.R. 1972. Predicting unfrozen water contents in frozen soils from surface area measurements. In *Frost Action in Soils.* Washington, D.C.: National Academy of Sciences, pp. 12-18 *(Highway Res. Rec.* 393).

Banin, A., Anderson, D.M. 1974. Effects of salt concentration changes during freezing on the unfrozen water content of porous materials. *Water Resour. Res. 10(1):* 124-28.

Barnes, D.F. 1963. Geophysical methods for delineating permafrost. In *Proc. Int. Conf. on Permafrost,* Lafayette, Ind. Publ. 1287. Washington, D.C: National Academy of Sciences-National Research Council, pp. 349-55.

Bates, R.E., Bilello, M.A. 1966 Defining the cold regions of the Northern hemisphere. U.S. Army cold reg. Res. Eng. Lab. Tech. Rep. 178 pp.

Brown, R.J.E. 1963. Relation between mean annual air and ground temperatures in the Permafrost Region of Canada. In *Proc. Int. Conf. on Permafrost*, Lafayette, Ind. Pub I.1287. Washington, D.C.: National Academy of Sciences National Research Council, pp. 241-47.

Carter. M., Bentley, S.P. 2016. Soil properties and their correlations. Second edition. Wiley. 236 pp.

Cass, J.R. 1959. Subsurface explorations in permafrost areas. *Soil Mech. Found. Div. Proc. ASEC* 85(SM5):31-41.

Dech, S.W., Tungalagsaikhan, P.. Preusser, C., Meisner, R.E., 1998. Operational value-adding to AVHRR data over Europe: methods, results, and prospects. *Aerospace Science and Technology*. 5, 335-346.

Dousset, B., Gourmelot, F., 2003. Satellite multi-sensor data analysis of urban surface temperatures and landcover. *ISPRS Journal of Photogrammetry & Remote Sensing.* 58, 43–54.

Farouki, O.T. 1981. *Thermal Properties of Soils.* u.s. Army Cold Reg. Res. Eng. Lab. Monogr. 81-1.

Hall, D. K., Riggs., G.A., 2016. *MODIS/Terra Snow Cover Daily L3 Global 500m Grid, Version 6*. Boulder, Colorado USA. NASA National Snow and Ice Data Center Distributed Active Archive Center.

Harris, S.A., Brouchkov, A., Guodong, C. 2017. Geocryology: Characteristics and Use of frozen ground and permafrost landforms. CRC press. 810 pp.

Johansen, O. 1975. Thermal conductivity of soils. Ph.D. diss., Norwegian Technical Univ., Trondheim; also, U.S. Army Cold Reg. Res. Eng. Lab. Trans!. 637, July 1977.

Johnson, T.C., Berg, R.L., Chamberlain, E.J., Cole, D.M. 1986. *Frost Action Predictive Techniques for Roads and Airfields: A Comprehensive Survey of Research Findings.* U.S. Army Cold Reg. Res. Eng. Lab. CRREL Rep. 86-18.

Johnston, G.H. 1963. *Soil Sampling in Permafrost Areas.* Nat. Res. Counc. Can. Div. Build. Res. Tech. Pap. 155 (NRC 7417).

Kaal, T., Jentson, M., 2011. *Muldkehade läbikülmumise, ilmastikutingimuste ja teede kandevõime seoste uuringuteks vajalike seadmete – Percostation mõõtejaam ja 6 vertikaalset temperatuuriandurit – ostmine ja paigaldamine*. AS Teede Tehnokeskus, Tallinn.

Kalman, B. 2018. Personal communication.

Klein, C.A., Wilson, C.R., Benson, B.D., Carpenter, G.W. 1986. Installation of thermistor strings in test borings: A comparison of methods and results. In *Proc. 4th Int. Conf. on Cold Regions Engineering,* Anchorage, Alaska. New York: ASCE, pp. 200-206.

Kļaviņš, M., .Zaļoksnis, J. 2016. Klimats un ilgtspējīga attīstība. Rīga: LU Akadēmiskais apgāds, 384. lpp

Kļaviņš, M., Blumberga, D., Bruņiniece, I., Briede, A., Grišule, G., Andrušaitis, A., Āboliņa, K. 2008. KLIMATA MAINĪBA UN GLOBĀLĀ SASILŠANA. Rīga, LU Akadēmiskais apgāds, 174 lpp.

Konrad, J.M. 1987. Procedure for determining the segregation potential of freezing soils. *Geotech. Test. 1. ASTM* 10(2):51-58.

Konrad, J.M. 1988. Influence of freezing mode on frost heave characteristics. *Cold Reg. Sci. Technol. 15(2):161-75.*

Konrad, J.M., Morgenstern, N.R. 1980. A mechanistic theory of ice lens formation in fine-grained soils. *Can. Geotech. J. 17(4):473-86.*

Konrad, J.M., Morgenstern, N.R. 1980. A mechanistic theory of ice lens formation in fine-grained soils. *Can. Geotech. J. 17(4):473-86.*

Konrad, J.M., Morgenstern, N.R. 1981. The segregation potential of a freezing soil. *Can. Geotech. J. 18(4):* 482-91.

Konrad, J.M., Morgenstern, N.R. 1982. Prediction of frost heave in the laboratory during transient freezing. *Can. Geotech. J. 19(3):250-59.*

Konrad, J.M., Morgenstern, N.R. 1984. Frost heave prediction of chilled pipelines buried in unfrozen soils. *Can. Geotech.* 1. 21(1):100-15.

Kummerow, C. D., Randel, D.L., Kulie, M., Wang N.-Y., Ferraro, R., Munchak, S.J., Petkovic, V., 2015. The evolution of the Goddard profiling algorithm to a fully parametric scheme. *J. Atmos. Oceanic Technol*. 32, 2265–2280.

Linell, K.A, KAPLAR, C.W. 1966. *Description and Classification of Frozen Soils.* U.S. Army Cold Reg. Res. Eng. Lab. Tech. Rep. 150.

LSA SAF, 2015. *Product user manual Land Surface Temperature (LST).* 2, 65.

Mackay, J.R. 1974. Seismic shot holes and ground temperatures, Mackenzie Delta Area, Northwest Territories. *Geol. Surv. Can.* Pap. 74-1, pt. A, pp. 389-90.

Meng, H., Dong, J., Ferraro, R., Yan, B., Zhao, L., Kongoli, C., Wang N.Y., Zadovsky, B., 2017. A 1DVAR-based snowfall rate retrieval algorithm for passive microwave radiometers. *Journal of Geophysical Research: Atmospheres.* 122 (12).

Morgenstern, N.R. 1981. Geotechnical engineering and frontier resource development. *Geotechnique 31(3):305-65.*

Nikodemus, O., Kļaviņš, M., Krišjāne, Z., Zelčs, V. 2018. Latvija, zeme, daba, tauta, valsts. Rīga: Latvijas Universitātes Akadēmiskais apgāds, 752 lpp.

Nixon, J.F. 1991. Discrete ice lens theory for frost heave in soils. *Can. Geotech.* 1. 28(6) 843-59.

Nixon, J.F. 1992. Discrete ice lens theory for frost heave beneath pipelines. *Can. Geotech.* 1. 29(3): 487-97.

Patterson, D.E., Smith, M.W. 1983. Measurement of unfrozen water content in saline permafrost using time domain reflectometry. In *Proc. 4th Int. Conf. on Permafrost,* Fairbanks, Alaska. Washington, D.C.: National Academy Press, pp. 968-72.

Shaker, A., Yan, W.Y., 2010. Trail road landfill site monitoring using multitemporal Landsat satellite data. *Canadian Geomatics Conference 2010 and ISPRS COM I Symposium*.

Stenberg, L. 1997. STÖR-96. VTI notat Nr 15-1997.

Tice, A.R., Anderson, D.M., Banin, A. 1976. *The Prediction of Unfrozen Water Contents in Frozen Soils from Liquid Limit Determinations.* U.S. Army Cold Reg. Res. Eng. Lab. CRREL Rep. 76-8.

Uddstrom, M.J., 1988. Retrieval of Atmospheric Profiles from Satellite Radiance Data by Typical Shape Function Maximum a Posteriori Simultaneous Retrieval Estimators. Journal of Applied Meteorology. 27(5), 515–549.

Vaitkus, A., Gražulyte, J., Skrodenis, E., Kravcovas, I. 2016. Design of Frost Resistant Pavement Structure Based on Road Weather Station (RWSs) Data. *Sustainability*.8, 1328. 1-13.

Velli, Y.Y.A., Grishin, P.A. 1983. *On the Functional Dependence of the Freezing Point of Soils on the Composition of Water-Soluble Salts in the Interstitial Solution* (transl. from Russian). Natl. Res. Counc. Can. Tech. Transl. TT- 2070.

Vikström, Lars., 1996. *Comparison between measured and calculated frost heave and frost depth*, Luleå Luleå tekniska universitet, Department of Civil and Mining Engineering, Division of Soil Mechanics.

Wan, Z., Hook, S., Hulley, G., 2015. *MOD11A1 MODIS/Terra Land Surface Temperature/Emissivity Daily L3 Global 1km SIN Grid V006*. NASA EOSDIS LP DAAC.

Wen, Y., Behragi, A., Kirstetter, P. E., 2016. Evaluation and Uncertainty Estimation of the Latest Radar and Satellite Snowfall Products Using SNOTEL Measurements over Mountainous Regions in Western United States. *Remote Sensing*. 8 (11).

World Meteorological Organization, 2011. Guide to Climatological Practices. WMO-No. 100, 2011 edn. Geneva, World Meteorological Organization. pp 117.

Zariņš, A., Kivilands, J., Krūmiņš, E., Gora, I. 2015. *Ieteikumi ceļu projektēšanai. Ceļa sega*. Rīga, 81 lpp.

Electronic sources

Avotniece, Z., Aņiskeviča, S., Maļinovskis, E. 2017. VSIA “Latvijas Vides, ģeoloģijas un meteoroloģijas centrs ”Climate change scenarios for Latvia”. Report. Available : http://www2.meteo.lv/klimatariks/zinojums.pdf Reviewed: 06.06.2019

CM SAF, 2019. *The CM SAF role in climate monitoring and research*. CM SAF. Available: https://www.cmsaf.eu/EN/Overview/Philosophy/Philosophy_node.html 25.02.2019.

Coppernicus, 2019. *Land Surface Temperature.* Coppernicus. Available: https://land.copernicus.eu/global/products/lst 25.02.2019.

Coppernicus, 2019. *Snow Cover Extent.* Available: https://land.copernicus.eu/global/products/sce 06.03.2019.

ESA, 2019. *Introducing Sentinel-3*. ESA. Available: https://www.esa.int/Our_Activities/Observing_the_Earth/Copernicus/Sentinel-3/Introducing_Sentinel-3 25.02.2019.

HSAF, 2019. *Snow*. HSAF. Available: http://hsaf.meteoam.it/snow.php 06.03.2019.

LSA SAF, 2019. *Land Surface Temperature*. LSA SAF. Available: https://landsaf.ipma.pt/en/products/land-surface-temperature-copy/ 25.02.2019.

LSA SAF, 2019(2). *MSG Toolbox*. LSA SAF. Available: https://landsaf.ipma.pt/en/products/land-surface-temperature-copy/ 25.02.2019.

LSA SAF, 2019(3). *Snow Cover*. LSA SAF, HSAF. Available: https://landsaf.ipma.pt/en/products/snow-cover/sc/ 06.03.2019.

NASA, 2019. *Precipitation Measurement Mission*. NASA. Available: https://pmm.nasa.gov/precipitation-measurement-missions 04.03.2019.

Ratier, A., S.a. *An introduction to EUMETSAT*. EUMETSAT. Available: https://www.eumetsat.int/website/home/AboutUs/index.html 25.02.2019.

USGS, 2019. *Landsat missions*. USGS. Available: https://www.usgs.gov/land-resources/nli/landsat 25.02.2019.

Standards*:*

ASTM D1883 – 16 ASTM Test method for CBR (California bearing ratio) of laboratory-compacted soils.

ASTM D2487 Standard practice for classification of soils for engineering purposes (Unified Soil Classification System)

ASTM D2974 – 14 Standard test methods for moisture, ash, and organic matter of peat and other organic soils" standard.

ASTM D4083 − 89 (Reapproved 2016) Standard practice for description of frozen soils (Visual-Manual Procedure).

ASTM D5918-13 Standard test methods for frost heave and thaw weakening susceptibility of soils.

BS 812-124:2009 Testing aggregates. Method for determination of frost heave.

DIN 18196 Earthworks and foundations - Soil classification for civil engineering purposes.

GOST 28622-2012. Грунты. Метод лабораторного определения степени пучинистости.

ISO 14688-1:2002 Geotechnical investigation and testing -- Identification and classification of soil -- Part 1: Identification and description.

ISO 14688-1:2017 Geotechnical investigation and testing -- Identification and classification of soil -- Part 1: Identification and description.

ISO 14688-2:2004 Geotechnical investigation and testing -- Identification and classification of soil -- Part 2: Principles for a classification.

ISO 14688-2:2017 Geotechnical investigation and testing -- Identification and classification of soil -- Part 2: Principles for a classification.

LVS 437 "Būvniecība. Gruntis. Klasifikācija".

LVS 190-5 Ceļu projektēšanas noteikumi. 5. daļa: Zemes klātne.

LVS EN 1997-1:2004. Eurocode 7: Geotechnical design - Part 1: General rules.

LVS EN 1997-2:2007. Eurocode 7: Geotechnical design - Part 2: Ground investigation and testing.

Appendix 1. Soils are classified in accordance with their suitability for civil engineering purposes using DIN 18196

Definition and designation									Frost-susceptibility class[1]	Distinguishing characteristics (including lines 16 to 21)			Examples
Line	Main groups	Particle size fraction in % by mass, Particle size ≤0.06 mm	≤ 2 mm	Plasticity index and position relative to A-line (see chart)				Letter symbol Group symbol		Dry strength	Response to vibration testing	Plasticity in kneading test	
1	Coarse-grained soils	<5%	≤ 60%	-	Narrow-graded gravels			GE	F1	Steep grading curve due to prevalence of one particle size range			River gravel and beach gravel Terrace gravel
2					Wide-graded gravel-sand mixtures			GW		Continuous grading curve extending over several particle size ranges			
3					Gap-graded gravel-sand mixtures			GI		Mostly staggered grading curve due to lack of one or several particle size ranges			Volcanic slag
4			> 60%	-	Narrow-graded sands			SE		Steep grading curve due to prevalence of one particle size range			Dune sand and drifting sand, quicksand, Berlin sand, basin sand, tertiary sand
5					Wide-graded sand-gravel mixtures			SW		Steep grading curve due to prevalence of one particle size range			Moraine sand, terrace sand, granitic sand
6					Gap-graded sand-gravel mixtures			SI		Steep grading curve due to prevalence of one particle size range			
7	Mixed-grained soils	5-15%	≤ 60%	-	Gravel-silt mixtures	5% to 15% by mass ≤ 0.06 mm		GU GT SU ST	F2*)	Wide-graded or gap-graded grading curve	Fines content is	silty	Moraine gravel Weathered gravel Talus deposits Boulder clay
8					Gravel-clay mixtures							clayey	
9			>60%		Sand-silt mixtures							silty	
10					Sand-clay mixtures							clayey	
11		15-40%	≤ 60%	-	Gravel-silt mixtures	5% to 15% by mass < 0.06 mm		GU* GT* SU* ST*	F3			silty	Tertiary sand
12					Gravel clay mixtures							clayey	Alluvial loam, sandy loess
13			>60%		Sand-silt mixtures							silty	Tertiary sand, creeping sand
14					Sand-clay mixtures							clayey	Boulder clay, glacial till
15	Fine-grained soils	> 40%	-	Ip ≤ 4% or below the A-line	Silts of low plasticity $w_L < 35\%$			UL	F3	low	quick	none to low	Loess, alluvial loam
16					Silts of medium plasticity $35\% \leq w_L \leq 50\%$			UM		low to medium	slow	low to medium	Lacustrine clay, basin silt
17					Silts of high plasticity $w_L > 50\%$			UA		high	none to slow	medium to high	Volcanic soils, pumice soils
18				Ip ≥ 7% and above the A-line	Clays of low plasticity $w_L < 35\%$			TL		medium to high	none to slow	none to low	Glacial till, varved clay
19					Clays of medium plasticity $35\% \leq w_L \leq 50\%$			TM		high	none	none to low	Loess loam, basin clay, saliferous clay, lacustrine clay
20					Clays of high plasticity $w_L > 50\%$			TA	F2	very high	none	none to low	Trass, Lauenburg clay, basin clay
21	Organogenic[2] soils and soils containing organic matter	>40%	-	Ip≥7% and below the A-line	Silts containing organic matter and organogenic silts	Not flammable	$35\% \leq w_L \leq 50\%$	OU	F3	medium	Slow to very quick	medium	Lacustrine marl, diatomaceous earth, topsoil
22					Clay containing organic matter and organogenic clays		$w_L > 50\%$	OT	F2	high	none	high	Alluvial mud, tidal mud, tertiary carboniferous clay
23		<40%	-	-	Corse-grained to mixed-grained soils containing humic matter			OH		Contains organic matter, mostly dark in colour, musty smell, loss on ignition of up to aprprox. 20% by mass			Topsoil, palaeosol
24					Coarse-grained to mixed-grained soils containing calcareous siliceous formations			OK		Contains non organic matter, mostly light in colour, low weight, high porosity			Calcareous sand, tuffaceous sand, bog lime
25	Organic soils	-		-	Non-degraded to moderately degraded peat	or		HN		Native humus formations	Degree of degradation 1 to 5, fibrous, rich in wood, light brown to brown in colour		Fan peat, Raised bog peat, Fen-wood peat
26					Degraded peats	Flammable smoulderable		HZ			Degree of degradation 6 to 10, blackish-brown to black		
27					Muds as a collective term for digested sludge, organic silt, gyttja, dy, sapropel			F		Underwater (sedimentary) muds consisting of organic matter, faeces and microorganisms, frequently interspersed with sand, clay and lime, blue-black or greenish to yellow-brown, occasionally dark grey-brown to blue-black, soft-strongy			Organic silt, Digested sludge

[1] In accordance with "Additional technical conditions of contract and directives for earthworks in road construction" (ZTV E-StB)

[2] Soils formed as a result of microorganism action

* To be classified as F1 if, where $U \geq 15,0$, the fines content ($d<0,063$) is $\leq 5\%$ by mass or, where $U \leq 6,0$, the fines content ($d<0,063$ mm) is $\leq$1`5% by mass. Where $6,0<U<15,0$, the particle fraction smaller 0,063 permissible for classifying as F1 may be interpolated linearly (see chart)